ADAPTIVE MOBILITY MANAGEMENT FOR NEXT-GENERATION SMALL CELL NETWORKS

by

Wahida Nasrin

A dissertation submitted to the faculty of
The University of North Carolina at Charlotte
in partial fulfillment of the requirements
for the degree of Doctor of Philosophy in
Electrical Engineering

Charlotte

2018

Approved by:

_____
Dr. Jiang (Linda) Xie

_____
Dr. Asis Nasipuri

_____
Dr. Yu Wang

_____
Dr. Isaac Sonin

ABSTRACT

WAHIDA NASRIN. Adaptive Mobility Management for Next-Generation Small Cell Networks. (Under the direction of DR. JIANG (LINDA) XIE)

Small cells are introduced as one of the key technologies of the new generation (5G) mobile networks. Among the existing small cell technologies, femtocells drew more research attention from both industry and academia because of their unplanned installation and management by users. Femtocell technology is a promising solution for offloading high volume cellular data traffic to low-powered indoor base stations. However, coexistence of femtocells with macrocell networks introduces special challenges to mobility management.

In this research, adaptive mobility management in femtocell networks is explored. The aim of this research is to provide seamless mobility and offloading to mobile users in different femtocell networks. Past research on mobility management in femtocell networks only focused on avoiding unnecessary handoffs and handoff failures while ignoring some important and practical issues, e.g., the ad-hoc nature of femtocells and offloading issues. Moreover, the effects of heterogeneous spectrum on mobility management in cognitive radio femtocell networks are never addressed. Furthermore, the service migration and the radio and computation offloading issues due to users' mobility are not well investigated.

In this research, six adaptive mobility management schemes are proposed to address these issues. First, two adaptive handoff decision algorithms are proposed for closed-access and open-access femtocell networks. Then, a secure target cell selection scheme is designed for femtocell networks. An analytical model is also proposed to analyze the total handoff signaling cost. Later, a power control scheme along with the detection sensitivity scheme and a mobility management scheme are proposed to address the issues of heterogeneous spectrum in cognitive radio femtocells. Last, a joint handoff

and offloading decision algorithm is proposed to reduce the service migration rate and the radio network congestion. The proposed mobility management schemes in this research are endowed with the ability to adapt to the existing practical challenges. Therefore, this research will provide important insights on next-generation femtocell networks.

ACKNOWLEDGEMENTS

Foremost, I would like to express my greatest and deepest gratitude to my advisor, Professor Dr. Jiang (Linda) Xie, for her continuous support, guidance, and supervision throughout these years. She has patiently spent countless hours to discuss and refine my cluttered research ideas and helped me to become an independent researcher. I could not have imagined having a better advisor than her.

Besides my advisor, I would like to thank my Ph. D. committee members: Dr. Asis Nasipuri, Dr. Yu Wang, and Dr. Isaac Sonin for their time and valuable advice. In addition, I appreciate the GASP grant from UNC-Charlotte and Research Assistantships from National Science Foundation (NSF) as the financial assistance for this work.

In the end, I would like to thank my family and friends. Their wishes and supports made the journey easier. Special thanks to my husband Md Majharul Islam Rajib. He has been extremely supportive, and was always there for me.

TABLE OF CONTENTS

LIST OF FIGURES

LIST OF TABLES

CHAPTER 1: INTRODUCTION

1.1 Background on Femtocell Networks

Though the specification of 5G is not standardized yet, currently, five emerging technologies are considered as the platform of the 5G network: millimeter waves, small cells, massive multiple-input multiple-output (MIMO), full duplex, and beamforming. In 5G networks, small cells will be deployed to overcome the drawbacks of using millimeter waves. However, the objective remains unchanged from 4G small cells deployment, which is providing coverage and capacity to end users. The senior vice president of technology planning and engineering for AT&T said, "As you build small cells for Long Term Evolution (LTE) networks, it pre-positions you for the infrastructure we are going to need for 5G as well" [1]. Small cells are low-powered and short-ranged (10 meters to a few kilometers) indoor or outdoor cellular base stations (BSs). There are three types of small cells: *femtocells*, *picocells*, and *microcells*. These small cells coexist with the traditional cellular networks (macrocells) and share the same spectrum band. Comparing with other small cells, femtocells have the characteristic of unplanned installation and management by users that drew attention from the researchers. Moreover, the support of femtocells is a key feature of Long Term Evolution-Advanced (LTE-A) systems.

Femtocells are first introduced as a promising solution to improve indoor coverage and to offload data traffic from cellular networks (i.e., macrocells) [2, 3]. Femtocells are low-powered, short-ranged, and low-cost indoor base stations (BSs), which are deployed and managed by users. Femto base stations (FBSs) are connected to the core network via a broadband router and a femto-gateway (F-GW). A femtocell deployed macrocell network is shown in Figure 1.1. Femtocells can receive offloaded traffic from

cellular networks based on their access modes and the availability of user equipment (UE) within their coverage area. There are three access modes available in femtocell networks: closed, open, and hybrid. In closed-access femtocell networks, only a few registered users can access femtocells. Any user can access open-access femtocells when they are within the coverage area of an open-access femtocell. In hybrid-access mode, both registered and non-registered users can access these femtocells, however, the registered users have a higher priority.

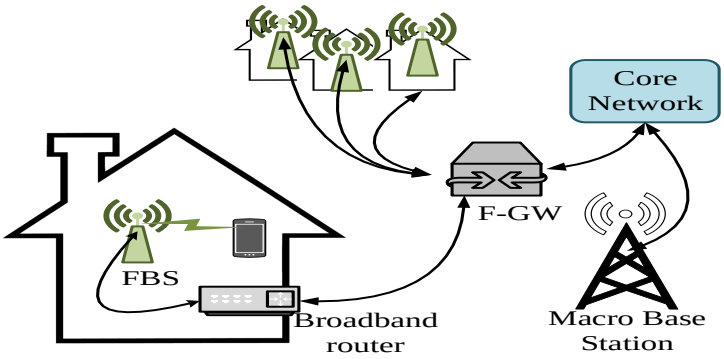

Figure 1.1: A femtocell network.

Femtocells usually use the same spectrum bands as the cellular networks. However, the volume of mobile data traffic is increasing exponentially in recent years due to the popularity of various mobile devices [4]. This increment of data traffic leads to a spectrum scarcity problem in cellular networks. Although femtocells are considered as a promising solution to provide cellular traffic offloading [2, 5], densely deployed femtocells may increase the demand of the cellular spectrum and interference to macrocell networks. The cognitive radio (CR) technology is then proposed to combine with femtocell networks to overcome these issues [6, 7, 8, 9, 10, 11]. This combined network is called CR femtocell network, where the CR femto-base stations (FBSs) act as secondary users (SUs) and they can access the licensed spectrum of both macrocell networks and TV white space in an opportunistic manner.

The evolution of femtocells does not stop with the CR technology. Recently, of-

floading computational data to the cloud has become the most promising solution to support the resource-hungry mobile and Internet of Things (IoT) applications. These applications are growing rapidly with the increasing popularity of smart mobile devices. As mobile devices are resource-constrained (limited computational resources and energy), cloud offloading allows them to use infrastructures, platforms, and software provided by cloud providers (e.g., Google, Microsoft Azure, and Amazon) at low cost [12, 13]. However, the remote execution of offloaded data in the cloud brings challenges to satisfying the delay requirement of end users. If an application is offloaded to the remote cloud, the delay requirement may not be satisfied because of the long transmission and offloading delay over the Internet. To overcome these issues, Mobile Edge Computing (MEC) is introduced as one of the key technologies for the new generation (5G) mobile networks. The main feature of MEC is to push computational resources and storage to the network edges (e.g., cellular base stations (BSs) and femtocells) in order to offload computation-intensive and latency-sensitive applications from smart mobile devices [14, 15].

Deployment of these femtocells and CR femtocells with macrocell networks, and integration of the MEC with femtocells or macrocells introduce special challenges to mobility management. Mobile users face several unique issues during performing a handoff (HO) due to the small coverage area and the unplanned and indoor deployment of femtocells by users. Three types of handoffs (HOs) are available in femtocell networks: macro-to-femto, femto-to-macro, and femto-to-femto. The closed-access mode supports macro-to-femto and femto-to-macro HOs. Besides the two HOs available in closed-access, open-access mode also supports users in performing HOs from a femtocell to another femtocell (femto-to-femto). On the other hand, hybrid access mode supports all types of HOs. Each of these types of HOs have different decision criteria, and these HO decisions are affected by several unique challenges of femtocell networks. Similarly, the spectrum heterogeneity in CR femtocell networks introduces

new challenges to mobility management. In addition, the integration of MEC with the femtocell network adds the issue of computation offloading with the mobility management. To address these issues, the proposed mobility management schemes must be adaptive to serve not only seamless HOs but also efficient offloading.

1.2 Problem Statement and Research Motivation

1.2.1 HO Decisions in Femtocell Networks

HO plays an important role during data offloading in a femtocell-deployed macrocell network. Though femtocells operate on the same frequency spectrum as macrocells, the dense yet unplanned and indoor deployment of femtocells within the overlaid macrocell networks makes the HO decision more difficult and different from macrocell networks. The first difficulty is the difference in the transmission power of a femto-base station (FBS). The transmission power of a FBS (usually 10-15dB) is much lower than that of a macro-base station (MBS) which is usually 45dB [5]. Because of this low transmission power, a femtocell might be undiscovered by a UE. This can happen because a UE has the natural tendency to connect to the highest received signal strength (RSS) and it receives higher RSS from a macrocell rather than a femtocell.

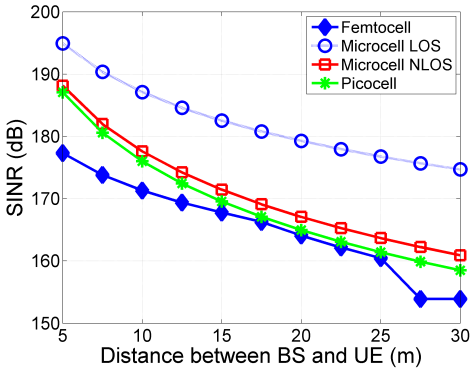

Figure 1.2: The comparison of SINR of different small cells.

The second problem is related to co-channel interference. Because of indoor deployment of femtocells, they suffer higher path-loss due to multi-path propagation,

wall penetration loss, and shadowing effects than other small cells [16]. As a result, an abrupt signal-to-interference-plus-noise-ratio (SINR) drop occurs at the boundary of femtocells. Simulation results on the SINR with respect to the distance between a UE and the BS of different small cells are shown in Figure 1.2. We use the ITU-R P.1238-7 path-loss model in our simulation [17]. The indoor deployment is indicated as NLOS (non-line-of-sight) and outdoor deployment is indicated as LOS (line-of-sight) here. From the figure, it is observed that a femtocell suffers from higher interference than others because of the low transmission power and indoor deployment. Hence, it has an abrupt signal drop at the cell boundary. How this abrupt signal drop and high interference affect the HO decision-making is explained in Figure 1.3.

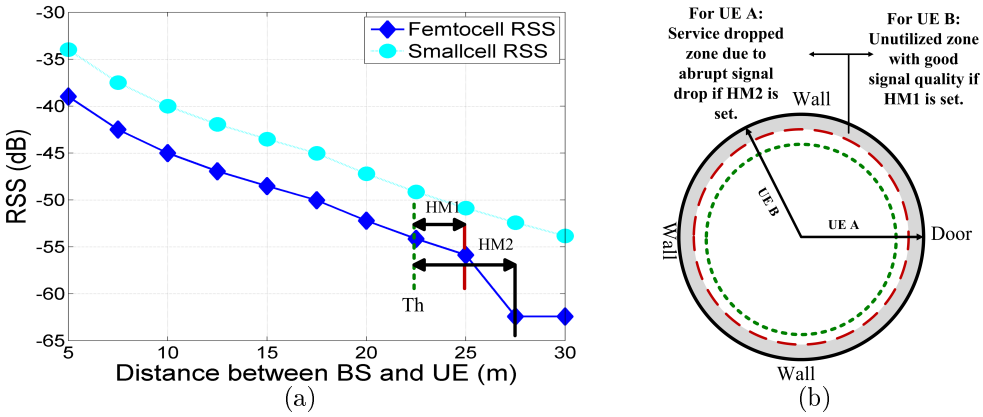

Figure 1.3: Effect of abrupt signal drop at the cell boundary in HO decision making.

The unplanned and unstable nature of neighboring femtocells introduces a third challenge. As femtocells are fully operated by users and the network operator does not have any control on this, the number and position of neighboring femtocells may vary randomly. This nature of neighboring femtocells will create an uneven interference effect on the boundary of femtocells from time to time. Figure 1.4 presents the SINR at the home femtocell boundary with different number of neighboring femtocells. We observe that the SINR changes randomly and unpredictably, which can increase the ping-pong effects for indoor femtocell users. This issue needs to be addressed in order

to provide seamless mobility support between femtocells and macrocells and to ensure a better user experience.

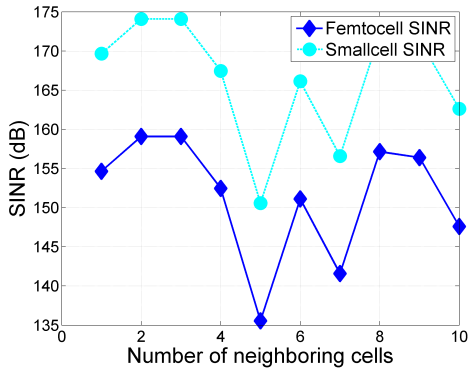

Figure 1.4: The effect of ad-hoc nature of neighboring femtocells on SINR at the boundary of the home femtocell.

Besides all of these challenges, different HO scenarios in femtocell networks have different criteria and purposes. They are:

- Macro-to-femto HO: To offload traffic from macrocell networks in order to avoid network congestion.
- Femto-to-macro HO: To provide seamless mobility management and better QoS while the indoor signal is poor and the macrocell network is not congested.

Each of these types of HOs have different decision criteria, and these HO decisions are affected by several unique challenges of femtocell networks. Due to indoor and unplanned deployment of femtocells, unnecessary HOs and ping-pong effects may happen frequently, which severely degrades the quality of connections and user experience. On the other hand, offloading in femtocells requires a high cell utilization. Therefore, it is necessary to design an HO decision algorithm that can reduce unnecessary HOs and improve cell utilization at the same time. Most of the existing works propose HO decision algorithms that reduce unnecessary HOs and ping-pong effects [18, 19, 20]. A few of them have considered cell utilizations while designing an HO

decision algorithm [21, 22]. All of these algorithms have used different parameters and techniques to design HO decision algorithms [18]. This practice adds extra HO signaling overhead at the core network and increases the HO signaling cost. Limited research has been conducted to analyze the HO signaling cost in femtocell networks [23, 24]. However, these works do not analyze the signaling cost of different types of HOs in open-access modes. Moreover, a comparison of the HO signaling cost for existing HO decision algorithms is necessary.

1.2.2 Attacks on Open-Access Femtocells

Though femtocells support necessary security features of a macro base station, due to the easy access of femtocells, femtocells are more vulnerable than a macrocell network. Moreover, though the nature of femtocells differs from wireless sensor networks and ad-hoc networks, the random deployment and the easy accessibility make them vulnerable to similar attacks of those networks. In this research, we discuss two of the most common attacks which may affect the target cell selection in open-access femtocell networks. These two attacks are: sinkhole and wormhole attacks.

1.2.2.1 Sinkhole Attack

In this attack, an attacker uses a signal booster to the antennas or increases the transmission power of a malicious or compromised femtocell to extend its coverage area. Therefore, the traditional HO decision algorithm, which selects the target cell with the maximum RSS to perform an HO, will hand off a UE to the malicious femtocell easily. As shown in Figure 1.5, a malicious FBS with increased transmission power has an extended coverage area. A UE moves towards the area will hand off to the malicious femtocell even though a number of secure FBSs exist there. Moreover, the UE will stay connected to the malicious FBS as long as the RSS is high enough to perform communications. As a result, the UE will not perform an HO to any other secure femtocell unless it crosses the border of the malicious femtocell. The longer

the UE stays connected to a malicious femtocell, the more harm it will face.

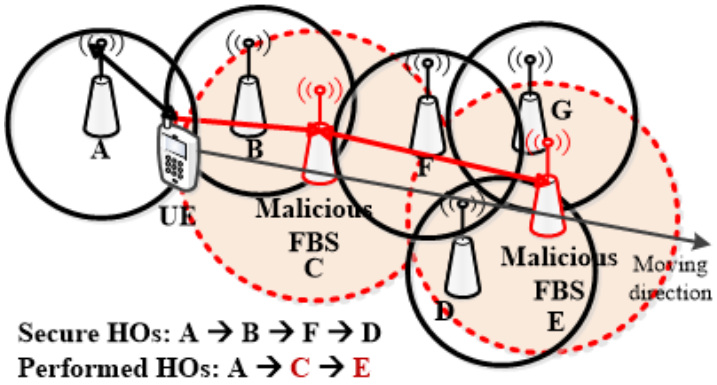

Figure 1.5: A scenario to show the effect of the sinkhole attack on HOs.

1.2.2.2 Wormhole Attack

In this attack, an attacker deploys a malicious femtocell and connects it to a registered femtocell [25]. The attacker is able to install the malicious FBS anywhere he desires and uses the location information of the registered femtocell. Therefore, a user when connected to the malicious femtocell assumes that it has been connected to the registered femtocell. On the other hand, it is very important that the location information of an FBS complies with radio communication license conditions and cell planning [26]. If an attacker deploys an FBS at any desired location and uses the real location information of a registered femtocell during location verification with the core network, then this mis-configured FBS may cause severe interference to other nearby FBSs and break the radio communication license policies obtained by the operator. The consequence of the wormhole attack on a mobile UE is shown in Figure 1.6. Placing a malicious FBS in a desired location will not only deceive a mobile UE to perform an HO to it, but also cause interference to nearby FBSs.

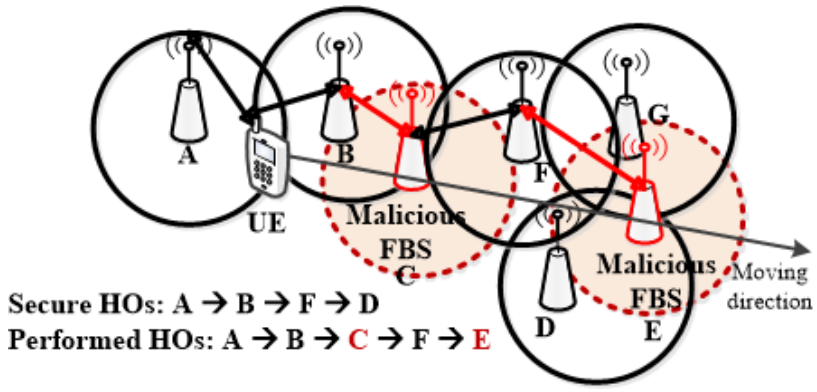

Figure 1.6: A scenario to show the effect of the wormhole attack on HOs.

1.2.3 Security in Femtocell Networks

The deployment of a large number of candidate femtocells each with a small coverage area makes HOs more challenging in open-access femtocell networks than other access modes [129]. As a result, cell selection plays a vital role in open-access femtocell networks. Because of the small coverage area and the random deployment of femtocells, a wrong selection of the target cell may cause unnecessary HOs, service failures, and HOs to malicious femtocells. These result in under-utilization of femtocells, performance degradation of UEs, increase of HO signaling costs, and sacrifice of UEs privacy. However, limited research has been conducted to select a proper target cell during HOs in femtocell networks. Most existing papers in literature are focused on avoiding unnecessary HOs, increasing femtocell utilization, and avoiding service failures [27, 28, 29, 30, 31, 32]. None of these schemes consider the selection of a trustworthy femtocell during HOs.

To demonstrate how existing algorithms cannot avoid malicious femtocells, we consider an open-access femtocell network consisting of n_f number of femtocells within the coverage area of a macrocell network. The FBSs are deployed inside apartments or offices which are located by the side of a road. A UE moves straight along the road with a constant speed. The deployment scenario is shown in Figure 1.7. We also consider m_f number of malicious FBSs randomly placed within the network. A

UE is able to access any femtocell whenever it is within the coverage area and meets the condition for HOs.

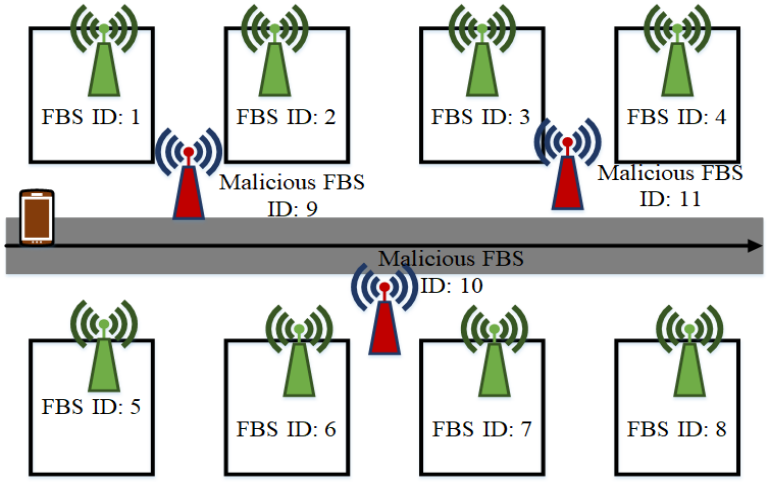

Figure 1.7: An open access femtocell network with malicious femtocells.

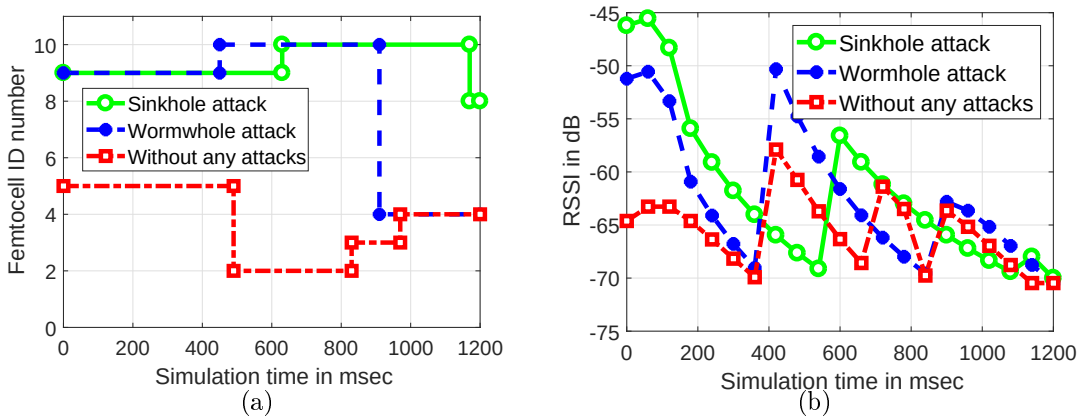

Figure 1.8: Effect of different attacks in HO-decision making.

To implement the sinkhole attack, we assign a high transmission power to malicious FBSs. On the other hand, malicious FBSs are placed randomly in the wormhole attack without changing any other parameters. We first observe HOs using simulations when a traditional target cell selection scheme is used based on the maximum RSS. The simulated result is shown in Figure 1.8. In the figure, both the selected target FBS IDs and their received signal strength indicators ($RSSI$s) are shown. The ITU-RP.1238-7

path-loss model [33] is used to determine the $RSSI$ from femtocells as:

$$RSSI = P_{tx} + G_f + G_u - PL, \tag{1.1}$$

$$PL = 20log_{10}(f) + Nlog_{10}(r_f) + L_f(n) - a(n), \tag{1.2}$$

where the carrier frequency $f = 1700$ MHz assuming that the femtocell operates on the LTE radio spectrum, r_f is the radius of a femtocell, N is the distance power coefficient, L_f is the floor/wall penetration loss, $a(n)$ is the shadow fading, and n is the number of floors/walls. We deploy three malicious femtocells with IDs 9, 10, and 11. The figure shows that in presence of attacks, a UE tends to perform HOs to malicious femtocells (which are 9 and 10).

Therefore, in open-access femtocell networks, selecting a trustworthy target cell is a unique issue for handoff management. Unlike traditional cellular networks, attackers can get physical access to femto base stations (FBSs) and perform a number of attacks utilizing these FBSs which may allow them to eavesdrop on user data, change software and configuration of FBSs, and inject false information to user data [34, 35, 36]. Existing target cell selection and HO decision algorithms use parameters, such as received signal strength (RSS), user's speed, and capacity of FBSs. Unfortunately, these parameters are not sufficient for a UE to differentiate malicious femtocells from secure femtocells. Therefore, selecting a trustworthy target cell during HOs is an important issue in open-access femtocell networks. Moreover, existing solutions to avoid these attacks in femtocell networks cannot be directly used in the HO scenario due to some strong assumptions.

1.2.4 Mobility Management in CR Femtocells

To support seamless traffic offloading, when an active user moves towards a femtocell, it is desirable that the user is handed off to the femtocell. On the other hand, while an active femtocell user (known as FUE) moves out of the femtocell coverage

area, it should be handed off to the macrocell in order to avoid service disconnection. Therefore, mobility management is a very important issue in femtocell networks [18]. Besides the existing challenges in traditional femtocell networks, such as transmission power difference and interference, adding cognitive capabilities to FBSs introduces more challenges in mobility management. Choosing channels from heterogeneous frequency bands is one of them. Each frequency band has different path-losses, transmission rates, channel-error rates, etc. Though heterogeneous channels are considered in spectrum sharing [37, 38, 39, 40] and spectrum handoffs (HOs) [41, 42, 43, 44, 45] in traditional CR networks, mobility management and the effect of heterogeneous channels on mobility management are never considered in CR femtocell networks.

The impact of spectrum heterogeneity in CR femtocell networks is investigated in this section. Heterogeneous spectrum have very different path-losses which may result in significantly different transmission ranges. The relationship between the transmission ranges (shown as coverage radius) and transmission frequencies under a *constant transmission power* is shown in Figure 1.9. In the figure, we use the ITU-RP.1238-7 indoor path-loss model [33] and assume that the cell coverage is defined as the region in which the received signal strength indicator (RSSI) is greater than the RSSI at the cell boundary of traditional femtocell networks. From the figure, it is shown that the cell coverage reduces drastically at high frequencies due to poor propagation.

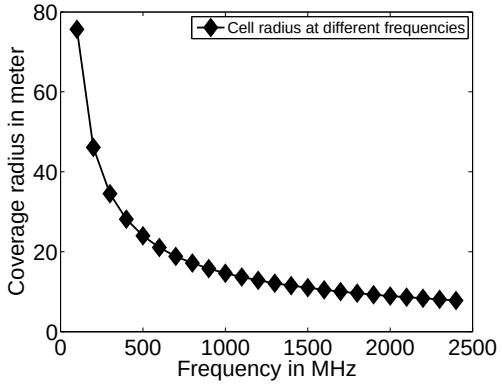

Figure 1.9: Transmission coverage under different transmitting frequencies.

Choosing channels from heterogeneous frequency bands during spectrum handoffs introduces unique challenges in CR femtocell networks. These challenges are caused by the change of two different ranges during a spectrum handoff. First, there are challenges caused by different transmission ranges. Each frequency band has different path-loss, therefore, a different transmission range for a *constant transmission power*. This difference in transmission ranges introduces two new issues in CR femtocell networks. When the operating frequency of a CR FBS changes from a low frequency to a high frequency, the coverage area of a CR femtocell shrinks due to larger path-loss at the high frequency. As a result, a number of FUEs within the uncovered area will either lose their connections or be forced to perform inter-cell handoffs. Therefore, the femtocell utilization becomes low. However, as CR femtocells are deployed to offload traffic from macrocell networks, low femtocell utilization is undesirable. On the other hand, when a CR FBS changes its operating frequency from a high frequency to a low frequency, its coverage area expands due to smaller path-loss at low frequencies. This expanded area can support more FUEs. However, this coverage area expansion can also cause interference to neighboring CR FBSs and their FUEs.

How this change of coverage area caused by spectrum heterogeneity affects the mobility management of FUEs during inbound HOs and outbound HOs is shown in Figure 1.10. In this figure, we use two transmission ranges to show the effect of heterogeneous channels. When a user (FUE_1) connecting to a macrocell moves towards a femtocell, the moment a macro-to-femto HO should be triggered depends on the channel availabilities. If the CR FBS chooses a low operating frequency for the FUE (which means that the coverage area of the femtocell is large due to a weak path-loss), the HO will be triggered early (at point A) if using a fixed HO-threshold. This early HO can enhance the femtocell utilization. However, this can also cause a number of unnecessary HOs at the cell boundary. On the other hand, if the CR FBS chooses a high operating frequency for the FUE, the coverage area of the femtocell

will be small. As a result, the HO should be triggered late (at point B). This late HO may lead to a low femtocell utilization. Although a proper channel selection algorithm can overcome these problems, it is possible that the selected proper channel might not be available at a certain time.

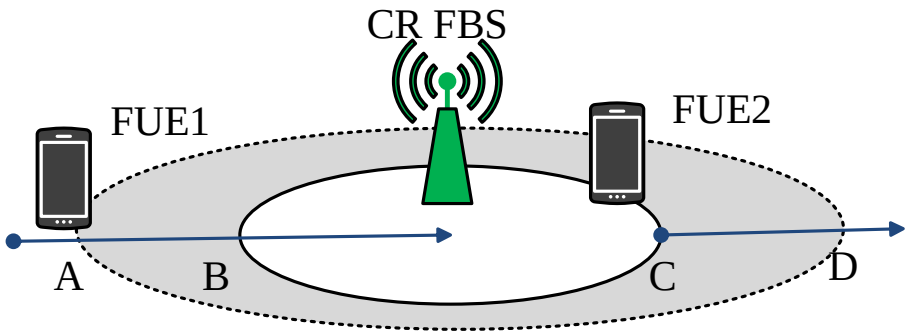

Figure 1.10: Effects of heterogeneous channels on mobile FUEs.

Similarly, when a user (FUE_2) moves out of a femtocell to a macrocell, either the femtocell utilization becomes low in the case of a high operating frequency or the probability of interference and unnecessary HOs is high in the case of a low operating frequency. To improve the femtocell utilization, a spectrum HO to a low frequency channel can be triggered (at point C). However, this spectrum HO may cause a high HO delay because of the additional sensing and channel switching delay. Another approach is the power control. However, increasing transmission power of the CR FBS can also increase the probability of interference to PUs and neighboring femtocells which are using the same channel. Moreover, a CR FBS may select different frequency channels at the same time. As a result, it is difficult for a CR FBS to adjust its transmission power for each frequency channel separately. Therefore, we propose an adaptive HO-threshold selection scheme which considers the probability of interference from PUs and neighboring femtocells to address these issues and design an analytical model based on this.

Second, there are challenges caused by different sensing ranges. The sensitivity

that a SU can detect the existence of a PU also depends on the path-loss between a PU and the SU (i.e., CR FBS in CR femtocell networks). Therefore, for a given detection sensitivity, the sensing area of a CR FBS also changes with the change of the operating frequency. This change of sensing range can introduce two new issues in CR femtocell networks. When a CR FBS senses a frequency higher than its operating frequency, the sensing area becomes smaller than the transmission area due to high path-loss. As a result, if there is any PU within the transmission area that is not covered by the sensing area, it cannot be detected and the CR FBS may cause interference to this PU. Similarly, when the CR FBS senses a lower frequency channel than its operating frequency, the sensing area expanded. Therefore, the CR FBS may sense some channels as unavailable when they are actually available within its transmission range, thus, cause false alarm.

All of these issues are very important and unique in CR femtocell networks. They have not been considered before. Only very few existing papers have considered the impact of operating frequency change during a spectrum handoff on the transmission range in CR networks [42, 43, 46, 47]. However, the impact is different in CR femtocell networks where FUEs are not cognitive because of the new consideration of femtocell utilization.

1.2.5 Mobility Management in MEC

1.2.5.1 Service Migration and Mobility Management in MEC

As mobile devices are resource constrained (limited computational resources and energy), offloading computation tasks to the remote cloud has become one of the most promising solutions to support energy-hungry mobile and Internet of Things (IoT) applications [13]. However, the remote execution of these offloaded applications to the cloud may not always fulfill the delay requirements. Therefore, mobile edge computing (MEC) is introduced recently to bring computational resources and storage closer to end users in order to reduce these delays [48, 14]. MECs are usually deployed with

cellular base stations (BSs), e.g., macrocells and small cells.

However, the deployment of MECs with cellular BSs introduces new research challenges in mobility management. First, as MECs are deployed with BSs, a MEC can only be accessed within the coverage area of that BS. Therefore, when a user equipment (UE) moves out of the coverage area of a cellular BS, it needs to not only perform a radio handoff (HO), but also perform a migration of the offloaded service. Second, unlike the remote cloud, MECs have limited resources. As a result, sufficient resources might not always be available at the target MEC. Therefore, when a UE moves out of the cell coverage area, it needs to find a target BS with both sufficient radio and computational resources at the MEC. However, since the serving BS cannot get the information of the available resources of the target BS until the UE is connected to the target BS, and as the migration and HO issues are never considered together, the migration decision is made after the UE has completed a radio HO in the traditional system. Therefore, in the traditional system, the UE may again need to find a new BS after performing a radio HO to a target BS without any available computational resources at its MEC, which causes unnecessary HOs and adds additional delay at the user's end. Moreover, different offloaded services have different migration requirements. For example, an offloaded video streaming needs immediate service migration when the UE moves out of the coverage area of the MEC. All these issues are more severe when MECs are deployed with small cells, e.g., femtocells.

Existing work on mobility management in MEC only considers the issues of performing service migration and reducing the migration delay. These existing works are mainly focused on designing mathematical models and migration decisions based on the prediction of a user's future status. However, they may cause a large overhead in the network and the prediction of a user's future information is not practical to access. On the other hand, the radio HO and service migration issues are never considered together in MEC. Moreover, the extra signaling cost introduced by the unnecessary

HOs are never analyzed. Therefore, a migration decision algorithm incorporating the radio HO decision is necessary to avoid extra signaling cost.

In the traditional MEC-deployed femtocell networks, when a UE moves out of the coverage area, it performs an HO and connects to a new FBS. As a result, the UE also moves out of the direct connection of the serving MEC, and the offloaded service also needs to be migrated to a new MEC associated with the new FBS. Each time a UE performs an HO, a service migration is required. However, it usually take a long transfer time to perform a migration. Moreover, the migration delays vary based on the type of the service that needs to be migrated. Sharing a MEC can reduce the number of migrations. The migration scenarios for the traditional and the proposed (which is described in Section 5.1.1) MEC-deployed femtocell networks are shown in Figure 1.11.

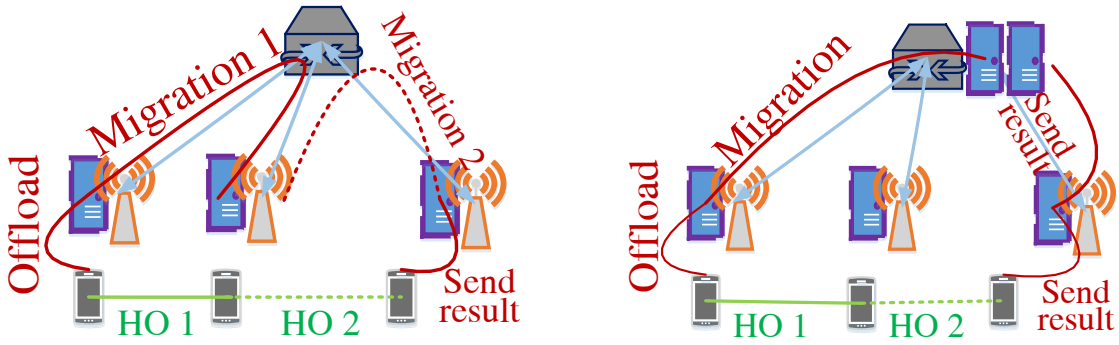

(a) Traditional network (b) Proposed network

Figure 1.11: Comparison of migration scenarios in the traditional MEC and the SharedMEC-deployed femtocell networks.

Additionally, simulation results showing the total number of migrations for both networks are presented in Figure 1.12. In the figure, it is shown that the proposed model can reduce the number of migrations. Moreover, as the number of migrations is lower in the proposed network, it can also reduce the total cost. Furthermore, since the target MEC is predetermined, the necessary information for a service migration can be collected during the HO signaling period. Therefore, the migration signaling

cost can also be reduced.

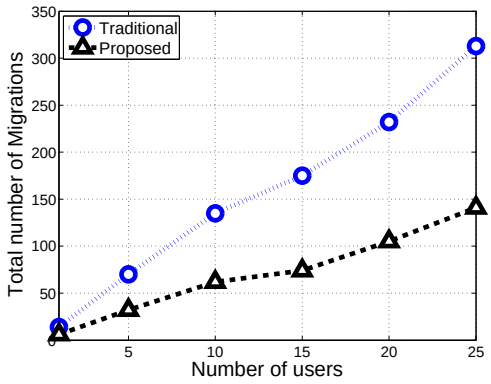

Figure 1.12: Comparison of the number of migrations.

1.2.5.2 HO and Offloading in MEC

Though both cloudlet and MEC are introduced to bring cloud closer to users to reduce the delay of offloading and to provide computational resources and storage to nearby mobile users [48, 49, 14, 50], there are differences between cloudlet and MEC. Cloudlet covers a small region which can be accessed only through Wi-Fi [15]. On the other hand, MEC enables end users to access cloud computing services within the range of Radio Access Networks (RAN), and each MEC is usually deployed with a cellular base station (BS) [14, 15].

However, the deployment of an edge cloud with a BS introduces new research issues. First, though offloading computation tasks to the MEC solves the problem of limited resources and delay requirements, it introduces a new issue in wireless networks. Since mobile users use wireless channels from the macro BS to offload computation tasks to the MEC, they create new traffic to the cellular network. Cellular networks are already crowded with the increased data and voice traffic. Therefore, how to manage the excess traffic becomes an important issue. Second, unlike the remote cloud, the MEC has limited computational resources. How to efficiently assign these limited computational resources is another foremost issue. Third, if the allocation of radio resources and computational resources is not considered jointly, the congestion

of computational resources may lead to the waste of radio resources and vice versa. Fourth, unlike in traditional cellular networks, the mobility of users triggers handoffs (HOs) not only between two BSs but also between two MECs. How to migrate unfinished-computation due to mobility is another critical issue.

Although research has been conducted on resource allocation and offloading decision in MEC systems, the mobility management issues have been utterly ignored. First, most of the papers on resource allocation in MEC systems only consider computational resource allocation. Only a few of them have considered both radio and computational resources together. However, in these papers, the available resources are assumed to be used by users only with computation traffic, which is not true because both communication and computation traffic need the radio resources to perform their operations, and delay-sensitive communication traffic should have a higher priority than the computation traffic. For example, a user with a voice call should be given a higher priority than a video game player. Moreover, the mobility management issue, e.g., HO, is not considered in all of these resource allocation papers. In addition, the HO issue is also ignored in existing papers when designing computation offloading decisions. An offloading decision without considering users' mobility may cause an offloading failure. Similarly, an HO decision without considering offloading decisions may cause a number of unnecessary HOs. Moreover, existing HO decision algorithms for traditional cellular networks cannot be directly applied to the MEC system because, in MEC systems, the radio connection from a user to both the BS and the MEC changes when the user moves out of a cell. As a result, the user has to perform an HO to a target BS with an MEC which has enough computational resources to perform the rest of the computation.

The above issues have a high impact on MEC systems and are the motivations of our research. If radio congestion in MEC systems is not addressed, all available radio channels may be assigned to the users only with communication traffic. This may lead

to the waste of computational resources at the MEC. Furthermore, any computation offloading may fail due to the unavailability of radio resources. Similarly, without a proper HO decision algorithm, a mobile user may perform HOs to a target cell following a traditional HO decision algorithm and fail to migrate the offloaded data if the needed computational resources are not available at the new MEC.

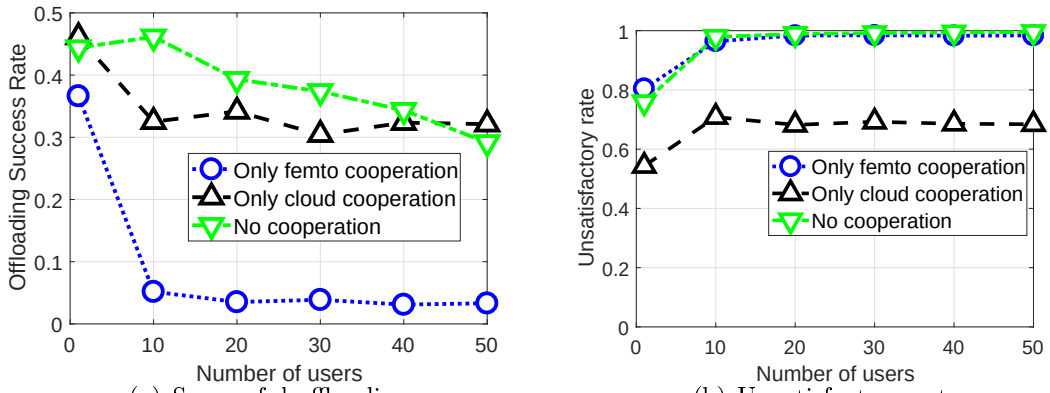

(a) Successful offloading (b) Unsatisfactory rate

Figure 1.13: The rate of successful computation offloading and user's unsatisfactory rate.

In order to illustrate the effect of applying traditional HO decision algorithms to MEC systems, we have conducted simulations of an MEC system. Based on the simulation results, the rate of successful computation offloading and user's unsatisfactory rate are shown in Figure 1.13 with respect to a different number of users. From the figure, we observe that traditional HO decision algorithms, even with radio offloading to femtocells and offloading with the cooperation of the remote cloud, can only offload less than 50% of the requested computation traffic successfully and have a high unsatisfactory rate. This indicates a large number of offloading failures. Therefore, we need a new HO decision algorithm along with proper offloading decisions to address the issues causing these offloading failures.

1.3 Overview of the Proposed Research

Figure 1.14 shows the overview of the proposed research. Two HO decision schemes along with an analytical model for HO signaling cost and a secure target cell selection scheme are proposed for femtocell networks. In addition, a power control scheme and a mobility management scheme are proposed for CR femtocell networks. Furthermore, a joint HO and offloading decision scheme is proposed for MEC integrated with femtocell networks. These adaptive schemes are proposed to address some unique and practical issues regarding users' mobility in small cell networks.

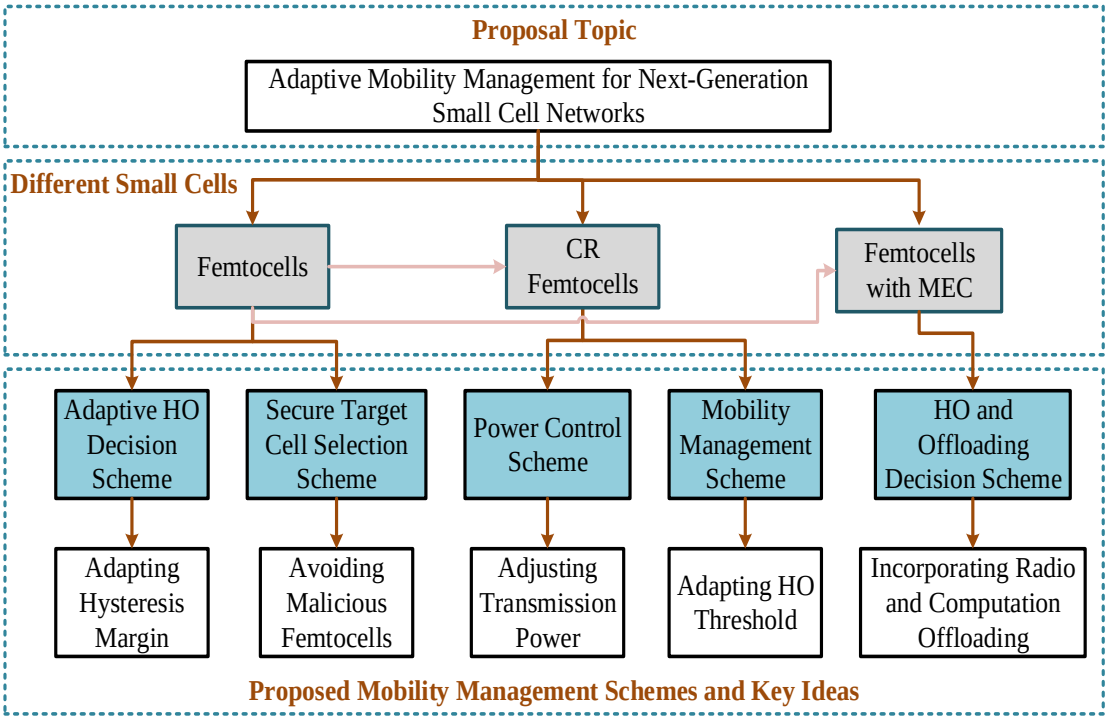

Figure 1.14: The overview of the proposed mobility management schemes.

First, a self-adaptive HO-decision algorithm is proposed to address the unique issues of both macro-to-femto and femto-to-macro HOs. The hysteresis margin (HM) of our algorithm can adapt not only with the deployment environment, but also with the mobility pattern of the user. The proposed algorithm is intelligent enough to set the HM to a proper value based on the history of previous HOs. A database

is proposed to contain the location fingerprinting of a user who has requested HOs before. The location fingerprinting is taken from the measurements of the neighboring femtocells. The goal of this self-adaptive HO-decision algorithm is to reduce the rate of unnecessary HOs and service failure, and at the same time, increase the cell utilization. Then, an analytical model is proposed to study the HO signaling cost of different HOs in open-access femtocell networks. In addition, previous work in [22] is extended to propose a target cell selection method and to propose HO decision algorithms that can reduce unnecessary HOs without increasing HO signaling costs and sacrificing the femtocell utilization. Finally, the HO signaling cost of existing HO decision algorithms are compared in femtocell networks.

Next, possible attacks on femtocell networks are discussed during an HO process. These are: sinkhole attack and wormhole attack. Then, the effects of these attacks on the HO decision are discussed in open-access femtocell networks. Finally, a target cell selection and HO decision scheme are proposed which help a UE to select a secure target femtocell during an HO. As the attacks are unlike in nature, it is very hard to come up with a single solution which can avoid both attacks. The received signal strength indicator (RSSI) and location database of FBSs are used to select a target cell in a way that the probability of HOs to a malicious femtocell is reduced without increasing the HO signaling cost significantly.

Then, a power control scheme and a detection sensitivity selection scheme are proposed to address the issues of channel heterogeneity. The proposed power control scheme is equally effective on addressing both the femtocell utilization problem and interference problem. Similarly, the proposed detection sensitivity scheme helps to reduce both the detection error and false alarm caused by sensing frequency changes. Both of the proposed schemes are easy for implementation. Simulation results show better performance of our proposed schemes, as compared to conventional CR femtocell networks.

Furthermore, the impact of channel heterogeneity on mobility management is considered in CR femtocell networks and propose a novel mobility management scheme for both inbound (macro-to-femto) and outbound (femto-to-macro) scenarios. In this scheme, some unique challenges caused by the channel heterogeneity are addressed and the use of a HO-threshold adaptation is proposed which considers the probability of interference from both primary users (PUs) and other CR femtocell networks. In this way, the proposed scheme is able to provide seamless offloading with reduced HO time and at the same time, enhanced femtocell utilization without interfering any PU or any neighboring FBS. The HO-threshold is adapted in a way that it can adjust the femtocell coverage area. This coverage area adjustment is challenging, because the CR FBS can only sense within its sensing area and when the coverage area expands with an increased transmission power, it cannot extend the sensing area. As a result, the CR FBS and its users can be affected by the interference from PUs and neighboring CR femtocells. In order to cope with this interference, a threshold-based adaptive HO scheme is proposed. An analytical model is proposed to calculate the probability of interference from PUs and neighboring CR FBSs and integrate this model to adapt the HO-threshold.

Last but not least, A new HO decision algorithm is proposed for MEC systems. The proposed algorithm is designed in a way that it can improve the Quality-of-Service (QoS) for both radio access networks and MEC systems. Both *radio offloading* and *computation offloading* decisions are incorporated in our proposed HO decision algorithm. The *radio offloading* is incorporated to reduce the effect of increased traffic in cellular networks due to the addition of computation traffic. This offloading allows users to perform HOs to a proper small-cell network, e.g., femtocells, to avoid traffic congestion [51]. In addition, in the proposed HO decision algorithm, different priorities for users are considered to better serve the delay requirement and user mobility. The cooperation with the remote cloud is also considered to reduce the

offloading failure rate. The proposed HO decision algorithm can increase the rate of successful computation offloading, reduce the rate of offloading failure, and reduce the computational migration costs.

1.4 Proposal Organization

The rest of the research is organized as follows. In Chapter 2, related work on the proposed research is introduced. In Chapter 3, two HO decision schemes, an analytical model for HO signaling cost, and a secure target cell selection scheme are presented to address the issues in femtocell networks. A power control scheme and a mobility management scheme for CR femtocell networks are proposed in Chapter 4. In Chapter 5, a service HO decision scheme and a joint HO and offloading decision is proposed for MEC deployed femtocells. Following that, the publications and remaining work are listed in Chapter 6.

CHAPTER 2: RELATED WORK

In this chapter, existing research on HO decision schemes, HO signaling cost analysis, and security in femtocell networks is discussed followed by the existing work on mobility management in CR femtocell networks. Additionally, existing work on mobility management in MEC is mentioned at the end of the chapter. Research approaches to solve these issues and their shortcomings are also described in this chapter.

2.1 Existing Research on HOs in Femtocell Networks

The problems addressed by existing research on HOs in femtocell networks include transmission power difference between MBS and FBS [52, 53, 54, 55], frequent and unnecessary HOs [56, 57, 58, 59, 60, 61, 62, 19, 63, 64, 65], selecting the target cell for HOs [66, 59, 64, 65], HO failure rate [57, 67], interference [55, 68, 57], energy saving strategy [69, 70], HO delay/cost minimization [24, 57], and ping-pong effects [71, 72, 73]. The power difference between FBS and MBS during an inbound (macro-to-femto) HO is considered in [52, 53, 54, 55]. In [52] and [53], a combination factor is proposed to compensate the power asymmetry in a way that the UE will be correctly assigned to a femtocell while maintaining the number of HOs at the same level. A window function is also proposed to prevent the RSS from varying abruptly. However, the abrupt signal drop cannot be ignored in real indoor scenarios. It is claimed in [54] that only considering this combination factor may increase the rate of unnecessary HOs. Therefore, another parameter, transmission loss, is proposed in [54] for HO decision-making. A cost-effective HO-decision algorithm is proposed in [55] considering the power discrepancy which will be discussed later.

Most of the existing works on HO decision in femtocell networks are focused on minimizing the unnecessary HO rate due to the dense femtocell deployment and small cell radius [56, 57, 58, 59, 60, 61, 62, 19, 63, 64, 65]. A mobility prediction method to predict the mobility pattern of a user, which is used to select the proper cell to HO, is proposed in [56, 64, 65]. The mobility prediction is based on the current mobility-history of a user. Different parameters, such as user's velocity, RSS, and traffic type are considered for HO decision-making in [58, 59, 57]. In addition, call admission control (CAC) is used in [60] and [62] for HO decision-making. A waiting time with a SINR threshold is proposed in [61] to avoid unnecessary HOs. Adaptive techniques to eliminate unnecessary HOs in femtocell networks are considered in [19, 63]. An adaptive HM is proposed based on the distance between a UE and a BS to avoid unnecessary HOs in [19]. The efficiency of two HO elimination techniques, i.e., windowing and HO delay timer are investigated in [63]. Both techniques are modified for femtocells based on the distance between a UE and the serving BS. In conclusion, existing works on eliminating unnecessary HOs consider user's speed, traffic type, waiting time, mobility pattern prediction, and distance-based adaptive HM for HO decision-making.

Another problem of making a HO-decision in densely deployed open-access femtocell networks is how to select the target cell properly. Large number of femtocells may create a long neighboring cell list and selecting a wrong target cell may cause unnecessary HOs. To overcome this problem, mobility-prediction is used to select a proper target cell [66] or to make an effective neighboring cell list [66, 59, 64, 65]. [66] considers that knowing the current position can help us know where a UE is going, which can later help to select the target cell. As described previously, [59] tries to avoid the long neighboring cell list problem in order to eliminate unnecessary HOs by considering user's speed and traffic type. A mobility-history database is proposed in [64, 65] which contains a list of target cells where users are recently handed over.

A few works have addressed the interference problem during an HO. Intracell HO (IHO) is considered in [55, 68, 57] to avoid the cross-tier interference. A cost-function based on the available bandwidth of the target cell is proposed in [57] to provide better QoS to users by reducing interference.

Along with these main issues, some other issues are also addressed, such as to avoid the HO failure rate which is one of the biggest challenges for designing a HO-decision algorithm [57, 67], to minimize the HO cost [24, 57], and to provide cost-effective service to users [74]. An intelligent HO management is proposed in [69] for energy efficient green femtocell networks and [70] works on reducing power transmission at the UE side by adapting the HM suitably with respect to the SINR from the target cell and the standard LTE measurements.

The location-based HO-decision algorithm for different small cell networks is discussed in [64, 65, 72, 73, 75, 76]. As described earlier, [64] and [65] keep the mobility-history of users to predict the target cell in small cell networks. Here, location is used to set the target cell and to minimize the HO delay. User's mobility and location are also used to provide better service during a HO. Geographical fingerprint for HOs are considered in [77, 78], where location-fingerprint is obtained using artificial neural networks. This fingerprint is used to select the target cell and neither a GPS nor a sensor is used.

2.2 Existing Research on HO Signaling Cost Analysis in Femtocell Networks

Though a number of papers on HO decision algorithms are available in the literature [18], only a few of the existing works consider the HO signaling cost in femtocell networks [23, 79, 24]. An architecture for LTE femtocell networks which introduces an intermediate node (HeNB GW) is presented in [23]. Two methods for mobility management are proposed in this research. In the first method, the HeNB GW acts as a mobility anchor to control HOs among femtocells, and it works as a relay in the second method. An analytical model to evaluate and compare HO signaling costs of

these two methods are described here. However, not all HO scenarios are considered. In [79], an HO decision algorithm based on users' speed and traffic types is discussed. The signaling procedure for both macro-to-femto and femto-to-macro HOs are also presented in this paper. A simple HO decision algorithm for the macro-to-femto HO scenario that considers users' speed is discussed in [24]. The HO signaling cost is also analyzed for this HO scenario, and the proposed algorithm is compared to a traditional HO decision algorithm. Both of the papers [23, 24] analyze the HO signaling cost for a simple general scenario. For example, a femto-to-femto HO scenario is considered in [23], and a macro-to-femto HO scenario is discussed in [24]. However, the rest of the HO scenarios in the open-access mode have not been considered.

2.3 Existing Research on Security in Femtocell Networks

Existing works on HOs in femtocell networks are rich. They are mainly focused on HO decisions in femtocell networks. A summary of these HO decision algorithms can be found in [80]. In open-access networks, target cell selection plays a vital role during the HO decision phase. Existing research on target cell selection is mostly on avoiding unnecessary HOs, increasing femtocell utilization, and avoiding service failures [27, 28, 29, 31, 32]. However, none of them considered the effects of attacks in femtocell networks. Therefore, research on selecting a trustworthy target cell during HOs is still being uncovered. Moreover, existing target cell selection algorithms are based on the RSS from neighboring cells, user's speed, the frequency of the serving FBS, and the capacity of FBSs. However, all of these parameters can be falsified by an attacker after gaining root-access to the FBS [34, 35, 36]. Therefore, only considering these parameters are not enough to select a trustworthy target cell.

On the other hand, though security issues of femtocell networks have been studied, most of these studies focus on security analysis and possible attacks of femtocell networks [81, 34, 35, 36, 82]. Only a few of them discuss possible solutions. The solution in [81] assumes that mobile operators have to decide where and how many

FBS to install when planning a cellular network. However, in practice, femtocells are deployed randomly by users. Another solution proposed in [25] cannot be applied in HO scenarios because it assumes that the UE has to be in a no-signal zone. In addition, though the attacks in femtocell networks are similar to the attacks in wireless sensor networks and ad-hoc networks, solutions of those networks cannot be applied to femtocell networks because those solutions require communications and time synchronization between nodes, which are not practical in femtocell networks, and communications through the macrocell will cause high latency.

2.4 Existing Research on Heterogeneous Spectrum and Mobility Management in CR Femtocell Networks

Existing work on CR femtocell networks is mainly focused on addressing the problem of interference, spectrum allocation and management, and spectrum sharing. Almost no existing paper has considered the effect of operating frequency changes during spectrum handoffs. Additionally, although research on spectrum handoffs is rich in conventional CR networks, only a few papers have discussed the issues of the frequency change in CR networks during spectrum handoffs.

Effects of heterogeneous spectrum during spectrum handoffs in pure CR networks are considered in [42, 43, 46]. The problem of cell outage during a low frequency to a high frequency change is discussed in [43]. Performing inter-cell handoffs is considered as a solution for overcoming this cell outage issue. However, though a low frequency to a high frequency change has similar effects in CR femtocell networks, the proposed solution cannot be used in CR femtocell networks. The reason behind this is the femtocell utilization. If FUEs perform inter-cell handoffs, CR femtocells will have low cell utilization, therefore, low traffic offloading, which is not desirable in CR femtocell networks. In addition, an optimal operating frequency selection scheme is proposed in [46]. However, choosing a different frequency channel other than the operating channel may cause cell outage or interference problems, which is

not considered in the paper. In [42], a cross-layer protocol for spectrum mobility and handoff is proposed for CR ad-hoc networks. This protocol considers when and how to make a decision for a spectrum handoff and an inter-cell handoff. The effect of the coverage range expansion is studied in [47] for femtocell networks. However, the infrastructure-based CR femtocell network needs further investigations to address the issue of frequency change in order to provide good cell utilization and at the same time to avoid interference to neighboring CR FBSs and FUEs. Moreover, none of the existing work considers the effects of frequency changes on the sensing range.

Existing work on CR femtocell networks is mainly focused on addressing the problem of spectrum sharing, resource allocation and management, interference avoidance, and power control. There is almost no existing work on mobility management in CR femtocell networks. Works on spectrum sharing take energy efficiency [11], dense deployment of femtocells [83], power allocation [84], and spatial reuse gain [85] into account. In addition, resource allocation and interference are considered together in CR femtocell networks [9, 86]. However, none of these existing work considers channel heterogeneity in CR femtocell networks. Additionally, although research on mobility management in traditional femtocell networks is rich, mobility management in CR femtocell networks still requires further investigations. All of the mobility management works in femtocell networks are designed to avoid frequent and unnecessary HOs, to reduce HO failure rate, and to minimize ping-pong effects [18, 22]. None of these techniques are suitable for CR femtocell networks when considering the channel heterogeneity.

In pure CR networks, the impact of heterogeneous channels on spectrum sharing and spectrum HOs is investigated in [37, 38, 39, 40, 41, 42, 43, 44, 45]. The energy constraint for heterogeneous channels during spectrum access is discussed in [38] where authors propose two schemes for spectrum allocation by taking propagation conditions of channels into account. A spectrum sharing algorithm based on

spectrum heterogeneity is presented in [39] where users are free to move and they perform channel HOs during multi-hop communications. In addition, the effects of heterogeneous spectrum during spectrum HOs in CR ad-hoc networks are considered in [43, 44, 45] where SUs are mobile. However, the CR femtocell network, which is an infrastructure based CR network, needs further investigations to address the issue of channel heterogeneity to support a number of mobile users which do not have cognitive capability.

2.5 Existing Research on Mobility Management in MEC

Though various issues have been well investigated in the MEC system, the mobility management issue still needs further investigation to ensure low signaling and migration cost [87]. The solutions for supporting mobility in MEC are categorized in three groups: power control [88], virtual machine (VM) migration [89, 90, 91, 92, 93, 94, 95, 96, 97, 98, 99, 8], and the selection of a new communication path between a UE and the MEC server [100, 101].

Power control solutions are considered for closed-access femtocells with computing capabilities. In these solutions, a power control algorithm is proposed to temporarily adjust the coverage of a femtocell in order to support mobile users [88]. The assumptions of these solutions are: femtocells can coordinate their transmission power and each femtocell supports only one user. Additionally, in these existing algorithms, the transmission power is controlled to adjust the coverage area in a way that the user is under the cell coverage until the offloaded computation is done and the result sends back to the user. However, FBSs cannot communicate with each other, and only considering one user per cell is not realistic. Moreover, existing solutions can only be applicable to low-speed indoor users who do not intend to leave home. However, other access modes of femtocells and users with an intention to leave home also need to be supported.

In VM migration solutions, existing works are mainly focused on designing mathe-

matical models for different MEC systems, e.g., Follow-me cloud [89, 90] and software clone (Avatar) of cloudlets [91]. Furthermore, an optimal threshold is calculated in the threshold-based solutions [92, 95]. However, a complete framework or protocol design for VM migration is missing. On the other hand, prediction is considered in [93, 94], where the mobility path of a UE and the time window to travel a road segment are assumed to be known before making a migration decision. However, these prediction-based VM migration solutions require future information about a user's location, movement, etc. This information is random and not easy to obtain. Besides, using this information and a large calculation to make a migration decision may cause a large overhead at the network. Moreover, even a modest mobility can result in a significant network degradation [97, 96].

Path selection and/or VM migration solutions worked on the selection of the most appropriate way between a UE and an edge cloud [100, 101]. Though this is like the routing decision in wireless sensor networks (WSNs), in WSN, the nodes can communicate with each other. However, FBSs need to communicate via a backhaul in MEC, which will cause a delay in communication. On the other hand, the lowest delay path selection cannot always guarantee seamless service migration or fulfill the delay requirement of a service. In addition, the path is selected without any knowledge of the available computation resources, which can cause unnecessary HOs. After this discussion, we can observe that all the existing VM migration and path selection solutions are only focused on the migration issue. The HO and migration issues are not considered together.

2.6 Existing Research on Offloading Decisions in MEC

Existing work on computation offloading for MEC systems is mainly focused on resource allocation and offloading decision. First, some papers on resource allocation have considered both radio and computational resource allocation [102, 103, 104]. The computational resources, e.g., the CPU time of virtual machines (VMs), are

distributed among the users who request for computation offloading. On the other hand, different scheduling algorithms are designed to allocate radio resources among users to ensure a better computation offloading. However, if radio and computational resources are considered separately in the MEC system, the congestion of computation traffic may lead to the waste of the radio resources and vice versa. Therefore, a few papers recently propose to consider radio and computational resources jointly [105, 106, 107]. However, these joint resource allocation papers are mainly focused on the congestion at the cloud side. The congestion in the radio network is being ignored. In cellular networks, congestion introduces a new offloading issue called *radio offloading*, where the cellular network offloads some of its traffic to different heterogeneous small-cell networks (e.g., Wi-Fi and femtocells) in order to reduce the radio congestion.

Second, existing papers on offloading decisions are mainly focused on whether to offload a computation task to the remote/edge cloud or to perform the computation locally based on the energy consumption of mobile devices [102]. In these papers, the cloud resources are assumed to be unlimited. Therefore, the impact of unavailable computational resources in MEC systems is not considered. Although some papers consider the cooperation between the local and the remote clouds to overcome this issue [108, 109], those offloading solutions cannot be directly applied to the MEC system because of the negligence of radio resources.

Finally, although the mobility issue has been considered for remote cloud computing and other types of computation offloading, it is not yet considered in MEC systems [110, 111, 112, 113]. Moreover, the mobility issue for the remote cloud and the mobile cloud is mainly focused on seamless HOs between different radio networks, which is the same as the HO issue in heterogeneous wireless networks. These existing HO decision algorithms cannot be directly used in MEC systems because they neglect the effects of computational resources. On the other hand, although some mobility-aware offloading

decision papers propose to let users make decisions on how to divide computation tasks based on users' mobility pattern, none of these solutions are suitable for MEC systems except the issue of computation migration [114]. The reason is that if the offloaded computation task is divided among MECs based on users' mobility, MECs cannot send back the computation result to the user as it is moving out of the current coverage area.

Observing these related work and unsolved issues, we can claim that the HO issue in MEC systems considering both radio and computation offloading has never been investigated before. Moreover, the issue of radio congestion in MEC systems is being unsolved.

CHAPTER 3: PROPOSED ADAPTIVE MOBILITY MANAGEMENT SCHEMES FOR FEMTOCELL NETWORKS

An HO decision algorithm for closed-access femtocell networks and an HO decision algorithm for open-access femtocell networks are described in this chapter. In these HO decision algorithms, the HM is adapted based on the history of previous successful HOs. Later an analytical model to analysis the total HO signaling cost is presented. The analytical model is designed based on different HO scenarios available in femtocell networks. Finally, a secure target cell selection scheme is presented in Section 3.4. In this scheme, a target cell is selected in a way that users can avoid malicious femtocells.

3.1 Proposed HO Decision Algorithm for Closed-Access Femtocells

In this section, the proposed self-adaptive HO decision algorithm for both macro-to-femto and femto-to-macro HOs is introduced. The proposed algorithm works in two phases: 1) initialization phase and 2) utilization phase. In the initialization phase, an HO between a femtocell and a macrocell is triggered using the LTE-A system-based HO criteria, and a database is built in this phase. The database contains the location-fingerprint of UEs that are successfully handed over to their target cells. The database is used in the utilization phase to adapt the HM for different UEs. During this phase, the database is updated with new information to handle the ad-hoc nature of femtocells. The notations used in our algorithm are listed in Table 3.1.

Table 3.1: Notations used in the Algorithms for Closed-Access Femtocells

$RSSI_m$	Received Signal Strength Indicator for macrocell
$RSSI_f$	Received Signal Strength Indicator for femtocell
$RSSI_{min}$	Minimum received signal strength indicator for macrocell
Th	Threshold for femtocell
HM_{max}	Optimized value of hysteresis margin
MME	Mobility management entity
FGW	Femto gateway
PCI	Physical cell identity
$RSSI_{fail}$	Minimum received signal strength indicator for femtocells

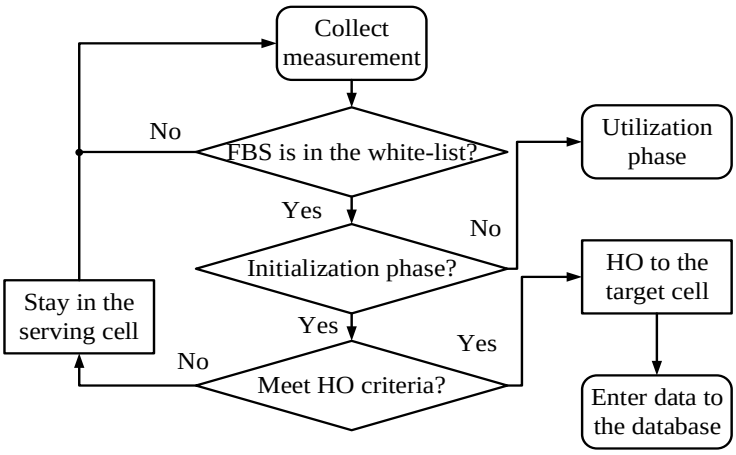

Figure 3.1: Flow chart for the initialization phase.

Algorithm 1: Macro-to-femto HO-decision algorithm

if $RSSI_f > Th$ **or** $RSSI_m < RSSI_{min}$, **and** $RSSI_f > RSSI_m + HM_{max}$ **then**
  HO to femtocell;
else
  Stay in macrocell;
End;

Algorithm 2: Femto-to-macro HO-decision algorithm

if $RSSI_f < Th$ **or** $RSSI_m > RSSI_{min}$, **and** $RSSI_f + HM_{max} < Th$ **then**
  HO to macrocell;
else
  Stay in femtocell;
End;

3.1.1 Initialization Phase

The initialization phase is activated at the time when a new FBS is plugged in. The flow chart for this phase is given in Fig. 3.1. The initialization phase is used to build

up the location-fingerprint database. In this phase, all HOs are performed based on a fixed HM and the measurement report of UEs. In LTE-A, the Radio Resource Control (RCC) protocol manages the events that a UE reports its HO measurement to the serving BS [115]. The measurement includes UE's ID, CSG ID, and available cell IDs (i.e., PCIs) along with their RSSIs. The PCI is not a unique ID for FBS (totally 504 PCIs from 0-503 are available for the LTE-A system). However, we assume that there will be a good distribution of offered PCIs within the coverage area of a macrocell. As shown in the flow chart, this measurement is used to check whether the UE is a registered-user for the closed-access femtocell. The HO process continues for the closed-group users and the HO decision. Whether the algorithm is in the initialization phase or not is determined from the database. An empty database indicates that the algorithm is in the initialization phase and the serving cell makes the HO decision based on the measurement report. The proposed HO algorithms for a macro-to-femto HO and a femto-to-macro HO are given in Algorithm 1 and Algorithm 2, respectively.

The selection of the Th and HM_{max} is explained later in the paper. After a successful HO, the location-fingerprint is entered in the database. We use both the neighboring cell IDs and their RSSIs as the location-fingerprint of UEs. The database has a specific length and the initialization phase ends as soon as the database is full.

3.1.2 Utilization Phase

When the database is full, it will be used for determining the adaptive HM in the utilization phase. Each time a user requests a HO, it sends location-fingerprint with its measurement report. After getting this report, MME (or FGW for femtocell) checks the database to find matches. Suppose the number of similar entries is N_d and the size of the database is d_s. Then the frequency of occurrence (P_{foc}) can be found as

$$P_{foc} = \frac{N_d}{d_s}. \tag{3.1}$$

P_{foc} is used for calculating the adaptive HM (HM_{ad}). A high value of P_{foc} indicates a frequent HO zone. As the frequent HO zones need a lower HM, P_{foc} and HM_{ad} are inversely proportional to each other. Hence, the relationship between them is $HM_{ad} \propto \frac{1}{P_{foc}}$ or $HM_{ad} \propto (1 - P_{foc})$ in dB. Given HM_{max}, the HM_{ad} is

$$HM_{ad} = (1 - P_{foc}) * HM_{max}. \tag{3.2}$$

After calculating the value of the adaptive HM, the serving BS checks the HO decision criteria. The proposed macro-to-femto and femto-to-macro HO criteria are given in Algorithm 3 and Algorithm 4, respectively. The HO is successful if the HO-decision criteria are met and the database is updated. The steps of the utilization phase are shown in Figure 3.2.

Algorithm 3: Macro-to-femto HO-decision algorithm

if $RSSI_f > Th$ **or** $RSSI_m < RSSI_{min}$, **and** $RSSI_f > RSSI_m + HM_{ad}$ **then**
  HO to femtocell;
else
  Stay in macrocell;
End;

Algorithm 4: Femto-to-macro HO-decision algorithm

if $RSSI_f < Th$ **or** $RSSI_m > RSSI_{min}$, **and** $RSSI_f + HM_{ad} < Th$ **then**
  HO to macrocell;
else
  Stay in femtocell;
End;

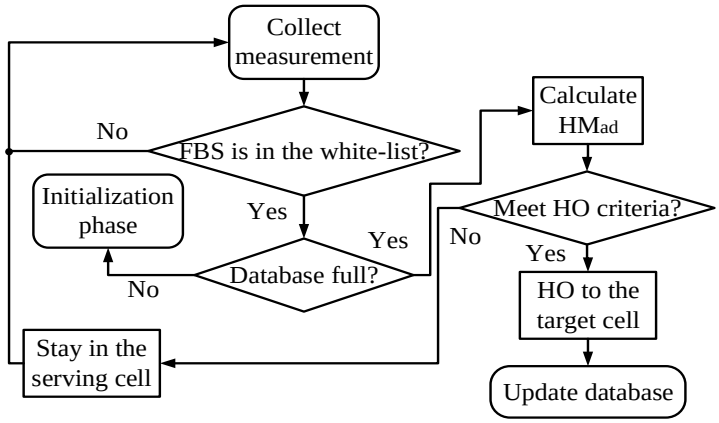

Figure 3.2: Flow chart for the utilization phase.

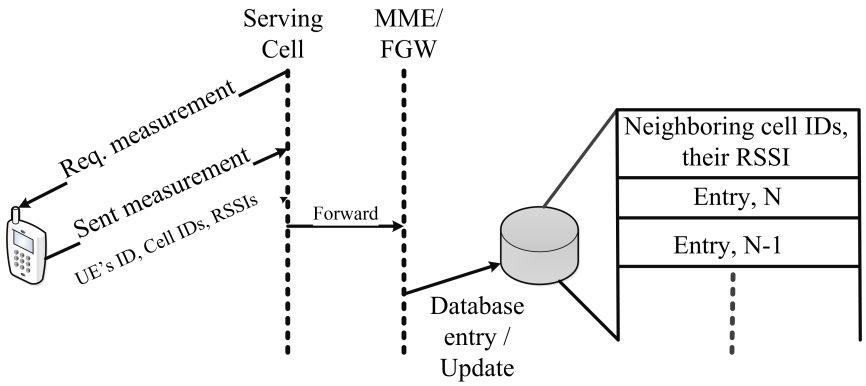

Figure 3.3: Database building and updating.

3.1.3 Location-Fingerprint Database

One of the important purposes of our proposed HO decision algorithm is to get the location of the user during an HO, because an HO is necessary at a few particular locations for indoor users. However, localization of indoor users is difficult. A number of localization techniques are available in the literature for indoor localization [116]. Most of them require complex algorithms. In our design, we consider RF fingerprinting [117] instead of calculating the coordinates of the user location, because our HO-decision algorithm does not require the actual position of a user. Determining the HO zone is our main purpose of building the database. If a location-fingerprint,

obtained from the neighboring cell list, is stored in the database each time an HO occurs, the serving BS can compare this list with the requested location-fingerprint, and can perform a quick HO triggering when necessary. The process of building the database is shown in Figure 3.3.

Algorithm 5: Database building and update

```
if Data matches a previous entry within a time x from the same UE then
    Delete both entries;
else
    if Database is full then
        Delete the oldest data and insert a new entry;
    else
        Insert the data;
End;
```

Each time a UE sends a measurement report to the serving BS, the serving BS determines the target BS and forwards the rest of the measurement to the MME/FGW. This forwarded message contains a list of neighboring cell IDs (with $RSSI > RSSI_{min}$) and their corresponding RSSIs. The MME/FGW stores this information in the database if the database is not full. This database is used in the utilization phase to calculate the adaptive values of the HM. To cope with the ad-hoc nature of femtocells, in the utilization phase, the database is updated in the FILO (first in last out) mode, i.e., the new location-fingerprint is entered and the oldest data is removed from the database if the database is full. The database building and updating algorithm is given in Algorithm 5.

3.1.4 Determining HO Parameters

The minimum received signal strength at the cell boundary of a macrocell and a femtocell is $RSSI_{min}$ and $RSSI_{fail}$, respectively. To find out these values, Okumura-Hata propagation model is used for macrocell networks and ITU-R P.1238-7 path-loss model is used for femtocell networks [17].

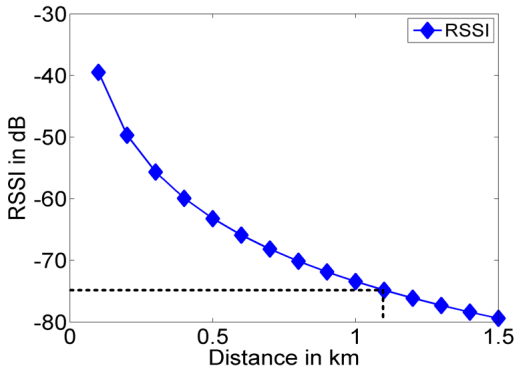

Figure 3.4: Selecting $RSSI_{min}$ at the macrocell boundary.

The radius of macrocells and femtocells is considered in the simulation as 1.2km and 15m. Fig. 3.4 presents the RSSI values for different distances from the macro BS. The $RSSI_{min}$ is calculated as -75dB at the macrocell boundary as shown in the figure. Similarly, the calculated $RSSI_{fail}$ value is -50dB at the femtocell boundary which is shown in Figure 3.5.

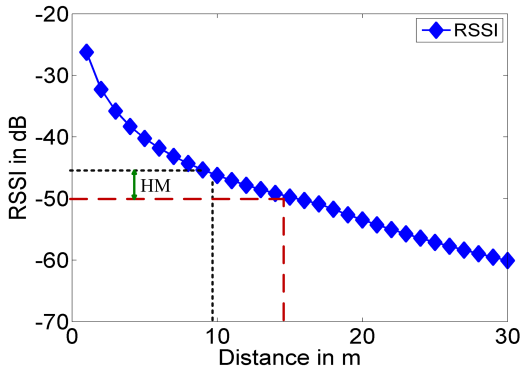

Figure 3.5: Selecting $RSSI_{fail}$ and Th for a femtocell.

The value of HM_{max} and Th can be obtained using simulations. We consider two contrary performance metrics of femtocell networks: rate of unnecessary HOs and cell utilization. The simulation results are shown in Figure 3.6 with respect to different values of Thresholds and HMs. From the figure, it is observed that when $HM = 5$dB and $Th = -45$dB, both metrics show better performance than others. Therefore, we set HM_{max} as 5dB. If the value of HM_{max} is 5dB in Figure 3.5, we can also find that

$Th = -45$dB. These values are used our simulation.

3.1.5 HO Signaling

Both the inbound and outbound signaling for self-adaptive HO decision in femtocell networks are given in Figure 3.7 and Figure 3.8.

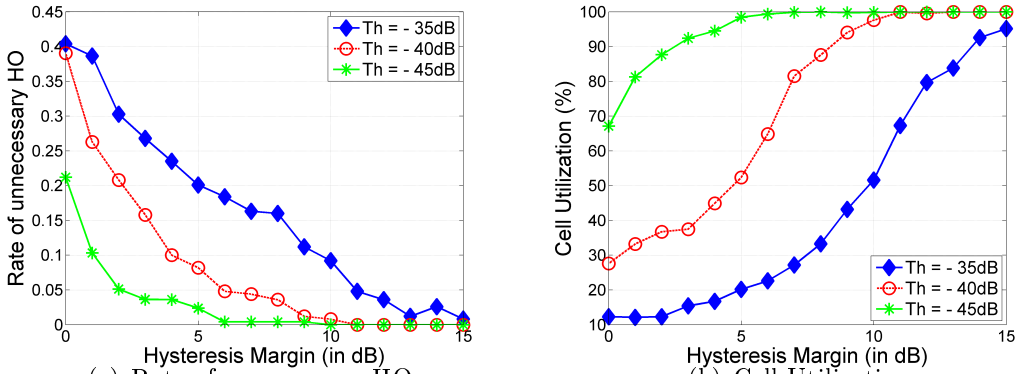

(a) Rate of unnecessary HOs (b) Cell Utilization

Figure 3.6: Rate of unnecessary HOs and cell utilization for different Th and HM.

The signaling procedure is considered during a macro-to-femto HO as the inbound signaling. In this state, the MME checks the location-fingerprint database for similar entries after getting the measurement report from the UE through the serving BS. If the database is empty, the MME considers that the initialization phase is activated and makes an HO decision. The location-fingerprint is added to the database after the HO is succeeded. In the utilization phase, this database is used to calculate the HM as described previously and the database is updated with new location-fingerprint. The database is shared by the MME and FGW so that it can be used for both inbound and outbound mobility. In the outbound signaling, i.e., in a femto-to-macro HO, the signaling procedure is similar to the inbound signaling. However, the FGW makes the HO-decision instead of the MME. The outbound signaling is shown in Figure 3.8.

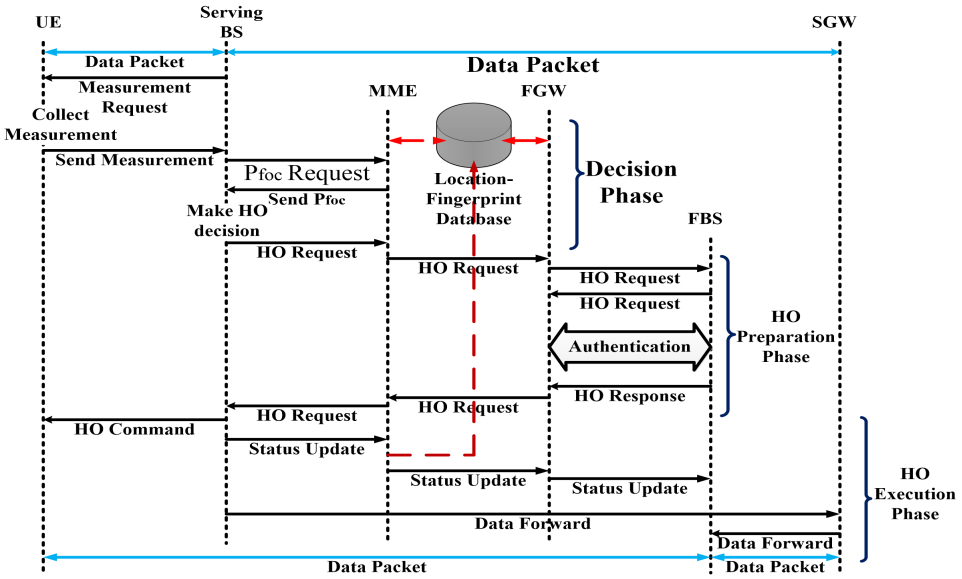

Figure 3.7: Inbound signaling for self-adaptive HO-decision algorithm.

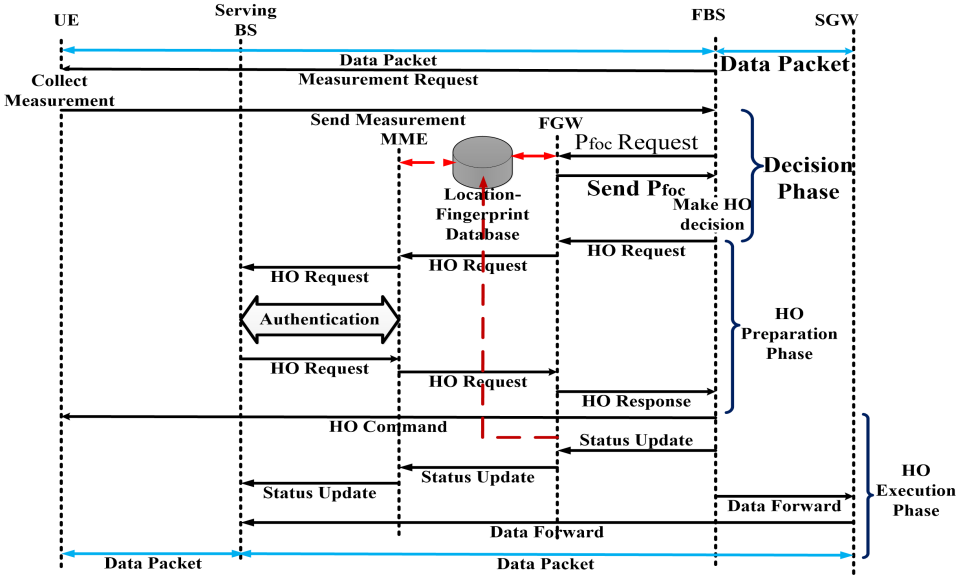

Figure 3.8: Outbound signaling for self-adaptive HO-decision algorithm.

3.2 Proposed HO Decision Algorithm for Open-Access Femtocells

In this section, the proposed target cell selection method and HO decision algorithms are presented. The proposed algorithms work in two phases: initialization and utilization. The initialization phase is used to build a location-history database, and this database is used in the utilization phase to adapt the hysteresis margin (HM).

The notations used in our algorithms are listed in Table 3.2.

Table 3.2: Notations used in the Algorithms for Open-Access Femtocells

$RSSI$	Received Signal Strength Indicator
$RSSI_m$	Received Signal Strength Indicator for the macrocell
$RSSI_{sf}$	Received Signal Strength Indicator for the serving femtocell
$RSSI_{tf}$	Received Signal Strength Indicator for the target femtocell
$RSSI_{min}$	Minimum received signal strength indicator for the macrocell
Th	Threshold for the femtocell
HM_{ad}	Adaptive hysteresis margin
MME	Mobility management entity
FGW	Femto gateway
MBS	Macro-base station
Th_{spd}	Threshold for users' speed
UE_{spd}	Users' speed

Despite the access policies, the requirements for a macro-to-femto and a femto-to-macro HO are the same for both closed-access and open-access femtocell networks. The proposed HO decision algorithms for these HOs are given in Algorithm 6 and Algorithm 7. We have modified the HO decision algorithms to make them applicable for open-access femtocell networks by considering the users' speed. The calculation of Th, $RSSI_{min}$, and HM_{ad} is shown in [22].

The most important issue during a femto-to-femto HO in open-access mode is how to select a proper target femtocell to perform an HO. We propose to use a location-history database that can store the ID of the target femtocell along with the location fingerprint. In the initialization phase, when the location-history database is built, each time a UE sends a measurement report to the serving BS, it determines the target cell based on the maximum $RSSI$ and forwards this information, along with the measurement report, to the MME/FGW. This forwarded message contains a list of neighboring cell IDs (with $RSSI > RSSI_{min}$), their corresponding $RSSI$s, and a target cell ID. The MME/FGW stores this information in the database until it is full. The database building and updating algorithm is shown in [22]. In the utilization phase, this database is used to adapt the HM and to select the target cell during a femto-to-femto HO scenario. In this manner, the serving BS can reduce the delay of selecting a target cell each time an HO request arrives. The proposed HO decision

algorithm for a femto-to-femto HO scenario is shown in Algorithm 8.

Algorithm 6: Macro-to-femto HO decision algorithm

```
if UE_spd < Th_spd then
    if RSSI_tf > Th or RSSI_m < RSSI_min, and RSSI_tf > RSSI_m + HM_ad then
        HO to femtocell;
    else
        Stay in macrocell;
else
    Stay in macrocell;
End;
```

Algorithm 7: Femto-to-macro HO decision algorithm

```
if UE_spd > Th_spd then
    HO to macrocell;
else
    if RSSI_sf < Th or RSSI_m > RSSI_min, and RSSI_sf + HM_ad < RSSI_m then
        HO to macrocell;
    else
        Stay in the femtocell;
End;
```

Algorithm 8: Femto-to-femto HO decision algorithm

```
if UE_spd > Th_spd then
    HO to the macrocell;
else
    if RSSI_sf < Th or RSSI_tf > Th, and RSSI_sf + HM_ad < RSSI_tf then
        HO to the target femtocell;
    else
        Stay in the serving femtocell;
End;
```

3.3 Proposed Analytical Model for Total HO Signaling Cost Analysis

In open-access femtocell networks, a macro-to-femto HO happens when an active UE moves towards a femtocell boundary, and a femto-to-macro HO happens when an active UE moves out of the boundary. There are four events that occur in open-access femtocell networks, including these HOs. All of these events are shown in Figure 3.9.

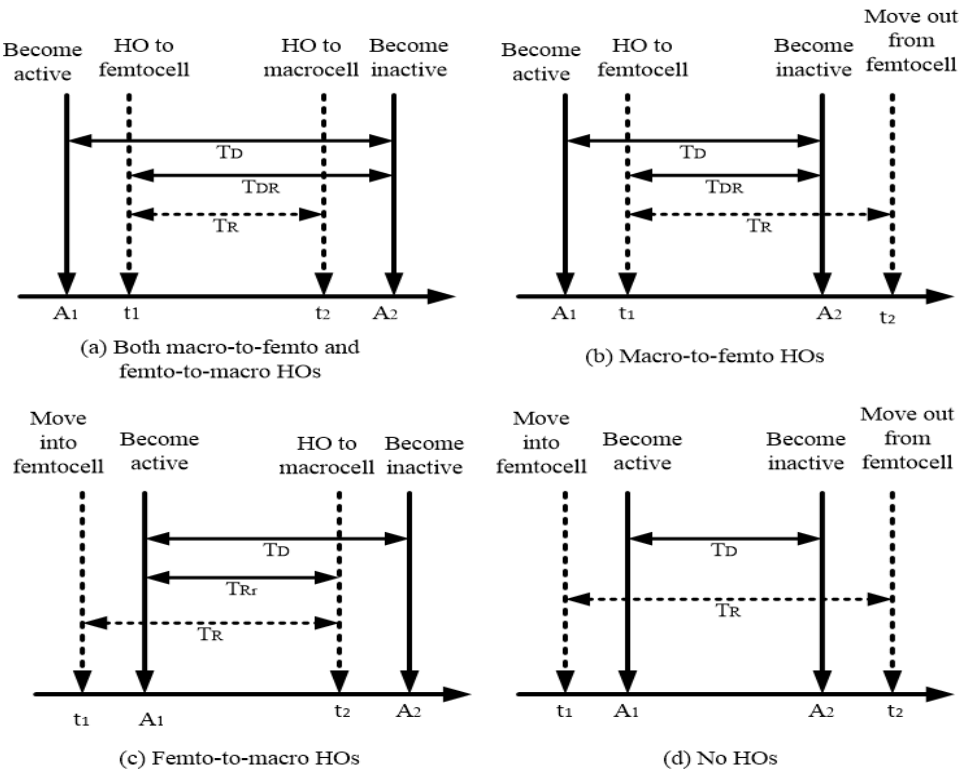

Figure 3.9: Timming diagrams for mobility events in marco-femto HOs.

In the timing diagram (Fiure. 3.9), it is assumed that a UE may become active at any moment (A_1), and the data session arrival rate (λ) is a Poisson process. On the other hand, A_2 is the moment when the data session ends. In addition, the moment when a UE enters the range of a femtocell is indicated by t_1, and the moment when it leaves the range of a femtocell is indicated by t_2. The first event shown in Figure 3.9(a) represents that an active UE moves into a femtocell coverage area and moves out while it is still active. Both macro-to-femto and femto-to-macro HOs happen in this case. In the second event (Figure 3.9(b)), an active UE moves into the femtocell coverage area, and the data session ends before it moves out of the area. A macro-to-femto HO happens in this case. During the third event (Figure 3.9(c)), a UE becomes active within a femtocell coverage area and moves out of the area while still active. In this case, the UE performs a femto-to-macro HO. In the fourth event (Figure 3.9(d)), since the UE becomes active, and the data session ends within the femtocell coverage

area, no HOs happen. The probabilities of these events are P_{r1}, P_{r2}, and P_{r3}.

Besides these four events, the open-access mode has five additional mobility events that can cause different HO scenarios. These five events are shown in Figure 3.10. In the timing diagram, the event in Figure 3.10(a) represents an active UE that moves into a femtocell coverage area from a macrocell and then moves into another femtocell coverage area. Both macro-to-femto and femto-to-femto HOs happen in this case. The event in Figure 3.10(b) represents an active UE that moves between femtocells while it is still active, and a femto-to-femto HO happens in this case. An active femtocell UE performs an HO to another femtocell when it moves into the next femtocell area and to a macrocell when it moves out of femtocells (Figure 3.10(c)). Femto-to-femto and femto-to-macro HOs happen in this case. The next event (Figure 3.10(d)) represents an active femtocell UE that moves into the coverage area of another femtocell, and the data session ends while within the area. Therefore, only a femto-to-femto HO happens in this case. On the other hand, a UE becomes active within a femtocell coverage area, and then it performs an HO to a femtocell (Figure 3.10(e)). If the probabilities of these events are P_{r4}, P_{r5}, P_{r6}, P_{r7}, and P_{r8}, then we can calculate probabilities of all three types of HOs in open access femtocell networks as:

$$P^{open}_{macro-to-femto} = P_{r1} + P_{r2} + P_{r4}, \tag{3.3}$$

$$P^{open}_{femto-to-macro} = P_{r1} + P_{r3} + P_{r6}, \tag{3.4}$$

and

$$P^{open}_{femto-to-femto} = P_{r4} + P_{r5} + P_{r6} + P_{r7} + P_{r8}. \tag{3.5}$$

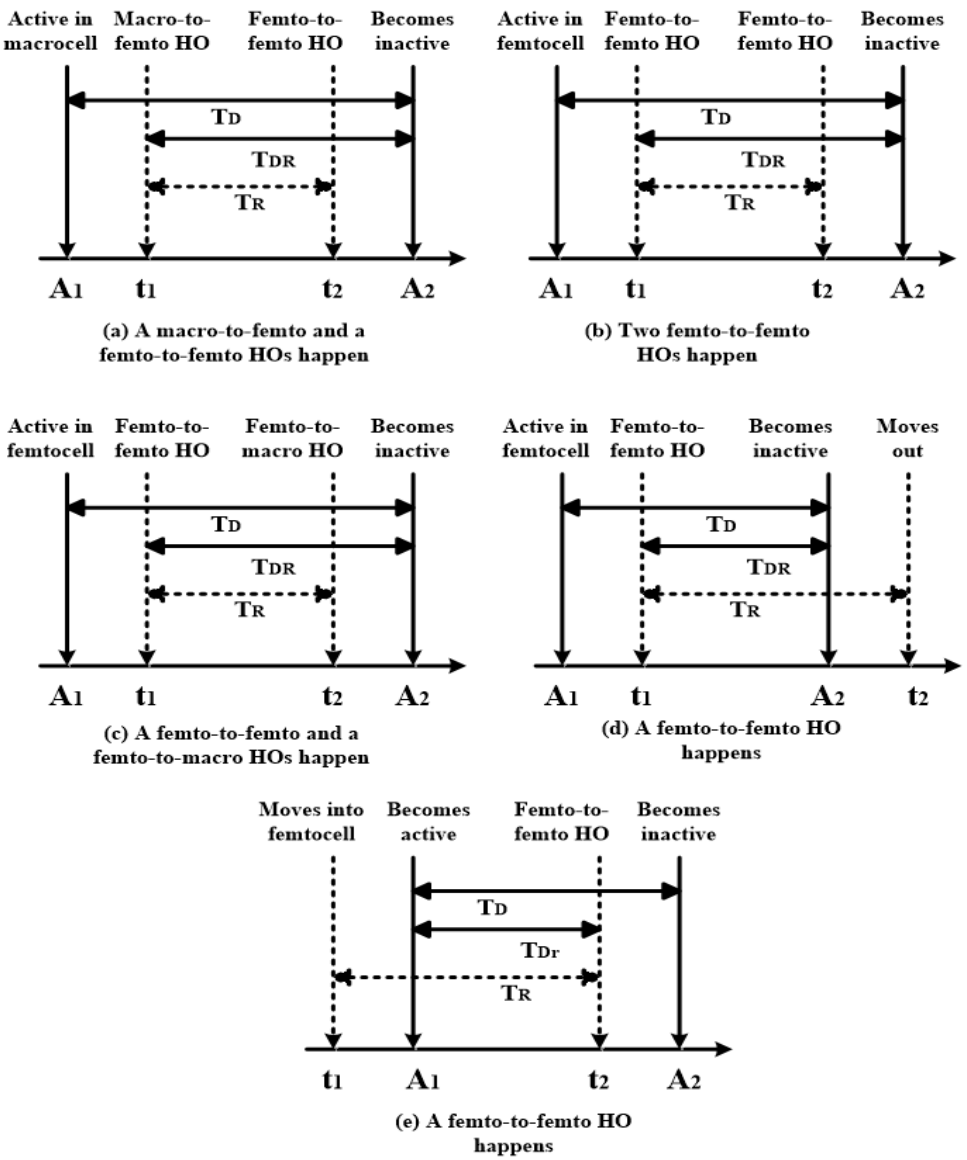

Figure 3.10: Timming diagrams for mobility events in femto-femto HOs.

Since both the session duration (T_D) and the duration that a UE stays within a femtocell coverage area (T_R) are exponentially distributed, we can calculate the probabilities of events in Figure 3.10 the same way as the events in Figure 3.9. Therefore, we can infer $P_{r4} = P_{r5} = P_{r6} = P_{r1}$, $P_{r7} = P_{r2}$, and $P_{r8} = P_{r3}$. Using these values in (3.3), (3.4), and (3.5), we obtain

$$P^{open}_{macro-to-femto} = 2P_{r1} + P_{r2}, \tag{3.6}$$

$$P^{open}_{femto-to-macro} = 2P_{r1} + P_{r3}, \tag{3.7}$$

and

$$P^{open}_{femto-to-femto} = 3P_{r1} + P_{r2} + P_{r3}. \tag{3.8}$$

In the timing diagrams, T_D and T_R are independent random variables. T_D denotes the session duration which is exponentially distributed with mean $1/\eta$, and the probability density function of this session duration is $f_{TD}(t) = \eta e^{-\eta t}$. Similarly, T_R is the duration of a UE being within the coverage area of a femtocell which is exponentially distributed with mean $1/\mu$, and the probability density function of this duration of stay is $f_{TR}(t) = \mu e^{-\mu t}$. T_{DR} and T_{Rr} in the timing diagram follow the memoryless property of the residence times, T_D and T_R, respectively. In addition, the probability density function of T_{DR} is f_{DR} (which is exponentially distributed with mean $1/\eta$) and the probability density function of T_{Rr} is f_{Rr} (which is exponentially distributed with mean $1/\mu$). Now, we can calculate P_{r1}, P_{r2}, and P_{r3} as:

$$P_{r1} = P(A_1 < t_1 < A_1 + T_D) \cdot P(T_{DR} > T_R), \tag{3.9}$$

$$P_{r2} = P(A_1 < t_1 < A_1 + T_D) \cdot P(T_{DR} \leq T_D), \tag{3.10}$$

and

$$P_{r3} = P(t_1 < A_1 < t_1 + T_R) \cdot P(T_D \geq T_{Rr}). \tag{3.11}$$

Here, (3.9) ensures that the session starts before the UE enters the femtocell coverage area, and the UE leaves the area before the session ends. Similarly, (3.10) indicates that the session starts before the UE enters the femtocell coverage area and ends before it leaves the area. (3.11) ensures that a session starts after the UE enters the femtocell coverage area and ends after it leaves the area. Using the Laplace transform, we have

$P_{r1} = \int_0^\infty \int_t^\infty \lambda t e^{-\lambda t} f_{TD}(y) dy dt \cdot$

$$(1 - \int_0^\infty \int_t^\infty \mu e^{-\mu x} f_{DR}(t) dx dt), \tag{3.12}$$

$P_{r2} = \int_0^\infty \int_t^\infty \lambda t e^{-\lambda t} f_{TD}(x) dx dt \cdot$

$$(1 - \int_0^\infty \int_t^\infty \eta e^{-\eta t} f_{DR}(y) dy dt), \tag{3.13}$$

and

$P_{r3} = \int_0^\infty \lambda t e^{-\lambda t} f_{Rr}(t) dt \cdot$

$$\int_0^\infty \int_t^\infty \eta e^{-\eta y} f_{Rr}(t) dy dt. \tag{3.14}$$

After solving (3.12), (3.13), and (3.14), we can find the probability of the three events as:

$$P_{r1} = \frac{\lambda \mu}{(\lambda + \eta)^2 (\mu + \eta)}, \tag{3.15}$$

$$P_{r2} = \frac{\lambda \eta}{(\lambda + \eta)^2 (\mu + \eta)}, \tag{3.16}$$

and

$$P_{r3} = \frac{\lambda \mu^2}{(\lambda + \eta)^2 (\mu + \eta)}. \tag{3.17}$$

Finally, these three probabilities can be calculated from (3.15), (3.16), and (3.17). Then, the total HO signaling cost of macro-to-femto, femto-to-macro, and femto-to-femto HOs in open-access femtocell networks are

$$C^{open}_{macro-femto} = P^{open}_{macro-femto} \cdot (\sum T^i_j + \sum P_i), \tag{3.18}$$

$$C^{open}_{femto-macro} = P^{open}_{femto-macro} \cdot (\sum T^i_j + \sum P_i), \tag{3.19}$$

and

$$C^{open}_{femto-femto} = P^{open}_{femto-femto} \cdot (\sum T^i_j + \sum P_i). \tag{3.20}$$

Here, T_j^i is the delivering cost of an HO message between node i and j, P_i is the processing cost of a message at node i, and the terms in the brackets are the signaling cost of a successful HO. The macro-to-femto and the femto-to-macro HO signaling procedures are given in [22]. By analyzing the HO signaling procedure, we get $\sum T_j^i$ and $\sum P_i$ for a macro-to-femto HO as:

$$\sum (T_j^i)_{macro-femto} = 3T_{UE}^{MBS} + 6T_{FGW}^{FBS} + 5T_{FGW}^{MME} + 5T_{MBS}^{MME}, \tag{3.21}$$

$$\sum (P_i)_{macro-femto} = P_{UE} + P_{FBS} + P_{FGW} + 2P_{MME}. \tag{3.22}$$

Similarly, we get $\sum T_j^i$ and $\sum P_i$ for a femto-to-macro HO as:

$$\sum (T_j^i)_{femto-macro} = 3T_{UE}^{FBS} + 5T_{FGW}^{FBS} + 3T_{FGW}^{MME} + 5T_{MBS}^{MME}, \tag{3.23}$$

$$\sum (P_i)_{femto-macro} = P_{UE} + P_{FBS} + 2P_{FGW} + P_{MME}. \tag{3.24}$$

In addition, we present the HO signaling procedure for a femto-to-femto HO in Figure 3.11. Now, we get $\sum T_j^i$ and $\sum P_i$ for a femto-to-femto HO as:

$$\sum (T_j^i)_{femto-femto} = 3T_{UE}^{FBS} + 10T_{FGW}^{FBS} + 2T_{FGW}^{MME}, \tag{3.25}$$

$$\sum (P_i)_{femto-femto} = P_{UE} + P_{FBS} + 2P_{FGW} + P_{MME}. \tag{3.26}$$

Notations for different costs and their values are given in Table 3.3 [24, 118, 23, 28, 119].

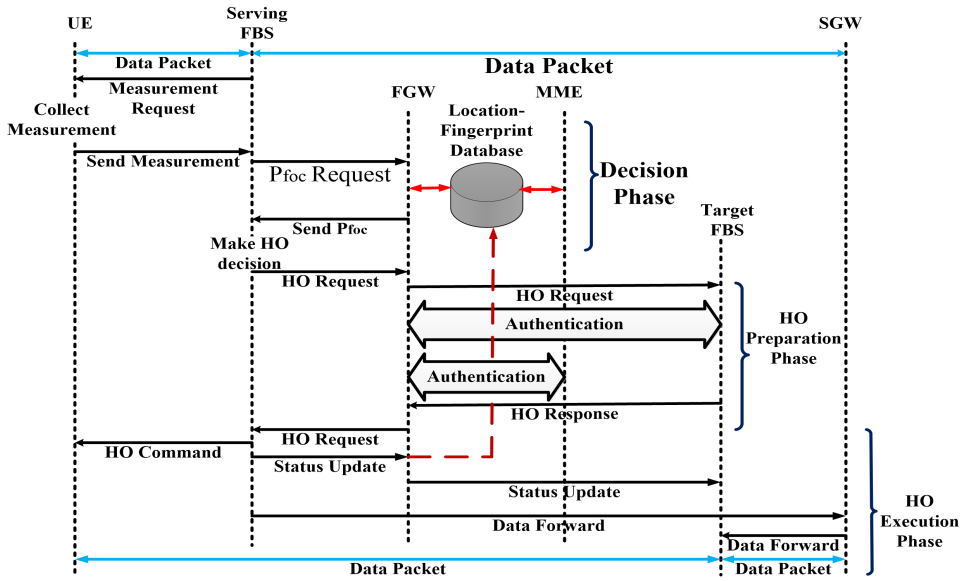

Figure 3.11: Femto-to-femto HO signaling procedures for the proposed HO decision algorithm.

Table 3.3: HO Signaling Cost Parameters

T_{UE}^{FBS}	Transmission cost between a UE and an FBS	2
T_{FBS}^{FGW}	Transmission cost between an FBS and an FGW	2
T_{FGW}^{MME}	Trnsmission cost between an FGW and an MME	4
T_{MBS}^{MME}	Transmission cost between an MBS and an MME	4
T_{UE}^{MBS}	Transmission cost between a UE and an MBS	2
P_{UE}	Processing time at UE	40
P_{FBS}	Processing cost at FBS	3
P_{FGW}	Processing cost at FGW	2
P_{MME}	Processing cost at MME	4

3.3.1 Performance Evaluation of HO Decision Algorithms

In this section, the performance of the proposed self-adaptive HO-decision algorithm is evaluated. The setting of scenarios in the simulation is introduced first. Then, the performance of the proposed HO-decision algorithm is evaluated. In this paper, we mainly investigate the following four performance metrics: 1) *rate of unnecessary HOs*: the probability that a UE temporarily hands over to the target cell and hands over back to the serving cell, 2) *HO failure rate*: the probability of a

call/service-drop before a successful HO is triggered, 3) *cell utilization*: the probability that a CSG UE stays connected to the femtocell while within the coverage area of it's home FBS, and 4) *total HO signaling cost*: total number of HOs for a particular scenario multiply with the HO signaling cost for one HO. In addition, we compare our proposed self-adaptive algorithm with three other algorithms: 1) *RSS TH HM*: HO decisions depend on both a threshold and a fixed HM, which does not adapt with the ad-hoc nature of femtocells; 2) *RSS ADHM*: HM adapts based on the formula from [120], which is $HM = max\{HM_{max} * (1 - 10^{\frac{d}{R}})^4; 0\}$. Here, R is the radius of the femtocell and d is the distance between the FBS and UE; and 3) *SINR ADHM*: adaptive HM is calculated from $HM = max\{HM_{max} * (1 - 10^{\frac{SINR_{act} - SINR_{min}}{SINR_{min} - SINR_{max}}})^4; 0\}$ [19].

3.3.1.1 Simulation Setup

Net Logo 5.0.5 [121] is used to simulate our proposed algorithm in an indoor environment for closed-access and open-access femtocell networks. A single-floored two-bedroom apartment with an FBS is designed, which has the capacity of supporting ten users surrounded by six neighboring FBSs in the coverage of a macrocell. Thirty users and all FBSs are placed in a random manner. These users follow a modified version of the Random Waypoint mobility model, and they have a probability of 0.7 to enter and exit the apartment. The mobility model is modified in a way that the users use the door only to go in/out of the apartment, and none of them cross the walls. The parameters used in our simulation are listed in Table 3.4 [17].

3.3.1.2 Rate of Unnecessary HOs

The rate of unnecessary HOs for the closed-access and open-access femtocell networks are shown in Figure 3.12(a) and Figure 3.13(a), respectively. The low rate of unnecessary HOs is desirable in order to provide better performance. Simulation results show that our proposed algorithm has a lower unnecessary HO rate than

other algorithms except the RSS TH HM algorithm for open-access networks. In open-access networks, as the RSS TH HM algorithm has a fixed HM, the rate of unnecessary HOs reduces for high values of HM. However, the results of HO failure in Figure 3.12(b) and Figure 3.13(b) and cell utilization in Figure 3.12(c) and Figure 3.13(c) show that the RSS TH HM algorithm has the highest HO failure rate and a lower cell utilization than the proposed algorithm. Moreover, the total signaling cost in Figure 3.14 and Figure 3.15 shows low signaling cost for the proposed algorithm despite of high unnecessary rates at the high HM. On the other hand, as RSS ADHM and SNR ADHM algorithms change the HM based on the distance and SINR, respectively, and select the minimum value of the HM throughout the cell boundary, both algorithms show worse performance than the proposed one.

3.3.1.3 HO Failure Rate

The HO failure rate should be as minimum as possible. Since a high value of the HM can lead to a high value of the HO failure rate because of the abrupt signal drop, it is necessary to minimize the HM where an HO is necessary. Additionally, femtocells suffer high interference at the cell boundary, which may lead to a high service failure if HO-decision cannot adapt to the change of the environment. If the RSSI of the UE

Table 3.4: Simulation Parameters for HO Decision Algorithm in Femtocells

Macrocell transmission power, P_m	45 dBm
Radius of macrocell	1.2 km
Femtocell transmission power, P_f	10 dBm
Radius of femtocell	15 m
Size of database, d_s	30
Users speed	5 km/hr
Threshold, Th	-45 dB
Wall penetration loss	5 dB
Outdoor penetration loss	2 dB - 10 dB
$RSSI_{min}$	-75 dB
$RSSI_{fail}$	-50 dB
HM_{max}	5 dB

goes below $RSSI_{fail}$ and an HO does not happen, we consider this as an HO failure. The performance of the HO failure rate of our proposed self-adaptive algorithm as compared to the other three algorithms is given in 3.12(b) for closed-access and in Figure 3.13(b) for open-access femtocell networks. It is observed that the proposed algorithm outperforms the other algorithms in terms of lower HO failure rate.

3.3.1.4 Cell Utilization

As femtocells are deployed for offloading cellular traffic and to provide cost-effective service to the closed-group users, it is expected that whenever a UE is within the coverage area of its home FBS, it should be connected to the femtocell. However, traditional HO-decision algorithms do not consider this issue. As a result, their cell utilization is lower than the proposed algorithm. The simulation results of cell utilization are shown in Figure 3.12(c) for closed-access and in Figure 3.13(c) for open-access femtocell networks. Simulation results show the highest cell utilization.

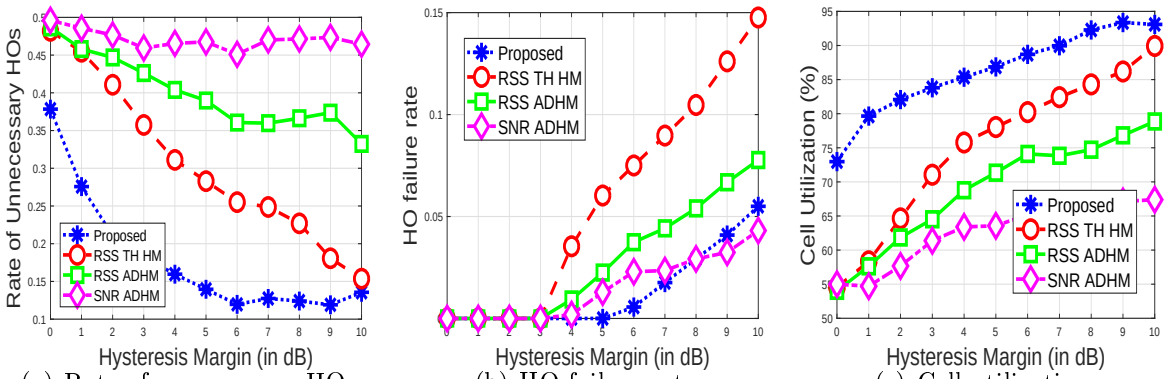

(a) Rate of unnecessary HOs (b) HO failure rate (c) Cell utilization

Figure 3.12: Performance evaluation of closed-access femtocell networks.

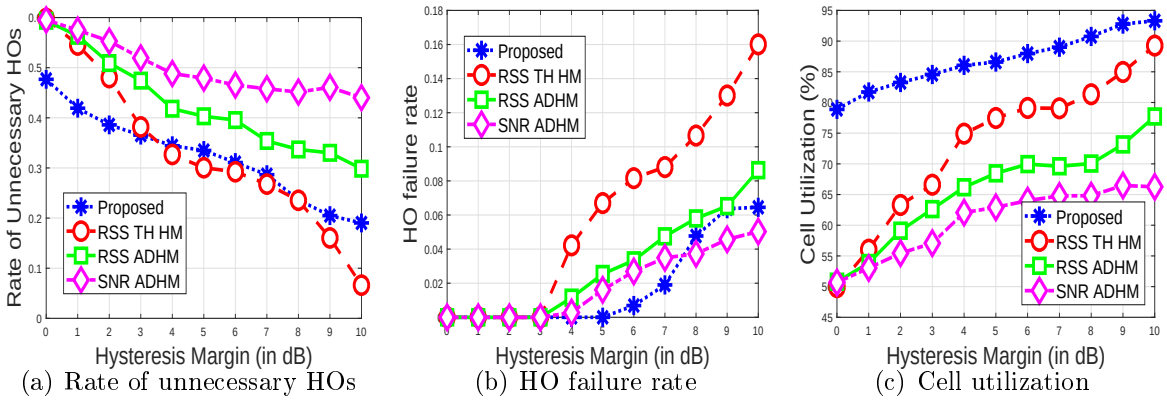

(a) Rate of unnecessary HOs (b) HO failure rate (c) Cell utilization

Figure 3.13: Performance evaluation of open-access femtocell networks.

3.3.1.5 Total HO Signaling Cost

The performance of the total HO signaling cost for all kinds of HOs in both closed-access and open access femtocell networks are given here. The HO signaling cost is determined by considering all transmission costs and processing costs during an HO. The HO signaling costs are calculated for an exponential session duration with mean $1/\eta = 3$, a residence time with mean $1/\mu = 10$, and the session arrival rate γ varied from 0.1 to 0.34. The total HO signaling cost for closed access and open access femtocell networks are shown in Figure 3.14 and Figure 3.15, respectively. Here the total costs are calculated by multiplying the cost of an HO with the total number of HOs that also includes unnecessary HOs. From the figures, we can observe that the HO signaling cost increases with the increment of HO decision criteria. We can also observe that using users' speed reduces the total HO signaling cost by reducing unnecessary HOs of users with high speed. The existing algorithms that adapt HMs have the highest total HO signaling cost. These existing algorithms adapt HM either based on the distance between the BS and the UE or the SINR received at the UE side. As a result, the UE has to notify the serving BS frequently, which causes additional signaling cost. Moreover, these methods cannot eliminate the number of unnecessary HOs. On the other hand, we can observe that our proposed algorithms show better results in both closed-access and open access modes.

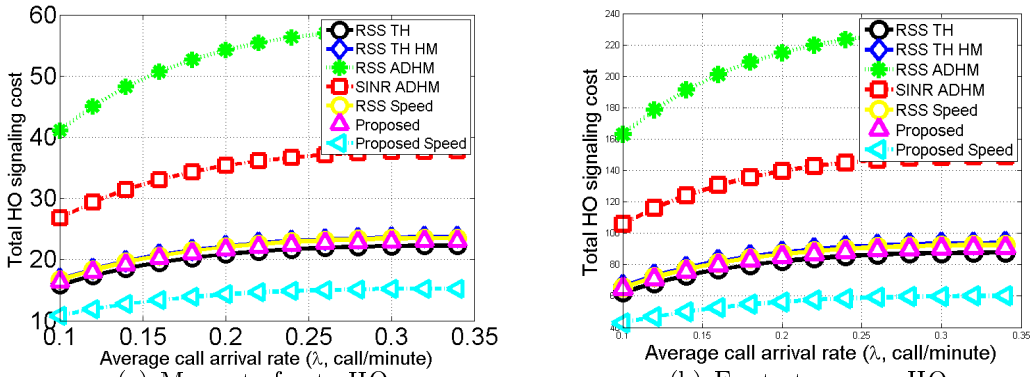

(a) Macro-to-femto HOs (b) Femto-to-macro HOs

Figure 3.14: Comparison of total HO signaling costs in closed-access femtocell networks.

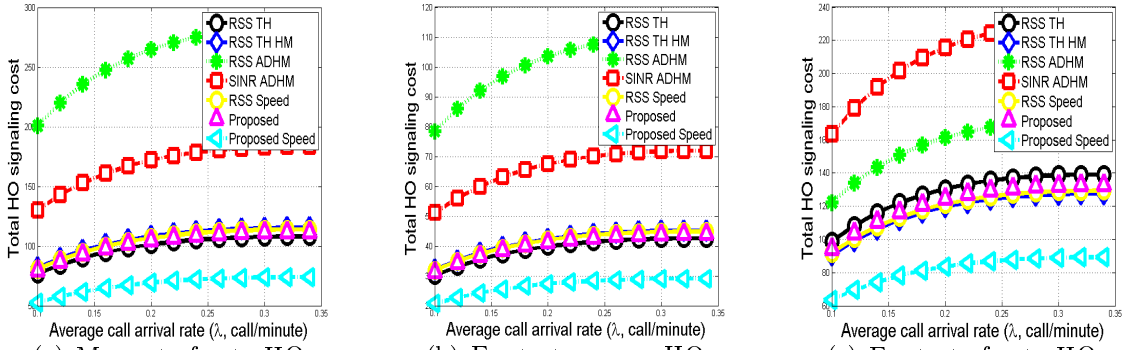

(a) Macro-to-femto HOs (b) Femto-to-macro HOs (c) Femto-to-femto HOs

Figure 3.15: Comparison of total HO signaling costs in open/hybrid-access femtocell networks.

3.4 Proposed Secure Target Cell Selection Scheme

In this section, we present our proposed target cell selection scheme in femto-to-femto HO scenarios by considering both sinkhole and wormhole attacks. Since all open-access femtocells have the same priority to a UE, the main challenge of designing such a scheme is how to avoid a malicious femtocell without reducing femtocell utilization and increasing HO signaling cost. In the HO decision phase, the serving cell uses the measurement report from UEs to select a target cell and make the HO decision. Since a UE is unable to detect any malicious femtocell, and femtocells are unable to communicate with each other, it is hard for a serving femtocell to differen-

tiate between a secure femtocell and a malicious femtocell. Therefore, our goal is *to avoid existing attacks, not to detect them.*

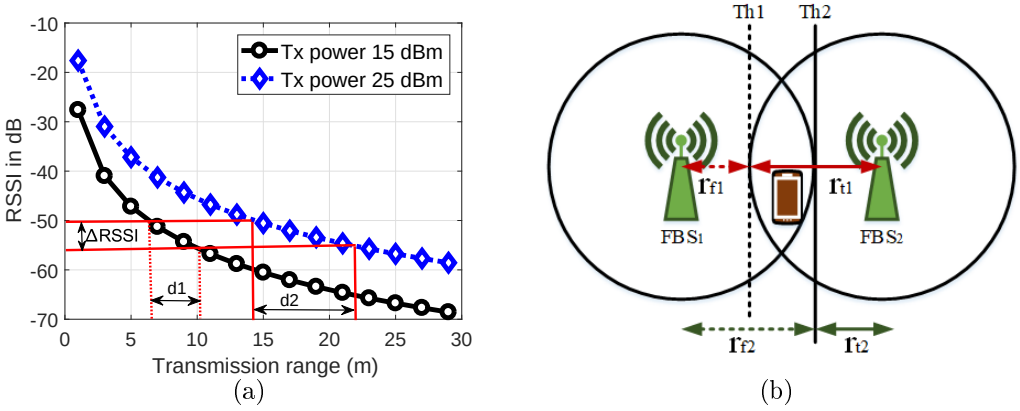

Figure 3.16: Effect of high transmission power, and a scenerio to select the target cell, where FBS_1 is the serving cell with radius r_{f2} and FBS_2 is the target cell with radius r_{t1}.

We already know that the attacker uses a high transmission power in the sinkhole attack. The effect of a high transmission power on the transmission range is shown in Figure 3.16(a). It is shown in the figure that the $RSSI$ is high for a high transmission power at the same distance. Moreover, we can also observe from the figure that in case of a high transmission power, the signal travels a longer distance for the same change of $RSSI$ ($\Delta RSSI$). Alternatively, for the same distance change, the change of $RSSI$ is lower for the high transmission power. We use this property to avoid the sinkhole attack.

A UE periodically sends a measurement report to the serving FBS. The measurement report contains the $RSSI$ from the serving cell as well as $RSSI$s from neighboring cells and their cell IDs. After getting the measurement report from the UE, when the RSSI of the serving cell goes below the threshold Th_1, the serving FBS generates a primary target cell list as:

$$List_{target1} = \{(i, RSSI(i)) : RSSI(i) > Th_2\}, \tag{3.27}$$

where Th_2 is the minimum RSSI which is required to transmit/receive a packet successfully, $i \in \{0, 1, \cdots, n_{nf}\}$, $RSSI(i)$ denotes the RSSI at the UE from FBS i, which is greater than the threshold, Th_2. n_{nf} represents the total number of neighboring femtocells in the measurement report. If no neighboring femtocell fulfills the requirement, the list becomes empty (ϕ) and the serving FBS prepares for performing an HO to the macrocell.

Now, if the $RSSI$ of the serving cell goes below a certain threshold Th_2, the serving FBS collects another measurement report from the UE. The HO scenario is shown in Figure 3.16(b). From the figure, the difference between Th_1 and Th_2 can be calculated as:

$$|Th_1 - Th_2| = |RSSI_{r_{f1}} - RSSI_{r_{f2}}|. \tag{3.28}$$

Here, we obtain $RSSI_{r_{f1}}$ and $RSSI_{r_{f2}}$ by using the path-loss model from (1.1).

$$RSSI_{r_{f1}} = P_{tx} + G_f + G_u - PL_{f1}, \tag{3.29}$$

and

$$RSSI_{r_{f2}} = P_{tx} + G_f + G_u - PL_{f2}. \tag{3.30}$$

Now, using the path-loss model from (1.2) we obtain $RSSI_{r_{f1}} = P_{tx} + G_f + G_u - 20log_{10}(f)$

$$-Nlog_{10}(r_{f1}) - L_f(n) + a(n), \tag{3.31}$$

and $RSSI_{r_{f2}} = P_{tx} + G_f + G_u - 20log_{10}(f)$

$$-Nlog_{10}(r_{f2}) - L_f(n) + a(n). \tag{3.32}$$

Putting the values of (3.31) and (3.32) in (3.28), we calculate

$$|Th_1 - Th_2| = |N\{log_{10}(r_{f2}) - log_{10}(r_{f1})\}|. \tag{3.33}$$

Similarly, the difference between $RSSI_{r_{t1}}$ and $RSSI_{r_{t2}}$ for all target femtocells from (3.27) can be calculated as:

$$|RSSI_{r_{t1}} - RSSI_{r_{t2}}| = |N\{log_{10}(r_{t2}) - log_{10}(r_{t1})\}|. \tag{3.34}$$

In both cases, the effects of transmission power, shadowing, and transmission frequency are canceled out, and the difference depends on distance only. Therefore, using the difference of RSSIs can eliminate the effect of transmission power change and using this difference to choose a target cell helps to eliminate effects of the sinkhole attack. We get from the properties of Figure 3.16(a) that the change of $RSSI$s for the same distance will be lower than the change of $RSSI$s of the target cell if the transmission power increases. Now, applying this property, the serving FBS can determine the new target cell list as $List_{target2} = \{(j, RSSI(j)) : |RSSI(j)_{r_{t1}}$

$$-RSSI(j)_{r_{t2}}| \geq |Th_1 - Th_2|\}. \tag{3.35}$$

In this way, the effect of the sinkhole attack may be reduced by avoiding malicious nodes with excessive transmission power in open-access femtocell networks. However, this method cannot reduce the effect of the wormhole attack, where the malicious femtocell acts as a traditional femtocell with a normal transmission power. Considering the fact that the wormhole attack needs to use the location information of a registered FBS for gaining a desire outcome, we decide to use the location database of FBSs from the core network to solve this problem. The core network keeps a database containing the registered femtocells and their locations. Each time an FBS turns on, it needs to perform a location verification, which is necessary to determine if the location of the FBS is inside a licensing area where it is permitted to operate [82]. Therefore, a malicious FBS can change its location and falsify the registered location information each time it is asked for location verification. Moreover, location

verification does not happen during HOs. Our plan is to use this location database during an HO to perform a location verification.

We propose two ways to perform the location verification. In the first way, the UE sends its own location coordinates $(xcor, ycor)$ with the measurement report. The serving FBS forwards location coordinates along with the updated list from (3.35) to the mobility management entity (MME) in the core network. The MME checks the location coordinates in the database for each FBS in this list. Then, the MME uses Algorithm 9 to judge whether the UE is inside the coverage area of each registered FBS and modify the list accordingly.

Algorithm 9: Location verification and cell list modification using UE's location coordinates

foreach j **do**
  Get $(xcor_j, ycor_j)$ from the location database.
  if $(\sqrt{(xcor - xcor_j)^2 + (ycor - ycor_j)^2} \leq r_f)$ **then**
    `// Check if the UE is within the range of the FBS`
    Put $(j, RSSI(j))$ in the modified list, $List_{locUpdate}$;
  else
    Discard the FBS from the list, $List_{target2}$;

However, a UE may turn off its location update process and the location verification cannot be performed using Algorithm 9 in this case. To address this issue, we propose a second method to verify the location of FBSs. In this proposed solution, a separate database can be created by assigning a group of femtocells within a specific zone with a zone ID. This database can be stored in the MME. We assume each sector of a macrocell is assigned with a zone ID. Moreover, using mobile edge computing (MEC) at the macro base station or FBS will allow them to get user's location (location zone) without the help of a GPS [48]. After getting the list from (3.35), the serving FBS forwards this list to the MME. The MME then checks the location zone for each FBS in the list and modify the list using Algorithm 10.

After the location verification, the MME sends back the modified list, $List_{locUpdate}$,

Algorithm 10: Location verification and cell list modification using location zone ID

```
Zone ID for the serving FBS← zone(s);
foreach j do
    Get zone(j);                    /* Checks zone ID for all FBSs from List_target2 */
    if zone(j) = zone(s) then
        Put (j, RSSI(j)) in the modified list, List_locUpdate;
    else
        Discard the FBS from the list, List_target2;
```

to the serving FBS. The list is shown as

$$List_{locUpdate} = \{(k, RSSI(k)) : RSSI(j)\}. \tag{3.36}$$

Finally, the FBS with the lowest $RSSI$ is written as

$$RSSI(k') = \arg\min_{k}(RSSI(k)), \tag{3.37}$$

where k' denotes the target femtocell and the UE is eventually handed off to the target femtocell. The algorithm to perform HOs is shown in Algorithm 11. The reason for choosing the lowest $RSSI$ is to choose a femtocell far away from the UE compared with other femtocells in the candidate target cell list. As a result, the UE can stay connected to the current femtocell for longer time and can avoid HOs with other femtocells. In this way, the UE can avoid unnecessary HOs and increase the femtocell utilization. This scheme is also applicable for a macro-to-femto HO in open-access femtocell networks.

3.4.1 Performance Evaluation of the Secure Target Cell Selection Scheme

In this section, we evaluate the effectiveness of the proposed target cell selection and HO decision scheme in terms of the rate of HOs to malicious femtocells, femtocell utilization, and total HO signaling cost. First, we introduce the setting of scenarios in the simulation. Then, the performance of the proposed scheme is evaluated.

Algorithm 11: HO decision algorithm

```
if RSSI_Serving < Th_1 then
    Get RSSI(i)_rt1;
    if RSSI_Serving < Th_2 then
        Get RSSI(i)_rt2;
        Find List_target2 using (3.35);
        Use Algorithm 9 or Algorithm 10 to get List_locUpdate;
        if List_locUpdate ≠ φ then
            Get k' using (3.37);
            if RSSI(k') > Th_1 then
                HO to the target femtocell, k';
            else
                HO to the macrocell;
        else
            HO to the macrocell;
```

3.4.1.1 Simulation Setup

To simulate the HO process of an open-access femtocell network, we use the system model scenario shown in Figure 1.7. Four single-floored apartments are considered by each side of a road within the coverage area of a macrocell network. Each of these apartments has an open-access FBS which is located randomly within an apartment. A UE moves straight along the road with a constant speed and performs an HO to the selected FBS using a given HO decision algorithm. A number of malicious FBSs are deployed randomly within the simulation area. Malicious FBSs are deployed to implement the sinkhole attack and the wormhole attack. We use Net Logo 5.0.5 [121] to simulate our proposed scheme. To minimize the randomness of the scenario, we use the average of 100 simulations for each case. The values of the parameters used in the simulation are listed in Table 3.5 [33, 5, 22, 20, 122].

To evaluate the performance of our proposed scheme, we investigate the following three performance metrics: 1) *Rate of HOs to a Malicious Femtocell*: the probability of a UE to hand off to a malicious femtocell; 2) *Femtocell Utilization*: total amount of time a UE stays connected to a secure femtocell divided by the total amount of time the UE stays connected to any femtocell; 3) *Total HO Signaling Cost*: average

signaling cost during a femto-to-femto HO. In addition, we compare our proposed cell selection and HO decision scheme with three existing cell selection schemes: 1) *MaxRSS Scheme*: in this scheme, the target femtocell is selected based on the maximum RSS from the neighboring cell list [123]; 2) *MinRSS scheme*: the minimum RSS and the speed of the user are considered to select the target femtocell to HO in this scheme; 3) *Direction and minRSS scheme*: a neighboring cell list optimization technique based on the location of FBSs is considered. However, the target cell selection method is not available in this scheme. Therefore, we use the minimum RSS to select the target cell in this scheme, so that our proposed scheme can be better compared.

Table 3.5: Simulation Parameters for Secure HOs

Macrocell transmission power, P_m	45 dBm
Radius of macrocell	1.2 km
Femtocell transmission power, P_f	15 dBm
Radius of femtocell	15 m
Wall penetration loss	5 dB
Outdoor penetration loss	2 dB to 10 dB
Distance power coefficient, N	28
Antenna gain of macrocells	15 dB
Antenna gain of FBSs, G_f	2 dB
HO threshold, Th_1, Th_2	-60 dB, -65 dB
User speed	5 km/hr
Number of malicious FBSs	0 to 15

3.4.1.2 Rate of HOs to a Malicious Femtocell

The rate of HOs to a malicious femtocell is determined by the probability of a UE to hand off to a malicious femtocell in presence of malicious femtocells in the network. The high rate presents less efficient HOs, therefore, more vulnerable networks. Figure 3.17 shows the results of the rate of HOs to a malicious femtocell in the sinkhole attack and the wormhole attack. The results vary with respect to the number of malicious femtocells in the networks. The figure shows that our proposed cell selection and HO decision scheme outperforms all the compared schemes under these attacks.

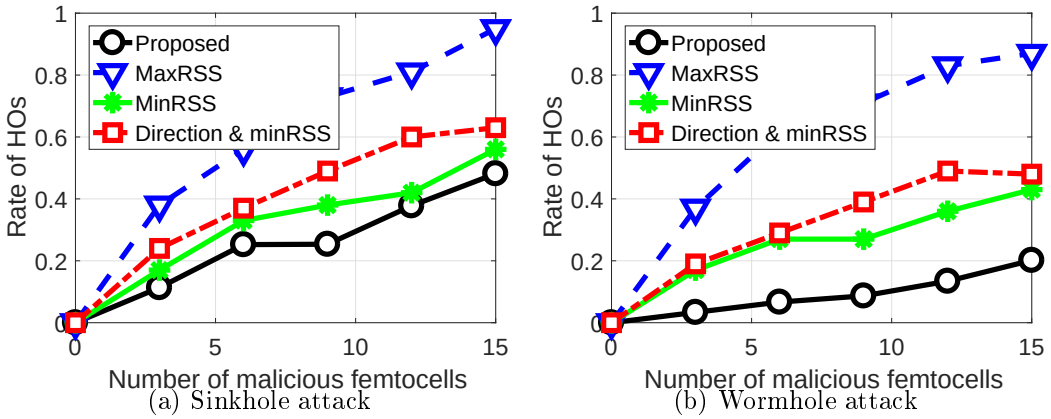

(a) Sinkhole attack (b) Wormhole attack

Figure 3.17: Comparison of the rate of HOs to a malicious femtocell.

3.4.1.3 Femtocell Utilization

The femtocell utilization represents the average time an active UE is served by a secure femtocell while connected to a femtocell network. To support good femtocell offloading, it is expected that a UE should be connected to a femtocell network as long as possible. However, connecting to a malicious femtocell is not desirable. Therefore, choosing a trustworthy femtocell to perform the HO is very important. Our proposed scheme can choose a secure femtocell more effectively, and it shows higher femtocell utilization than the compared schemes. The performance results are shown in Figure 3.18 with respect to different number of malicious femtocells in the network.

3.4.1.4 Total HO Signaling Cost

Here, the total HO signaling cost is determined by considering all transmission costs and processing costs during an HO [129]. The transmission cost is represented as a one-way transmission delay between a pair of nodes, and the processing cost is represented as the delay to process one message in one node. The HO signaling costs are calculated for an exponential session duration with mean $1/\eta = 3$, a residence time with mean $1/\mu = 10$, and the session arrival rate γ (varies from 0.1 to 0.34). We calculate the total HO signaling cost for femto-to-femto HO scenarios with three malicious femtocells under sinkhole and wormhole attacks. Though the neighboring

cell list update process adds additional signaling cost in the proposed scheme, we can observe from Figure 3.19, that our proposed scheme shows lower or similar HO signaling cost than the existing schemes. Moreover, by observing other performance metrics, we can state that adding some signaling cost is worthy in terms of avoiding malicious femtocells and increasing femtocell utilization.

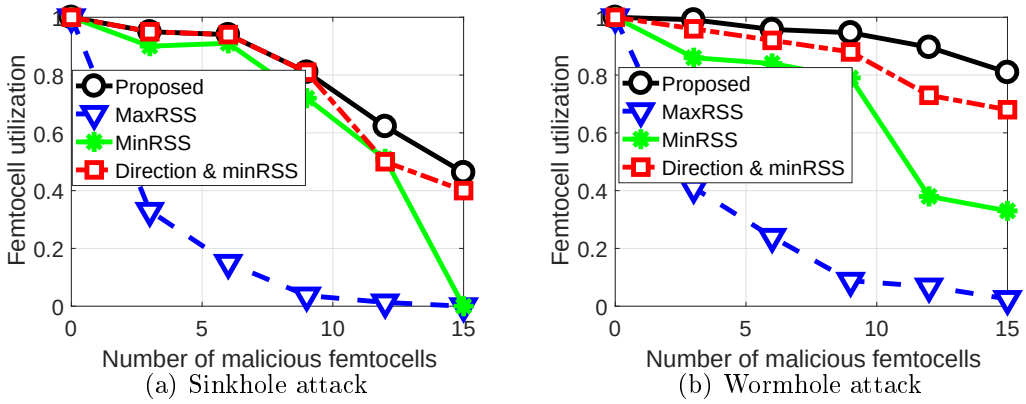

Figure 3.18: Comparison of the femtocell utilization for different attacks.

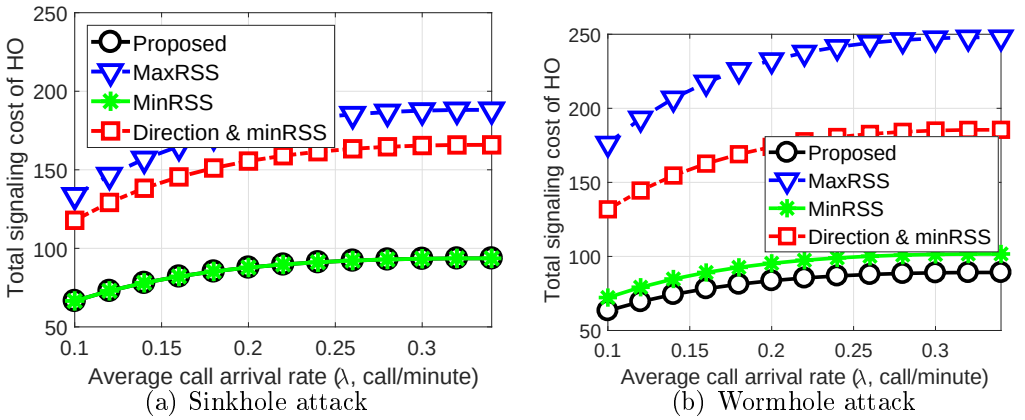

Figure 3.19: Comparison of total HO signaling cost for different attacks.

CHAPTER 4: PROPOSED MOBILITY MANAGEMENT SCHEMES FOR COGNITIVE RADIO FEMTOCELL NETWORKS

In this chapter, three schemes are proposed to avoid spectrum heterogeneity in CR femtocell networks. A power control scheme and a detective sensitivity scheme are presented for a CR femtocell network, where all channels are selected from the same spectrum band. On the other hand, a mobility management scheme is proposed for the CR femtocell network where channels are selected from different spectrum bands. The HO threshold is adapted based on the probability of interference with primary users and neighboring femtocells.

4.1 System Model

We consider a communication system that includes multiple primary networks and a femtocell-based heterogeneous network. Primary networks consist of macrocell networks, TV networks, macrocell users, and TV users. Users in primary networks are known as PUs. We consider an extension of the conventional femtocell concept under which FBSs are equipped with cognitive radios. Each cognitive radio femtocell has a number of FUEs. FUEs act as traditional femtocell users and have no cognitive capabilities. The network architecture of such a CR femtocell network is shown in Figure 4.1.

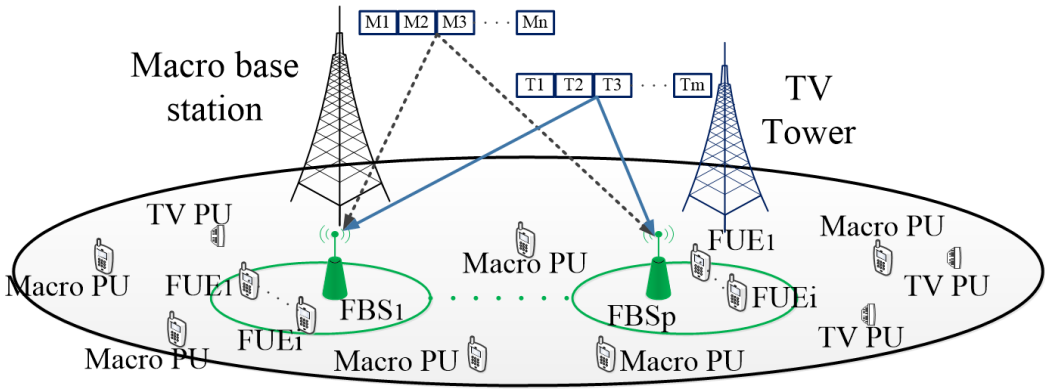

Figure 4.1: A cognitive radio femtocell network.

In this model, PUs use the licensed spectrum whenever necessary. CR FBSs actively sense the spectrum and allocate the available spectrum resources to FUEs which are not being used by any PU. CR FBSs maintain a list of the available spectrum based on the sensing outcome and update it in a time-to-time manner. Whenever a FUE becomes active within the femto-coverage area, the CR FBS assigns an available channel from the list to the FUE. If a PU appears on the channel the FUE is using, the CR FBS will ask the FUE to perform a spectrum handoff. To support multiple FUEs, a CR FBS may access different spectrum bands from different networks based on their availabilities. Therefore, the CR femtocell network acts as a multi-carrier multi-radio system with heterogeneous channels.

Under this system, we assume that there are p heterogeneous primary networks which consist of both cellular (macrocell) and TV networks. Denote M_i as the set of channels used by the ith macrocell and T_j as the channels of the jth TV tower, where $i, j = \{1, 2, 3, \dots\}$. Assume that there are q CR femtocells available in the system. Each CR FBS individually detects the available channels. The set of available channels is different from one CR FBS to another depending on their location. Consider a CR FBS within the coverage area of the ith and jth primary networks. Denote c as the set of available channels observed by femtocell r. Hence, $(c \subseteq M_i) \cup (c \subseteq T_j)$, which means the list of available channels for CR FBSs are either from macrocell

frequency band or from TV white space or both. Each time a FUE becomes active or moving towards the femtocell, the CR FBS assigns a channel to the FUE by considering the channel heterogeneity and adjusts its transmission power for the selected channel when necessary.

4.2 Proposed Power Control Scheme and Detection Sensitivity Selection Scheme

In this section, the proposed power control scheme is introduced, followed by the proposed detection sensitivity selection scheme. Both of the proposed schemes are equally effective for a low-to-high frequency change and a high-to-low frequency change during a spectrum handoff.

In the proposed power control scheme, the transmission power is controlled in a way that the RSS at the CR femtocell boundary remains the same as the RSS at the conventional femtocell boundary for any operating frequency. In this way, both the low femtocell utilization introduced by the low-to-high frequency change and the interference introduced by the high-to-low frequency change during a spectrum handoff can be avoided. The RSS at the femtocell boundary can be calculated as

$$P_{rx} = P_{tx} + G_f + G_u - PL, \tag{4.1}$$

where P_{tx} is the transmitting power of a FBS, G_f is the antenna gain of the FBS, G_u is the antenna gain of the FUE, and PL is the path-loss at the femtocell boundary. In the proposed scheme, we use the ITU-RP.1238-7 indoor path-loss model [33] to calculate the path-loss, PL, at the femtocell boundary as

$$PL = 20log_{10}(f) + Nlog_{10}(r_f) + L_f(n) - a(n), \tag{4.2}$$

where the operating carrier frequency $f = 1700$ MHz by assuming that the conventional femtocell operates on the LTE radio spectrum, r_f is the radius of a femtocell,

N is the distance power coefficient, L_f is the floor/wall penetration loss, $a(n)$ is the shadow fading, and n is the number of floors/walls. From conventional femtocell networks, we know that femtocells are designed to provide indoor coverage. Hence, femtocells have a small but enough coverage to cover a home, usually 10 meters to 15 meters in radius [3].

Whenever a CR FBS performs a spectrum handoff either from a low frequency to a high frequency or from a high frequency to a low frequency, it needs to adapt its transmission power so that the RSS at the femtocell boundary does not change drastically. This can be obtained as

$$P_{newtx} = P_{rx} - G_f - G_u + PL_{opt}, \tag{4.3}$$

where PL_{opt} is the path-loss for the new operating frequency, f_{opt}, which can be calculated using equation (4.2).

Now, we adapt the detection sensitivity of a CR FBS in order to minimize the effect of frequency variation during a spectrum handoff. The detection sensitivity is defined as the minimum signal-to-noise ratio (SNR) at which the primary signal can still be accurately (e.g., with a probability of 0.99) detected by the cognitive radio. The detection sensitivity is expressed as

$$\lambda = \frac{P_{PU} * PL(D)}{N_p}, \tag{4.4}$$

where P_{PU} is the transmission power of the primary signal, $PL(D)$ is the path-loss for the interference range of the CR, and N_p is the noise power [124, 125]. In dB, (4.4) can be expressed as

$$\lambda = P_{PU} + PL(D) - N_p. \tag{4.5}$$

Therefore, the sensing range of SU transmitters has to cover the maximum inter-

ference range in order to avoid interference at PU receivers. For the simplification of the calculation, we consider the interference range and the transmission range the same. Therefore, $PL(D) = PL$, where $D = r_f$. Now, we can calculate the sensing range as

$$r_s = 10^{\frac{\lambda + N_p - P_{PU} - 20log_{10}(f_{opt}) - L_f(n) + a(n)}{N}}. \tag{4.6}$$

The required detection sensitivity, λ_{new}, is obtained under the sensing range, r_s, which is

$$\lambda_{new} = P_{PU} + 20log_{10}(f_{new}) + Nlog_{10}(r_s) + L_f(n) - a(n) - N_p, \tag{4.7}$$

where f_{new} is equal to the operating frequency, f_{opt}, if a channel with a carrier frequency higher than or equal to the operating frequency is sensed. Otherwise, f_{new} is equal to the new sensing frequency, f_s. This adaptive detection sensitivity scheme allows a CR FBS to sense a certain range despite of the sensing frequency variation. The flow chart of our proposed power control scheme and the detection sensitivity selection scheme is presented in Figure 4.2.

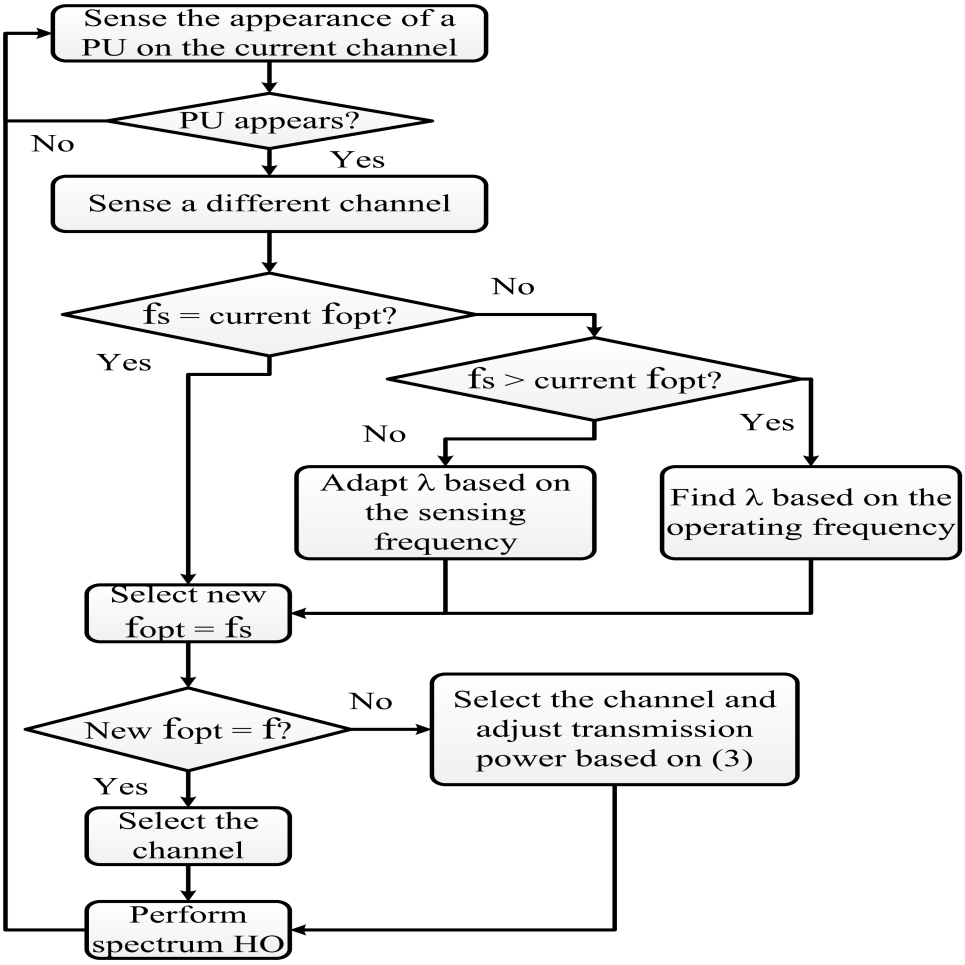

Figure 4.2: Flow chart for the proposed power control and the detection sensitivity selection scheme.

4.3 Performance Evaluation of the Power Control and Detection Sensitivity Scheme

In this section, we evaluate the performance of our proposed power control scheme and detection sensitivity selection scheme using simulations. We use Net Logo 5.0.5 to simulate our proposed algorithm in an indoor environment [121]. A single-floored two-bedroom apartment is designed to have a CR FBS which has the capacity of supporting up to eight FUEs. The CR FBS has six neighboring CR femtocells and all of them are within the coverage area of primary networks containing a macrocell and a TV tower. We consider 30 users, where each user has a probability of 0.7

to enter or exit the apartment in a random manner. All users are placed randomly and they follow a modified version of the Random Waypoint mobility model. The mobility model is modified in such a way that users only use the door to get in/out of the apartment and none of them can cross the walls. The power control scheme and the adaptive detection sensitivity scheme are evaluated under the spectrum handoff scenario of a low-to-high frequency change and a high-to-low frequency change. The simulation parameters are given in Table 4.1 [33, 46, 3].

Table 4.1: Simulation Parameters for Power Control and Detection Sensitivity Scheme

Transmission power of PUs	45 dBm
Transmission power of conventional FBS	10 dBm
Operating frequency	100 MHz to 3500 MHz
Range of femtocell (radius)	15 m
Wall penetration loss	5 dB
Outdoor penetration loss	2 dB to 10 dB
Distance power coefficient, N	28
Antenna gain of PUs	15 dB
Antenna gain of FBS, G_f	2 dB
Antenna gain of FUEs, G_u	0 dB
Shadow fading, $a(n)$	28
Number of FUEs, m	8
Number of PUs, n	30
The probability that a PU is active, σ_p	0.1 (ON/OFF process)

4.3.1 Performance Evaluation of the Power Control Scheme

To evaluate the performance of the power control scheme, we investigate the following two performance metrics: 1) *femtocell utilization:* the probability that a FUE stays connected to the femtocell while within the coverage area of the serving femtocell; 2) *the probability of interference:* the probability that a CR FBS interferes with neighboring CR FBSs and FUEs. In addition, we compare the performance of our proposed power control scheme with conventional CR femtocell networks, where no power control is used.

4.3.1.1 Femtocell Utilization

While a CR FBS performs a spectrum handoff from a low frequency to a high frequency, the transmission range of the CR FBS shrinks. As a result, some FUEs may lose their connections to the FBS. Therefore, to continue their communications, femto-to-macro handoffs are performed. Because of this shrunk transmission area, the utilization of femtocell decreases when a CR FBS changes its operating frequency from a low frequency to a high frequency. In our proposed power control scheme, the transmission power is controlled in a way that the transmission range of the femtocell remains constant. Therefore, our proposed power control scheme shows better femtocell utilization as compared to the conventional CR femtocell networks. In both cases, the femtocell utilization is calculated as the total duration a FUE is connected to a CR FBS divided by the total duration that the FUE is within the coverage area of the home FBS. The femtocell utilization of the proposed scheme and the conventional scheme is shown in Figure 4.3. The figure shows results of femtocell utilization during a low operating frequency to different high frequency changes. From the figure, it is shown that the femtocell utilization of our proposed scheme is much better than the traditional scheme.

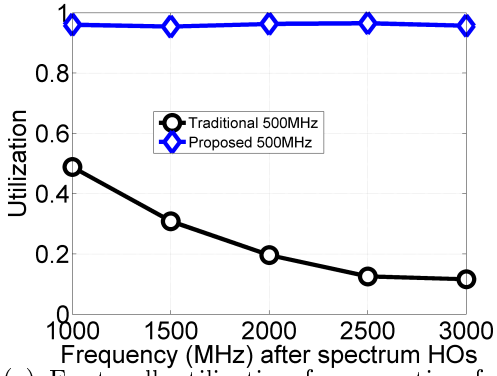

(a) Femtocell utilization for operating frequency 500MHz

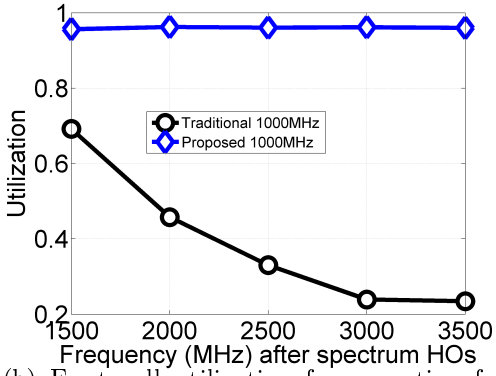

(b) Femtocell utilization for operating frequency 1000MHz

Figure 4.3: Comparison of the femtocell utilization in CR femtocell networks.

4.3.1.2 The Probability of Interference

A high-to-low frequency change extends the transmission coverage area because of the low path-loss. This extended transmission area may generate interference to other FUEs and other FBSs (i.e., neighboring femtocells). As a result, we consider the probability of interference to a neighboring CR FBS to evaluate the performance of a high-to-low frequency change during a spectrum handoff. The probability of interference under the conventional femtocell networks and the proposed scheme is shown in Figure 4.4 for a high operating frequency to a low frequency change. From the figure, it is shown that the probability of interference is high during a spectrum handoff from a high frequency to a very low frequency. However, the probability of interference is very low and almost constant under the proposed scheme, which indicates that the frequency change does not increase the probability of interference under the proposed power control scheme.

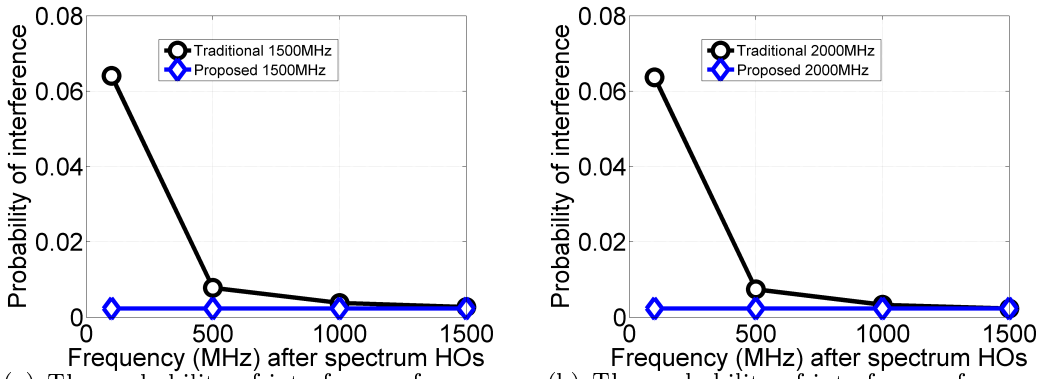

(a) The probability of interference for operating frequency 1500MHz

(b) The probability of interference for operating frequency 2000MHz

Figure 4.4: Comparison of the probability of interference.

4.3.2 Performance Evaluation of the Detection Sensitivity Selection Scheme

To evaluate the performance of the proposed detection sensitivity selection scheme, we consider two different performance metrics: 1) *detection error rate:* the probability that a PU is within the sensing area of a CR FBS, but cannot be detected by the CR

FBS; 2) *false alarm rate:* the probability that a CR FBS senses the presence of a PU which is not within the sensing range of a CR FBS. We compare our proposed scheme with conventional CR femtocell networks, which do not use any detection sensitivity scheme. In addition, we also compare the results by using only the power control scheme and by using both power control and detection sensitivity schemes together.

4.3.2.1 Detection Error Rate

When a CR FBS senses a channel with a frequency lower than the operating frequency, it can only sense an area smaller than its current transmission area. As a result, any PU within the area that is not covered by the sensing range is most likely to be undetected. The detection error rate is high in conventional CR femtocells for this reason and this may cause collision not only between PUs and FUEs, but also between FUEs from different CR femtocells. The simulated results of the detection error rate are shown in Figure 4.5, where the detection error rate is obtained under the conventional CR femtocell networks (without power control and sensitivity detection, shown as “traditional"), the proposed adaptive sensitivity selection scheme (shown as “DS"), the proposed power control scheme (shown as “power control"), and the proposed power control and adaptive sensitivity detection scheme together (shown as “combined"). The performance is shown for operating frequencies 500MHz and 1000MHz, and sensing frequencies are 1000MHz to 3000MHz and 1500MHz to 3500MHz, respectively. From the figure, it is shown that the performance of the conventional CR femtocell network and the power control scheme are almost similar, which indicates that controlling transmission power of a CR FBS does not have much effects on the sensing range. It is also shown in the figure that both the detection sensitivity scheme and the combination scheme show better results than the conventional one.

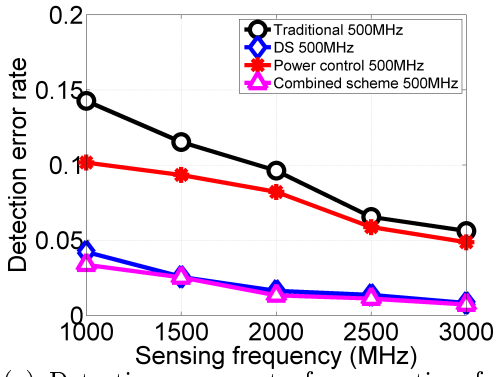

(a) Detection error rate for operating frequency 500MHz

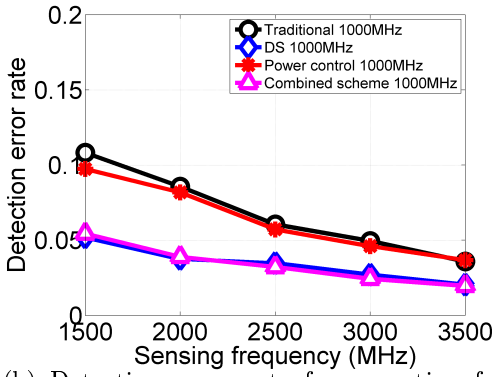

(b) Detection error rate for operating frequency 1000MHz

Figure 4.5: Comparison of the detection error rate.

4.3.2.2 False Alarm Rate

False alarm happens when a CR FBS senses the presence of a PU, which is not within the interference range. In CR femtocell networks, when the CR FBS senses a channel with frequency lower than the operating frequency, its sensing range extended. In this case, as the CR FBS senses larger area than its transmission area, it may sense some available channels as unavailable and cause false alarm. The rate of false alarm for a high-to-low frequency change is shown in Figure 4.6 for operating frequencies 2000MHz and 2500MHz. From the figure, it is shown that when a CR FBS senses a lower frequency than the operating frequency, the rate of false alarm is higher in conventional CR femtocell networks than in the CR femtocell network using our proposed detection sensitivity scheme. It is also shown in the figure that using both the power control scheme and the detection sensitivity scheme can achieve better performance than others.

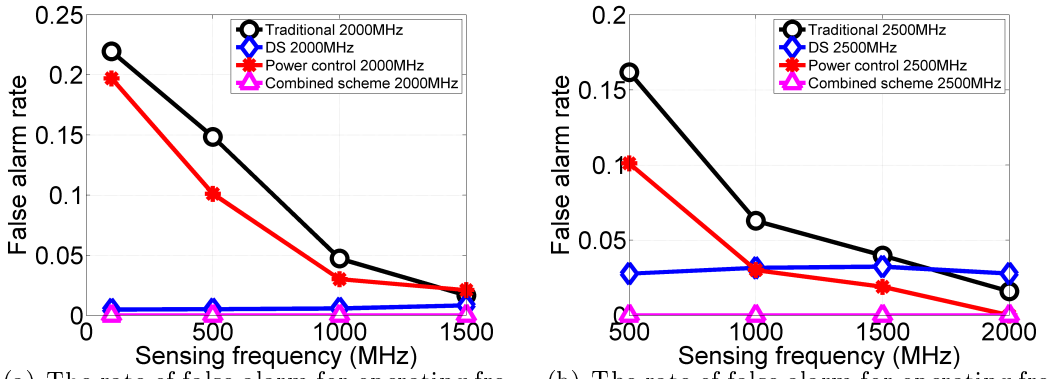

(a) The rate of false alarm for operating frequency 2000MHz

(b) The rate of false alarm for operating frequency 2500MHz

Figure 4.6: Comparison of the false alarm rate.

4.4 Proposed HO Decision Scheme

In this section, an adaptive HO-threshold selection scheme for different operating frequencies is proposed for both inbound (macro-to-femto) and outbound (femto-to-macro) HO algorithms. Our design goal is to utilize available channels as long as they are not occupied by PUs within the femtocell coverage area and at the same time, avoid possible interference from undetected PUs and from neighboring femtocells that are using the same channels. The notations used in the algorithms for our proposed scheme are shown in Table 4.2.

Table 4.2: Notations used in the HO Decision Scheme

$RSSI$	Received Signal Strength Indicator
$RSSI_f$	RSSI of a CR femtocell
$RSSI_{minFemto}$	RSSI at a traditional femtocell boundary
$RSSI_m$	RSSI of a macrocell
$RSSI_{minMacro}$	RSSI at a macrocell boundary
r_f	Coverage radius of a CR femtocell at frequency f
$P(I)$	The probability of interference
r_I	The radius of the interfered area
I_{Th}	The threshold of the probability of interference
Th_{adp}	The threshold of the adaptive RSSI
Δr	The radius of the extended interference-free area
δr	The radius of the reduced interference-free area

4.4.1 HO Threshold Adaptation and HO Decision Algorithms

In order to avoid early and late HOs, an adaptation of the HO-threshold to the operating frequency is very important for CR FBSs. In this scheme, we adapt the HO-threshold of a CR FBS based on the current operating frequency in order to compensate the difference in signal propagations on different frequency channels and to improve the femtocell utilization. The detailed spectrum sensing and selection design is out of the scope of this paper. We consider that each CR FBS has a proper sensing strategy and the channel selection is random. The selection varies based on PU activities. Parameters required for this adaptive HO-threshold scheme are $RSSI_{minFemto}$, r_f, $P(I)$, r_I, and I_{Th}.

After selecting an operating frequency, the CR FBS can calculate its coverage radius, r_f, from the ITU indoor path-loss model for urban area [33]. The path-loss is

$$PL = P_{tx} + G_t + G_u - RSSI_{minFemto}, \tag{4.8}$$

and

$$PL = 20log(f) + Nlog(r_f) + L_f(n) - a(n), \tag{4.9}$$

where P_{tx} is the transmission power of a CR FBS, G_t and G_u are the antenna gains for the CR FBS and the FUE, respectively, f is the operating frequency, L_f is the floor penetration loss factor, N is the distance power-loss coefficient, n is the number of floors/walls, and $a(n)$ is the shadow fading. Therefore, the cell radius can be calculated from (4.8) and (4.9) as

$$r_f = 10^{\frac{P_{tx}+G_t+G_u-RSSI_f-20log(f)-L_f(n)+a(n)}{N}}. \tag{4.10}$$

Now, from [125] we get

$$r_I = 1.5r_f. \tag{4.11}$$

The algorithm to determine the adaptive HO-threshold is shown in Algorithm 12.

In this algorithm, Δr is the extended distance in cell radius for which $P(I)$ is below the threshold. Δr can be calculated in two different ways. In the first approach, $\Delta r(i) = ivcos\theta$, where $i = \{1, 2, \dots\}$ represents increments in time, v is the speed of the FUE in m/s, and θ is measured in degree and is used to represent the direction of the FUE movement. However, it is not practical for a CR FBS to know the speed and the moving direction of a FUE. Considering this fact, we adopt the second approach to find Δr. In this approach, $\Delta r(i) = i$, where $i = \{1, 2, 3, \dots\}$ represents increments in distance. Now, the distance Δr can be calculated using Algorithm 13. Additionally, δr is the distance in radius for which the value of $P(I)$ is lower than the threshold. Now, δr can be calculate using Algorithm 14.

Algorithm 12: Calculation of Th_{adp}

Inputs: f, $RSSI_{minFemto}$, I_{Th};
The CR FBS determines r_f and r_I using (4.10) and (4.11), respectively;
Calculate $P(I)$ based on r_I; // the calculation is shown in Section 4.4.3
if $P(I) < I_{Th}$ **then**
    Calculate Δr using **Algorithm 2**;
    $r_{fnew} = (\Delta r + r_I)/1.5$;
else
    Calculate δr using **Algorithm 3**;
    $r_{fnew} = \delta r/1.5$;
End;
Calculate Th_{adp} for r_{fnew} using (5) and (6);

Algorithm 13: Calculation of Δr

$i = 1$;
while $i \neq 0$ **do**
    $\Delta r(i) = i$;
    Calculate $P(I)$ for $\Delta r(i) + r_I$ (as explained in Section 4.4.3);
    if $P(I) < I_{Th}$ **then**
        $i = i + 1$;
    else
        $i = 0$;
End;
$\Delta r = \Delta r(i) - 1$;

Algorithm 14: Calculation of δr

```
i = 1;
while i ≠ 0 do
    δr(i) = r_I;
    Calculate P(I) for δr(i) (as explained in Section 4.4.3);
    if P(I) > I_Th then
        r_I = r_I − 1;
        i = i + 1;
    else
        i = 0;
End;
δr = δr(i);
```

The adapted HO-threshold Th_{adp} can be obtained from

$$Th_{adp} = P_{tx} + G_t + G_u - PL_{new}, \tag{4.12}$$

where PL_{new} is the path-loss for distance r_{fnew} and

$$PL_{new} = 20log(f) + Nlog(r_{fnew}) + L_f(n) - a(n). \tag{4.13}$$

After determining the value of the adaptive HO-threshold, the serving CR FBS checks the HO decision criteria. Similar to the LTE-Advanced system, in CR femtocell networks, the Radio Resource Control (RCC) protocol manages the event that a UE reports its HO measurement to the serving BS [126]. The measurement includes UE's ID, CR femtocell's ID, and their RSSIs. When a UE sends a measurement report to the CR FBS, the CR FBS makes a decision of whether to HO or not, based on the HO decision criteria. Our proposed inbound (macro-to-femto) and the outbound (femto-to-macro) HO algorithms are given in Algorithm 15 and Algorithm 16.

Algorithm 15: Inbound HO-decision algorithm

```
if RSSI_f > Th_adp or RSSI_m < RSSI_minMacro, and RSSI_f > RSSI_m + HM then
    Perform a HO to the femtocell;
else
    Remain connected to the macrocell;
End;
```

Algorithm 16: Outbound HO-decision algorithm

if $RSSI_f < Th_{adp}$ **or** $RSSI_m > RSSI_{minMacro}$, **and** $RSSI_f + HM < Th_{adp}$ **then**
  Perform a HO to the macrocell;
else
  Remain connected to the femtocell;
End;

The selection of $RSSI_{minFemto}$, $RSSI_{minMacro}$, and I_{Th} are shown later in the paper. The calculation of $P(I)$ is also presented in Section 4.4.3 in the paper. The value of HM is taken from [22].

4.4.2 Calculation of HO Parameters

The values of $RSSI_{minFemto}$, $RSSI_{minMacro}$, and I_{Th} are determined in this section. To calculate $RSSI_{minFemto}$, we consider the traditional LTE femtocell networks operating at the 1700MHz frequency band. Fig. 4.7 presents the RSSI values for different distances from the FBS. The ITU-R.P.1238-7 indoor path-loss model is used for the RSSI calculation [33]. From the figure, it is shown that at the cell boundary, which is considered as 15m for our simulations, the $RSSI$ is -60.54dB. This $RSSI$ value is considered as $RSSI_{minFemto}$.

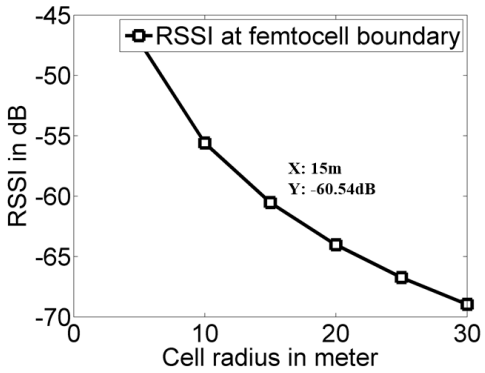

Figure 4.7: Selecting $RSSI_{minFemto}$ at the femtocell boundary.

The Okumura-Hata propagation model is used for calculating the RSSI of macrocell networks against different distances, which is shown in Figure 4.8. The $RSSI$ at macrocell boundary, which is considered as $500m$ for our simulations, is taken as

$RSSI_{minMacro}$.

On the other hand, since the probability of interference depends on various factors, such as noise, femtocell placement, and neighboring femtocells, it is difficult to select a single threshold for the probability of interference. Considering this fact, we take I_{Th} from a range of 0.1 to 0.3.

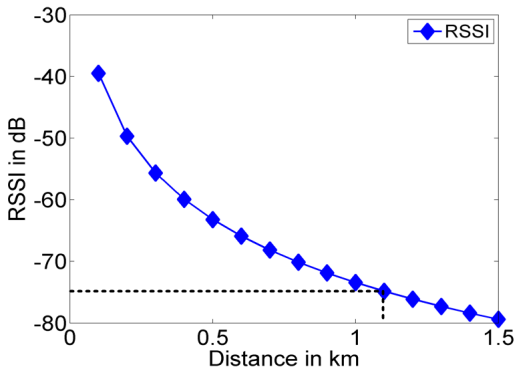

Figure 4.8: Selecting $RSSI_{minMacro}$ at the macrocell boundary.

4.4.3 Calculation of the Probability of Interference

In this section, the probability of interference from PUs and from neighboring femtocells which are using the same channels as the serving CR FBS is calculated. The probability of interference from PUs is denoted as $P(I_{PU})$ and the probability of interference from neighboring femtocells is denoted as $P(I_n)$. Now, the total probability of interference is

$$P(I) = P(I_{PU}) + P(I_n). \tag{4.14}$$

4.4.3.1 The Probability of Interference from PUs

We assume that the sensing area of a CR FBS is similar to the interference area of the CR FBS. Therefore, the CR FRS can sense the presence of any PU within the interference area. Now, to calculate the probability of interference from PUs, we consider two different scenarios. In the first scenario, PUs appear in the interference area of CR FBSs. In this case, the CR FBS can sense the appearance of PUs. Therefore,

the probability of interference from PUs in this case is $P(I_{PU}) = 0$. This first scenario is applicable for Algorithm 12, where we consider the probability of interference for r_I and for Algorithm 14, where we consider the probability of interference for δr. In both cases, the PU is within the sensing area. In the second scenario, PUs appear within the area which is larger than the sensing area of the CR FBS. We use this scenario to calculate the P(I) for Algorithm 13.

To determine $P(I_{PU})$ for the second scenario, we consider the Venn diagram shown in Figure 4.9. We assume that K PUs are evenly distributed within the coverage area of a primary network A_m, which is equivalent to the coverage area of the macrocell with a radius of r_m. The interference area of a CR femtocell is $A_f = \pi(r_I)^2$ and the extended area is $A_{new} = \pi r_{new}^2$, where $r_{new} = \Delta r + r_I$. Since the probability of interference from PUs is equal to zero in the interference area, to calculate $P(I_{PU})$ we need to calculate the probability of interference from PUs within the extended area. Now, $P(A^c \cap B) = \frac{r_{new}^2 - r_I^2}{r_m^2}$ is defined as the probability that an event happens in the extended area. Therefore, the probability that k_1 PUs are within the extended area of A_{new} is

$$P(k_1) = \binom{K}{k_1} (\frac{r_{new}^2 - r_I^2}{r_m^2})^{k_1} (1 - \frac{r_{new}^2 - r_I^2}{r_m^2})^{K-k_1}. \tag{4.15}$$

The probability that k_2 PUs are active given that k_1 PUs are within the new interference area of a femtocell is

$$P(k_2|k_1) = \binom{k_1}{k_2} \sigma^{k_2} (1-\sigma)^{k_1-k_2}, \tag{4.16}$$

where σ is the probability that a PU is active. And

$$\sigma = \frac{E[ON]}{E[ON] + E[OFF]}, \tag{4.17}$$

where $E[\cdot]$ is the average value of the ON period and OFF period. If c channels

are available for a CR femtocell and each CR femtocell can support M users, the probability that a CR FBS chooses a set M channels from c channels is equal to $1/\binom{c}{M}$. Then the probability that any PUs are using the same channels = 1− the probability of no PUs are using the same channels = $1 - \binom{c-M}{1}/\binom{c}{1}$, because a PU can only choose one channel at a time. Therefore, the probability that k_3 PUs are using the same channels as the serving CR femtocell given that k_2 PUs are active is

$$P(k_3|k_2) = \binom{k_2}{k_3}(1 - \frac{\binom{c-M}{1}}{\binom{c}{1}})^{k_3}(\frac{\binom{c-M}{1}}{\binom{c}{1}})^{k_2-k_3}. \tag{4.18}$$

Hence, the probability that any PUs are using the same channel within the femtocell extended area is

$$P(I_{PU}) = \sum_{k_1=1}^{K}\sum_{k_2=1}^{k_1}\sum_{k_3=1}^{k_2} P(k_1)P(k_2|k_1)P(k_3|k_2). \tag{4.19}$$

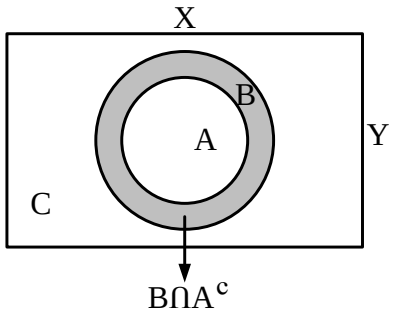

Figure 4.9: A Venn diagram representing the coverage area of a primary network denoted by C, A denotes the interference area of a CR femtocell, and B denotes the extended area of the CR femtocell, for which the $P(I_{PU})$ needs to be calculated.

4.4.3.2 The Probability of Interference from Neighboring Femtocells

Similar to the probability of interference from PUs, we consider two different scenarios for determining the probability of interference from neighboring femtocells. For the first scenario, we consider the Venn diagram shown in Figure 4.10 to calculate

$P(a)$, which is the probability that an event happens within the overlapping interference area of the serving femtocell and its neighboring femtocells. From the figure, we determine the overlapping area between the serving CR femtocell A and neighboring femtocells as $\{(A \cap f_1) \cup (A \cap f_2) \cup \cdots \cup (A \cap f_m)\}$. However, neighboring femtocells may also overlap with each other. Considering this overlap, the total overlapping area is $\{(A \cap f_1) \cup (A \cap f_2) \cup \cdots \cup (A \cap f_m)\} - \{(f_1 \cap f_2) \cup (f_2 \cap f_3) \cup \cdots \cup (f_{m-1} \cap f_m) \cup (f_m \cap f_1)\}$. Therefore, we calculate the probability that an event happens in the overlapping area between neighboring femtocells for the first scenario as

$$P(a) = \{P(A \cap f_1) + \cdots + P(A \cap f_m)\} -$$

$$\{P(f_1 \cap f_2) + \cdots + P(f_{m-1} \cap f_m) + P(f_m \cap f_1)\}. \tag{4.20}$$

Since the placement of neighboring femtocells is random, it is nearly impossible to determine the actual overlapping area between neighboring femtocells. Therefore, we consider $P(a)$ as a variable and $0 \leq P(a) \leq 1$.

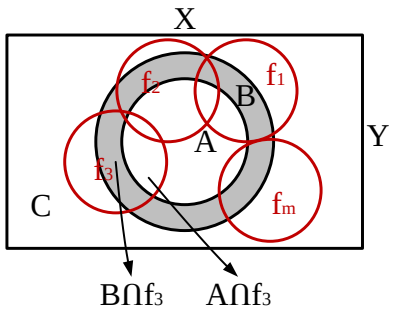

Figure 4.10: A Venn diagram representing the transmission area of a primary network denoted by C, a serving CR femtocell, which is surrounded by m neighboring femtocells, and the interference area of femtocell as A and the extended area as B.

In the second scenario, as the area is extended, the probability that any event happens within the overlapping area will be equal to the summation of the probability that any event happens within the overlapping interference area and the probability

that any event happens within the extended area. Therefore, the probability that an event happens within the overlapping area of the expanded area of a femtocell and its neighboring femtocells is

$$P(b) = P(a) + \frac{r_{new}^2 - r_I^2}{r_m^2}. \tag{4.21}$$

Now, we obtain the probability that any FBS is within that overlapping area. We assume that Q CR FBSs are evenly distributed among the coverage area of πr_m^2. The probability of t_1 FBSs from Q FBSs within the overlapping area as

$$P(t_1) = \binom{Q}{t_1} P(b)^{t_1} (1 - P(b))^{Q - t_1}. \tag{4.22}$$

The probability that t_2 FBSs are active given that t_1 FBSs are within the overlapping area and the probability of t_3 FBSs using the same channels as the serving femtocell given that t_2 FBSs are active can be calculated as

$$P(t_2|t_1) = \binom{t_1}{t_2} \lambda^{t_2} (1 - \lambda)^{t_1 - t_2}, \tag{4.23}$$

and

$$P(t_3|t_2) = \binom{t_2}{t_3} (1 - \frac{\binom{c-M}{M}}{\binom{c}{M}})^{t_3} (\frac{\binom{c-M}{M}}{\binom{c}{M}})^{t_2 - t_3}, \tag{4.24}$$

where λ is the probability that a CR FBS is active, c is the number of channels available for a CR femtocell, and M is the total number of channels used by a CR femtocell as described before. Using these probabilities, $P(I_n)$ can be found as

$$P(I_n) = \sum_{t_1=1}^{Q} \sum_{t_2=1}^{t_1} \sum_{t_3=1}^{t_2} P(t_1) P(t_2|t_1) P(t_3|t_2). \tag{4.25}$$

Then, $P(I)$ can be calculated using (4.14).

4.4.4 Performance Evaluation of the HO Decision Scheme

In this section, we evaluate the performance of the proposed mobility management scheme. First, we introduce the setting of scenarios in the simulation. Then, the performance of the proposed scheme is evaluated in terms of femtocell utilization, required transmission time, and throughput.

4.4.4.1 Simulation Setup

We simulate the HO process of a closed-access (only the registered users have access to a femtocell) CR femtocell network. We use Net Logo 5.0.5 [121] to simulate our proposed scheme in an indoor environment. We investigate the HOs, triggered by FUEs, in an area of πr_m^2 for a certain simulation time. A single-floored two-bedroom apartment is designed to have a CR FBS which has the capacity of supporting up to eight FUEs. The CR FBS has six neighboring CR femtocells and all of them are within the coverage area of primary networks containing a macrocell and a TV tower. We consider 20 users with a probability of 0.7 to enter and exit the apartment in a random manner. The neighboring CR FBSs are placed in a way that the overlapping area is between 0 and 0.3 with the serving CR femtocell. All users are placed randomly and they follow a modified version of the Random Waypoint mobility model [127]. The mobility model is modified in such a way that users only use the door to get in/out of the apartment and none of them cross the walls. The values of the parameters used in the simulation are listed in Table 4.3.

We mainly investigate the following three metrics to evaluate the performance of our proposed scheme. These metrics are 1) *femtocell utilization*: the probability that a FUE stays connected to the femtocell while within the coverage of its home FBS, 2) *required transmission time*: total transmission time required to transmit a specific length of video traffic including all delays, and 3) *Throughput*: the amount of traffic the CR FBS can transmit in a unit time. In addition, we compare our pro-

posed scheme with the traditional mobility management scheme, where the HO RSSI threshold is fixed and does not change with the variation of operating frequencies. We take three different values for both $P(a)$ and I_{Th} to show the variation and the comparison of the proposed scheme with the traditional scheme.

Table 4.3: Simulation Parameters for Power Control and Detection Sensitivity Scheme

Macrocell transmission power, P_m	45 dBm [5]
Radius of macrocells	500 m
Femtocell transmission power, P_{tx}	15 dBm [5]
Radius of femtocells	15 m [22]
Operating frequencies of PUs	$500 - 2500$ MHz
Users speed	5 km/hr[22]
Minimum femtocell RSSI, $RSSI_{minFemto}$	-60.54 dB
Minimum macrocell RSSI, $RSSI_{minMaco}$	-62.21 dB
Interference threshold, I_{Th}	0.1 to 0.3
Overlapping area, $P(a)$	0.1 to 0.3
Floor penetration loss, L_f	5 dB[33]
Distance power loss coefficient, N	28 [33]
Shadow fading, $a(n)$	28 [33]
Antenna gain of FBSs, G_t	2 dB[33]
Antenna gain of FUEs, G_u	0 dB[33]
Total number of PUs, K	20
The probability that a PU is active, σ	0.7 [45]
Total number of femtocells, Q	7
The probability that a femtocell is active, λ	0.6
Number of channels in the system, c	200
Delivered data	10000000 bps
Channel bandwidth	5 MHz
Total simulation time	20000 secs

4.4.4.2 Femtocell Utilization

The femtocell utilization is determined as the average time an active FUE is served by the CR femtocell while it is within the area of the femtocell. As CR femtocells are deployed for offloading cellular traffic and to provide cost-effective service to FUEs, it is expected that when a FUE is within the coverage area of its home CR FBS, it should be connected to it. The femtocell utilization is shown in Figure 4.11 with

respect to different operating frequencies. From the figure, it is shown that the femtocell utilization decreases when the serving CR FBS interferes more with the neighboring femtocells. A high value of $P(a)$ shows a high probability of overlapping area, therefore, a high interference from neighboring femtocells. On the other hand, the selection of a high I_{Th} represents a high femtocell utilization. This is because a high value of I_{Th} means a more interference tolerant network. We also observe that the traditional mobility management scheme shows worse femtocell utilization in each of these scenarios as compared to the proposed mobility management scheme.

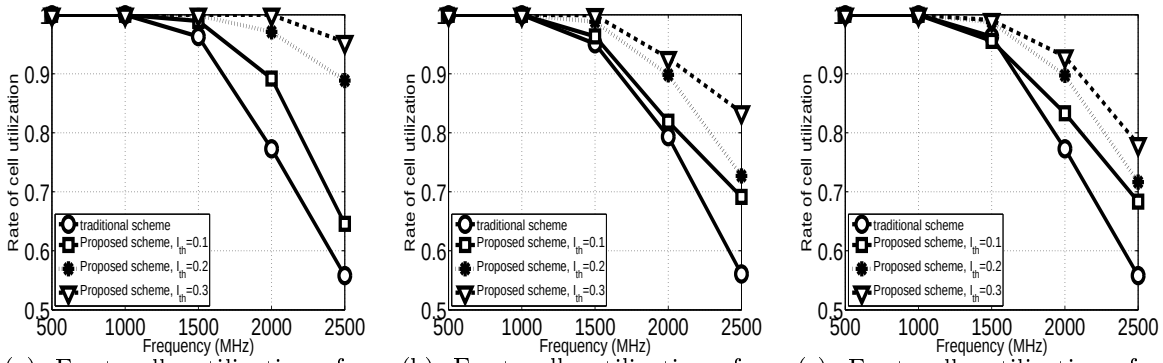

(a) Femtocell utilization for $P(a) = 0.1$

(b) Femtocell utilization for $P(a) = 0.2$

(c) Femtocell utilization for $P(a) = 0.3$

Figure 4.11: Comparison of the femtocell utilization for different femtocell overlapping area.

4.4.4.3 Required Transmission Time

To simulate the performance of the required transmission time, we use the method from [42]. When a FUE performs an HO, it requires a high transmission time due to the HO delay. Our proposed mobility management scheme uses the adaptive HO-threshold to reduce unnecessary HOs, which are caused by the channel heterogeneity in CR femtocell networks, therefore, reduces HO delay. In the simulation, we determine the required transmission time for a traffic of 10 Mb for both proposed and traditional schemes. Figure 4.12 shows the required transmission time with respect to various operating frequencies. From the figure, it is observed that the traditional

scheme requires more time to transmit the same data traffic than the proposed one. We also observe that the required transmission time increases with the interference from the neighboring femtocells and it decreases with the I_{Th}.

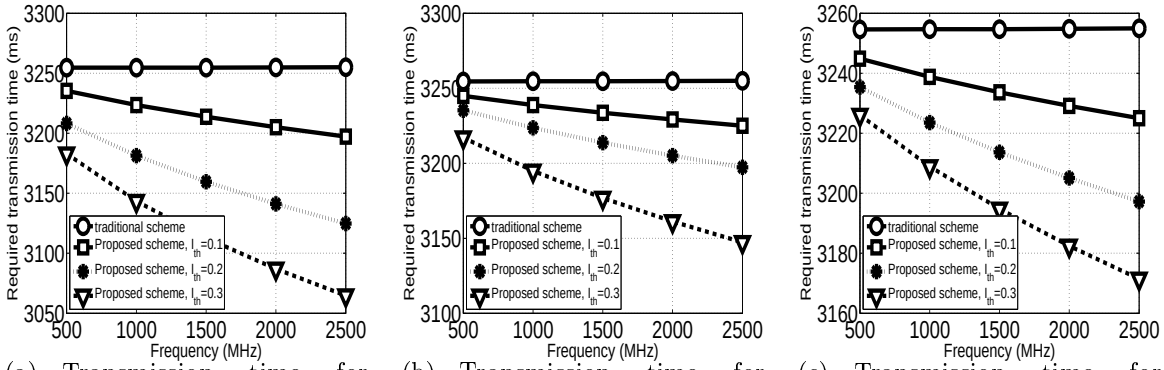

(a) Transmission time for $P(a) = 0.1$

(b) Transmission time for $P(a) = 0.2$

(c) Transmission time for $P(a) = 0.3$

Figure 4.12: Comparison of the required transmission time.

4.4.4.4 Throughput

Throughput is calculated as the total size of transmitted data divided by the total required time to transmit the data. A high throughput indicates a more reliable network. The comparison of throughput of our proposed mobility management scheme and the traditional mobility management scheme is shown in Figure 4.13. It is observed from the figure that the increment of both $P(a)$ and I_{Th} reduces the throughput of CR femtocell networks. The reason behind this is that the increment of $P(a)$ and I_{Th} increases interference in femtocell networks.

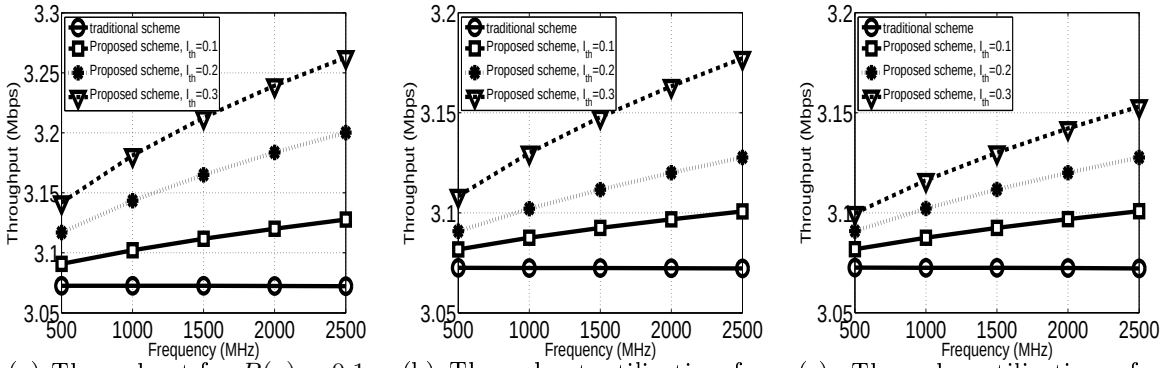

(a) Throughput for $P(a) = 0.1$ (b) Throughput utilization for $P(a) = 0.2$ (c) Through utilization for $P(a) = 0.3$

Figure 4.13: Throughput comparison.

CHAPTER 5: PROPOSED HO DECISION ALGORITHM FOR MOBILE EDGE COMPUTING

A migration decision algorithm along with an HO decision algorithm and an HO decision algorithm with the incorporation of radio offloading and computation offloading are presented in this chapter. the deployment of MEC with a BS introduces special challenges to mobility management. First, a MEC can only be accessed within the coverage area of its BS. Therefore, a user needs to perform both a radio handoff (HO) and a service migration when moving out of the cell coverage range. Second, as MECs have limited computational resource and storage, the target MEC may not have sufficient available resources to support new users. Therefore, a user with computation task may be forced to perform a radio HO to a different target BS in order to successfully migrate the service. These cause unnecessary HOs in cellular networks, especially when MECs are deployed with small cells, e.g., femtocells. These unnecessary HOs and service migrations incur a large signaling and migration cost. In this chapter, a novel architecture, SharedMEC, to support user mobility is presented first. Then, a service HO decision algorithm and an analytical model to analyze the total cost which considers the total HO signaling cost, total migration signaling cost, and total migration cost is explained. On the other hand, femtocells are deployed to serve radio offloading and both MEC and the core cloud are deployed to serve computation offloading. When an HO is triggered, the user selects a target cell and a cloud to fulfill both of these offloading issues. In addition, how to select the proper HO decision parameters is shown in this chapter.

5.1 Proposed Service HO Decision Algorithm and Total Cost Analysis

In this section, we propose a service HO decision algorithm in MEC systems based on our proposed SharedMEC architecture. An analytical model analyzing the total cost of an HO and a service migration for a mobile user is also presented.

5.1.1 System Model

The architecture of the SharedMEC is presented in this section. In this architecture, each BS has a MEC with it, and a group of BSs share a MEC server which does not exist in the traditional MEC-deployed systems. Additionally, this SharedMEC can be implemented in any edge cloud networks, e.g., in MEC-deployed femtocell networks, in MEC-deployed macrocell networks, and in Cloudlets. Furthermore, though in this paper we consider this architecture in MEC-deployed femtocell networks, the proposed service HO decision algorithm and the analytical model can be applied to any edge cloud systems with or without considering this architecture. In the system model shown in Figure 5.1, several FBSs form a cluster and all FBSs in the cluster share a MEC (which has larger computational resources and storage than the edge cloud at the FBS). The shared MEC may or may not be connected to the femto gateway (FGW). However, we propose to place the MEC with the FGW, so that it can be shared by all FBSs connected to the FGW. Therefore, the shared-MEC and FBSs are wire connected via the FGW. In addition, all wire connections in the proposed architecture are the same as in the traditional femtocell architecture. A number of such femtocell clusters can be within a macrocell coverage area.

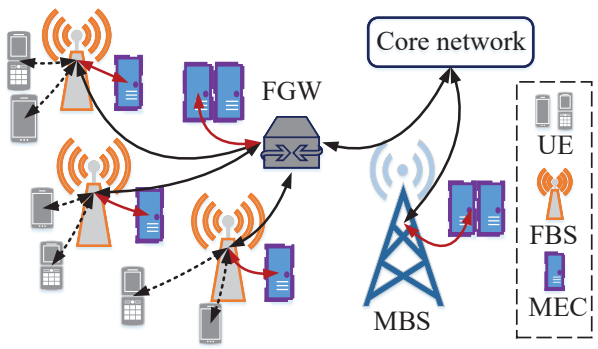

Figure 5.1: The architecture of the SharedMEC.

The proposed architecture has several characteristics and advantages over the traditional MEC-deployed femtocell networks. First of all, this system can be easily deployed without any major changes in the traditional MEC-deployed networks. Second, both femto-MEC and shared-MEC are at most two-hops away from UEs. Third, sharing the information of available resources between the serving MEC and the target MEC is easier because they are wire connected, therefore, the migration cost can be reduced. Finally, a path selection between the serving MEC and the target MEC is not necessary, which reduces the delay of performing a migration.

In addition to the proposed architecture, to support the seamless service transfer between two MECs, we use the 3-layer container system as described in [128]. In the proposed SharedMEC, all MECs are deployed by the same service provider. Therefore, all MECs have the same “bins/libs" layer of the container. Now, our goal is to transfer the data instance when the application is available at the target MEC or transfer both the data instance and the application if the application is not available at the target MEC. Since we only focus on transferring the service between MECs, we named this process as *service HO*.

5.1.2 Service HO Decision Algorithm

In the service HO decision algorithm, the service HO decision is made based on available resources, application type, and application availability. As the proposed

Algorithm 17: Service HO Decision Algorithm

```
if Application availability = 1 then
    if 0MB < RAM utilization < 300MB then
        Perform service HO;
    else
        Find T_Time = dataSize_Remaining / Speed_FBS-FGW;
        Find P_Time = dataSize_Remaining / Speed_MEC;
        if T_Time < P_Time then
            Perform service HO;
        else
            Sent result after completing the task;
else
    if 0MB < RAM utilization < 100MB then
        Perform service HO;
    else
        Find T_Time = (dataSize_Remaining + appSize) / Speed_FBS-FGW;
        Find P_Time = (dataSize_Remaining + appSize) / Speed_MEC;
        if T_Time < P_Time then
            Perform service HO;
        else
            Sent result after completing the task;
End;
```

SharedMEC architecture uses a MEC that is shared by a group of FBSs, it is not difficult to get this information before making a service HO decision. Therefore, the resource availability and the application availability can be obtained from the FGW. In addition, the type of an application can be determined based on the RAM utilization. Different application types have different memory requirements, e.g., a video streaming requires approximately 30MB and a game requires approximately 1MB RAM utilization, and the application that uses more memory needs longer migration time [128]. Our proposed service HO decision algorithm is shown in Algorithm 17.

In the algorithm, T_{Time} represents the time to transfer a service, P_{Time} represents the time to process a service at the serving MEC, $dataSize_{Remaining}$ is the size of the remaining computation, $appSize$ is the size of the application, $Speed_{FBS-FGW}$ is the speed of the wire connection between an FBS and an FGW, and $Speed_{MEC}$ is the CPU speed of a MEC. The application availability is represented by $\{0, 1\}$, where 1

means an application is available. The proposed algorithm is designed in a way that all real-time applications perform migration to avoid disconnection.

5.1.3 Total Cost Analysis

In a MEC-deployed femtocell network, a service HO is triggered only when a radio HO is performed. Therefore, the mobility events that cause different radio HO scenarios are responsible for the service HOs. Now, in any homogeneous network, there are four mobility events that cause HOs. These events are shown in Figure 5.2 and Figure 5.3.

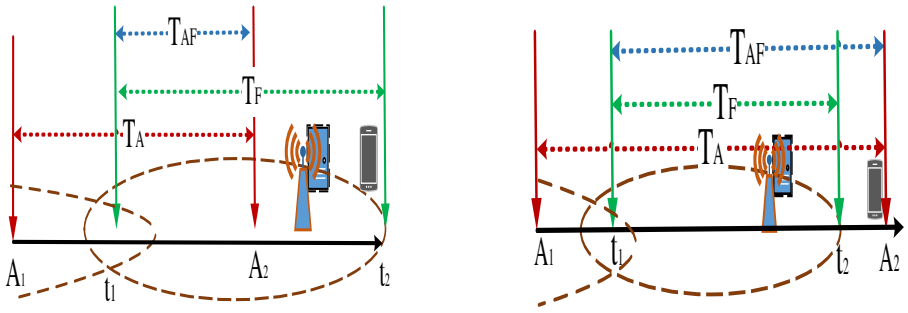

(a) A HO happens at t_1 (b) Two HOs happen at t_1 and t_2

Figure 5.2: Timing diagram for mobility events in MEC one and two HO scenarios.

The event in Figure 5.2(a) represents an active UE performs an HO to a target cell, then becomes inactive. An active UE performs an HO to a target cell, then performs another HO before becoming inactive is the event shown in Figure 5.2(b). Similarly, an inactive UE moves into a MEC coverage area, then becomes active and performs an HO to another cell is the event shown in Figure 5.3(a). In Figure 5.3(b), no HOs happen since the UE becomes active and finishes its task before moving out of the cell area. If the probability of the events in Figure 5.2(a), 5.2(b), and 5.3(a) are considered as P_{b1}, P_{b2}, and P_{b3}. Then, we can get the probability of service HOs as:

$$P_{serviceHO} = P_{b1} + 2P_{b2} + P_{b3}. \tag{5.1}$$

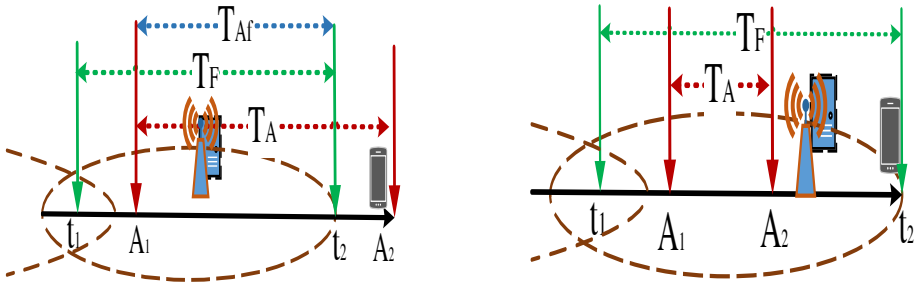

(a) A HO happens at t_2 (b) No HOs happen

Figure 5.3: Timing diagram for mobility events in MEC for one and no HO scenarios.

In the timing diagrams, T_A and T_F are independent random variables. T_A denotes the session duration which is exponentially distributed with mean $1/\eta$, and the probability density function of this session duration is $f_{TA}(t) = \eta e^{-\eta t}$. Similarly, T_F is the duration of a UE being within the coverage area of a femtocell which is exponentially distributed with mean $1/\mu$, and the probability density function of this duration of stay is $f_{TF}(t) = \mu e^{-\mu t}$. T_{AF} and T_{Af} in the timing diagram follow the memoryless property of the residence times, T_A and T_F, respectively. In addition, the probability density function of T_{AF} is f_{AF} (which is exponentially distributed with mean $1/\eta$) and the probability density function of T_{Af} is f_{Af} (which is exponentially distributed with mean $1/\mu$). Now, we can calculate P_{b1}, P_{b2}, and P_{b3} as:

$$P_{b1} = P(A_1 < t_1 < A_1 + T_A) \cdot P(T_{AF} \leq T_A), \tag{5.2}$$

$$P_{b2} = P(A_1 < t_1 < A_1 + T_A) \cdot P(T_{AF} > T_F), \tag{5.3}$$

and

$$P_{b3} = P(t_1 < A_1 < t_1 + T_F) \cdot P(T_A \geq T_{Af}). \tag{5.4}$$

Using the Laplace transform, we have

$P_{b1} = \int_0^\infty \int_t^\infty \lambda t e^{-\lambda t} f_{TA}(x) dx dt \cdot$

$$(1 - \int_0^\infty \int_t^\infty \eta e^{-\eta t} f_{AF}(y) dy dt), \tag{5.5}$$

$P_{b2} = \int_0^\infty \int_t^\infty \lambda t e^{-\lambda t} f_{TA}(y) dy dt \cdot$

$$(1 - \int_0^\infty \int_t^\infty \mu e^{-\mu x} f_{AF}(t) dx dt), \tag{5.6}$$

and $P_{b3} = \int_0^\infty \lambda t e^{-\lambda t} f_{Af}(t) dt \cdot$

$$\int_0^\infty \int_t^\infty \eta e^{-\eta y} f_{Af}(t) dy dt. \tag{5.7}$$

Solving (5.5), (5.6), and (5.7), we can obtain the probabilities as:

$$P_{b1} = \frac{\lambda \eta}{(\lambda + \eta)^2 (\mu + \eta)}, \tag{5.8}$$

$$P_{b2} = \frac{\lambda \mu}{(\lambda + \eta)^2 (\mu + \eta)}, \tag{5.9}$$

and

$$P_{b3} = \frac{\lambda \mu^2}{(\lambda + \eta)^2 (\mu + \eta)}. \tag{5.10}$$

Finally, the total cost can be calculated as:

$C_{total} = P_{serviceHO} \cdot (\sum T_j^i$

$$+ \sum P_i + \sum CT_j^i + \sum CP_i + \sum M_j^i), \tag{5.11}$$

Here, T_j^i is the delivering cost of an HO message between node i and j, P_i is the processing cost of a message at node i, CT_j^i is the delivering cost of a service HO message between node i and j, CP_i is the processing cost of a service message at

node i, and M_j^i is the migration cost of a service between node i and j. The radio and service HO signaling procedure is given in Figure 5.4. We can get T_j^i, P_i, and CT_j^i from the HO signaling procedure as:

$$\sum(T_j^i) = 2T_{UE}^{FBS} + 10T_{FGW}^{FBS} + 2T_{FGW}^{MME}, \tag{5.12}$$

$$\sum(P_i) = P_{UE} + P_{FBS} + 2P_{FGW} + P_{MME}, \tag{5.13}$$

and

$$\sum(CT_j^i) = 2T_{FGW}^{FBS} + 5T_{MEC}^{FBS}. \tag{5.14}$$

However, $4T_{MEC}^{FBS}$ does not add extra cost in the process because they happen when another radio signaling is in action. Therefore,

$$\sum(CT_j^i) = 2T_{FGW}^{FBS} + T_{MEC}^{FBS}. \tag{5.15}$$

In addition, CP_i and M_j^i can be obtained from the HO signaling procedure as:

$$\sum(CP_i) = P_{FBS} \tag{5.16}$$

and

$$\sum(M_j^i) = T_{FGW}^{FBS} + 2T_{MEC}^{FBS}. \tag{5.17}$$

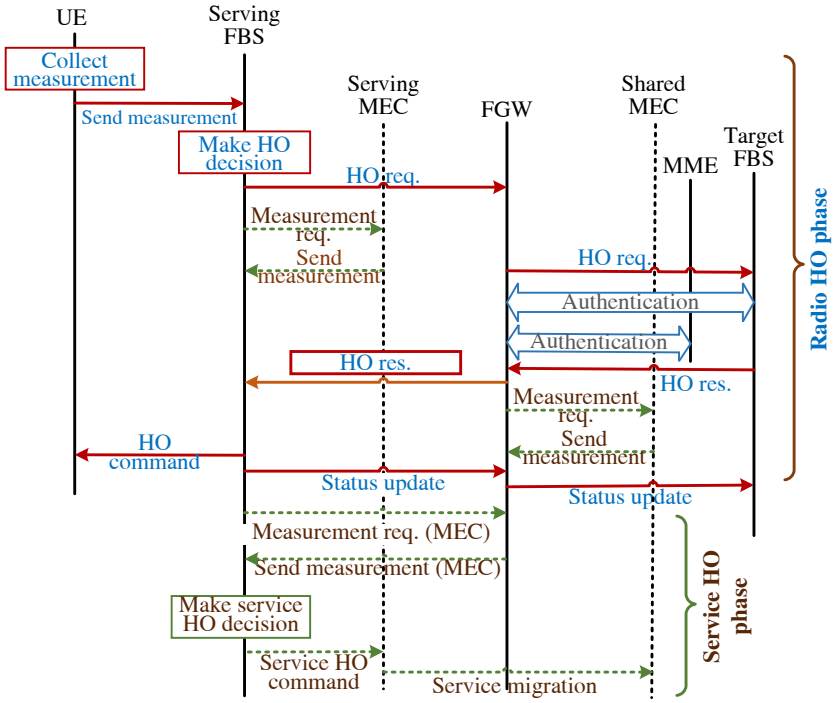

Figure 5.4: Total HO and migration signaling.

Notations for different costs and their values are given in Table 5.1 [24, 20, 118, 122, 131, 129, 130] and Table 5.2 [128]. In Table 5.2, AppType 1 (memory size: 0MB to 30MB) represents gaming applications, AppType 2 (memory size: 31MB to 99MB) represents audio or video streaming, AppType 3 (memory size: 101MB to 299MB) represents detection and editing applications, and AppType 4 (memory size: over 300MB) represents simulation and computation applications.

Table 5.1: HO Signaling Cost Parameters

T_{UE}^{FBS}	Transmission cost between a UE and an FBS	2
T_{FBS}^{FGW}	Transmission cost between an FBS and an FGW	2
T_{FGW}^{MME}	Trnsmission cost between an FGW and an MME	4
T_{FBS}^{MEC}	Transmission cost between an FBS and an MEC	1
P_{UE}	Processing time at UE	40
P_{FBS}	Processing cost at FBS	3
P_{FGW}	Processing cost at FGW	2
P_{MME}	Processing cost at MME	4

5.1.4 Performance Evaluation

In this section, we evaluate the performance of the proposed service HO decision scheme in terms of total signaling cost. We use NetLogo 6.0.1 [121] to simulate the SharedMEC environment. We deploy fifteen femtocells in a random manner and each FBS has a MEC that is deployed with it. We also deploy three shared-MECs, each of these MECs is shared by five FBSs. All users follow the Random Waypoint mobility model. We use 1 to 25 users in the system. The Okumura-Hata propagation model is used for the macrocell network, and the ITU-R P.1238-7 indoor path-loss model [33] is used for the femtocell network. The parameters used in our simulation are listed in Table 5.3 [22].

To evaluate the performance of the proposed model and algorithm, we investigate the following two performance metrics: 1) *Total cost of service HOs*: the summation of the total HO signaling cost, total migration signaling cost, and total migration cost when a user performs both radio and service HOs from the serving FBS to the target FBS; 2) *Total cost of results forward*: the summation of the total HO signaling cost, processing cost of the service at the service MEC, and the cost of result transfer when the serving FBS decides to process the service and send the result back to the UE via the shared-MEC. Additionally, we compare our proposed model and

Table 5.2: Migration Cost

Application available at the shared-MEC			
App Type	**Data Transfered**	**Migration Time**	**Migration Cost**
AppType 1	1.6MB	6.4s	20
AppType 2	7.4MB	8.5s	6
AppType 3	10MB	15.5s	8
AppType 4	97.1MB	19.8s	1
Application not available at the shared-MEC			
AppType 1	2.7MB	10.9s	34
AppType 2	184.6MB	37.3s	25
AppType 3	365MB	70.1s	35
AppType 4	97.6MB	27.2s	2

algorithm with the traditional MEC model and two other variations of our proposed model to analyze the worst and the best case scenarios. These algorithms are: 1) *No SharedMEC*: MECs are only deployed with each FBS and our proposed service HO decision algorithm is used; 2) *SharedMEC: With App*: our proposed system model and service HO decision algorithm are used, however, it is considered that applications are always available at the target MEC; 3) *SharedMEC: No App*: our proposed system model and service HO algorithm are used, however, it is considered that applications are never available at the target MEC.

5.1.4.1 Total Cost of Service HOs

The performance of the total cost for service HOs is given in Figure 5.5(a). The total cost is determined by considering all radio HO signaling cost, all migration signaling cost, and the migration cost. It is calculated for an exponential session duration (mean $1/\eta = 3$), an exponential residence time (mean $1/\mu = 10$), and the Poisson session arrival rate λ (0.1 to 0.34). Then, the total HO signaling cost is calculated by multiplying the signaling cost of an HO by the rate of HOs, which also includes the rate of unnecessary HOs. From the figure, we can observe that the total cost in our proposed model is lower than that in the traditional MEC model. Furthermore, we can observe that our proposed model shows better performance than

Table 5.3: Simulation Parameters for Service HO

Macrocell transmission power, P_m	45 dBm
Radius of macrocell	1.2 km
Femtocell transmission power, P_f	10 dBm
Radius of femtocell	15 m
Users speed	0 to 10 km/hr
Threshold, Th	-45 dB
Wall penetration loss	5 dB
Outdoor penetration loss	2 dB - 10 dB
$RSSI_{min}$	-75 dB
Th_{spd}	5 km/hr
HM_{max}	5 dB

the traditional one even in the worst case (no applications are available at the target MEC) and the best case (all applications are always available at the target MEC) scenarios. The availability of applications at the target MEC encourage more services to be handed over to the target MEC, therefore, the migration cost is higher in this case than in the no application available case, which also forces the total cost to be higher.

5.1.4.2 Total Cost of Results Forward

In Figure 5.5 (b), the performance of results forwarding cost for our proposed and the traditional models is presented. Here, the total cost of results forwarding is determined by considering all radio HO signaling cost, all migration signaling cost, the processing cost of the service at the serving MEC, and the result forwarding cost. From the results in Figure 5.5(b), we can observe that our proposed model presents better performance than the traditional MEC model. We can also observe that the total cost of results forwarding is lower in our proposed model than that in the traditional one even in the worst case and the best case scenarios. Additionally, the total cost of results forwarding is higher in SharedMEC: No App. This is because when applications are not available at the target MEC, all services that do not require live migration check whether the migration cost is higher than the result transfer cost. If the migration cost is higher, then these services are executed at the serving MEC.

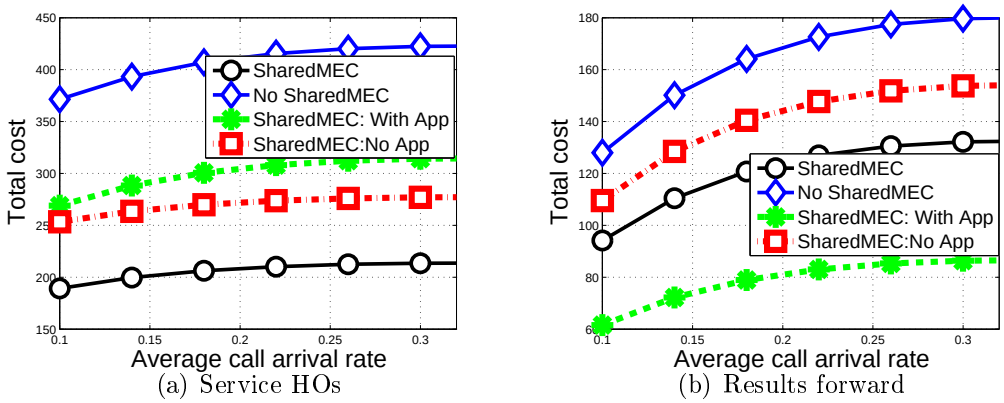

(a) Service HOs (b) Results forward

Figure 5.5: Total cost of service HOs and results forward.

5.2 Proposed HO Decision and Offloading Decision Algorithms

In this section, we present our proposed HO decision algorithm along with the joint offloading decision algorithm. Both algorithms are executed at the serving macro BS. Previously, most of the computation offloading algorithms are proposed to be executed at end user devices because the offloading only focuses on the energy and computational resource savings at end devices. However, this is not only inappropriate for MEC systems but also introduces several new issues. Therefore, papers on MEC systems are focusing on designing computation offloading decision algorithms at the BS [109]. Though the BS has the information on the available computational resources at the MEC which is deployed with the BS, it still needs additional information to decide whether to offload a user's computation task or not based on user's priority. Otherwise, offloading delay-tolerant computation tasks from one user may cause the delay-sensitive task from another user unable to be accepted by the MEC but have to be offloaded to the remote cloud or in the worst-case scenario, may lead to an offload failure. Moreover, adding radio offloading and user mobility requires extra information to perform a radio offloading and an HO. Furthermore, the BSs (or MECs) do not share information with each other. Therefore, coming up with a single solution to address both HO and offloading problems is challenging.

Here, we first present the system model, then, propose a solution to assign priorities to users based on their speeds, delay requirements, and traffic conditions of the network. Then, we propose two solutions: a joint radio and computation offloading algorithm for static users and an HO decision algorithm for mobile users which incorporates the joint radio and computation offloading decision algorithm. The notations used in our algorithms are given in Table 5.4.

5.2.1 System Model

We consider a computation offloading system that includes multiple MECs deployed with macro BSs, multiple femtocells, multiple users, and a remote cloud. The system

Table 5.4: Notations used in the HO and Offloading Decision Algorithms

$RSSI_{serv}$	RSSI in the serving macrocell
$RSSI_{targ}$	RSSI in the target macrocell
$RSSI_{femto}$	RSSI in a femtocell
$RSSI_{femtoMin}$	Minimum acceptable RSSI in a femtocell
Th_{RSSI}	Threshold for the macrocell network
Th_{femto}	Threshold for the femtocell network
HM	Hysteresis margin
P_u	User's priority
Th_{pr}	Priority threshold
Ch_{avM}	Available channels in a macrocell
Ch_{avF}	Available channels in a femtocell
$compRes_{avl}$	Available computational resources
$comRes_{req}$	Required computational resources
$comRes_{rem}$	Computation needs to be migrated

model is shown in Figure 5.6. In the system, all macro BSs, MECs, and the remote cloud are deployed by the same service provider [14, 48]. Each MEC is co-located with a macro BS. Each macrocell contains multiple femtocells within it. The coverage area of each femtocell is much smaller than the coverage area of a macrocell. Femtocells can serve less number of users and they share the same spectrum band with the macrocell. We consider an OFDMA system to assign channels (subcarriers) for both macrocells and femtocells in order to avoid interference between users.

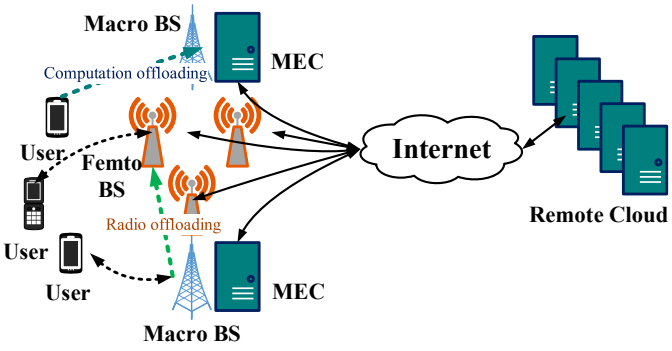

Figure 5.6: A femtocell-deployed cellular network with MECs and the remote cloud.

In the system, each MEC can be accessed via cellular channels from the macrocell, while the remote cloud can be accessed over the Internet. Mobile users are connected either to a macro BS or to a femto BS based on their priorities and resource availabilities at the BS. The priority of a user is selected based on its speed, delay requirement

of the computation task, and the network congestion situation. The details of the priority selection are given in Section 5.2.2. Each user can offload its computation tasks to the remote cloud while connected to a femto BS. On the other hand, whether to offload to the MEC or to the remote cloud while users are connected to the macro BS is based on the resource availability.

5.2.2 Users' Priority Assignment

When designing a computation offloading decision algorithm, the most straightforward way to assign priority to different traffic is based on their delay requirements. In this way, the delay-sensitive computation task is offloaded to the MEC and the delay-tolerant computation task is offloaded to the remote cloud. However, the delay requirements of *communication* tasks do not have much impact on the radio offloading decision algorithm because users with communication tasks can meet their delay requirements by using channels from either macro BSs or femto BSs. The only problem is that if a high-speed user is connected to a femto BS, a number of frequent HOs may increase the rate of unnecessary HOs. Now, to avoid unnecessary HOs, priority can be assigned to users based on their speed during designing a radio offloading decision algorithm. Thus, the radio offloading has different priority requirements than the computation offloading. Therefore, the straightforward ways of assigning priority separately based on delay requirements or speed are not the best options.

Now, if we consider both delay requirements and user's speed together to design a joint radio and computation offloading decision algorithm and an HO decision algorithm, we have four types of users: 1) high delay-sensitive and low-speed, 2) high delay-sensitive and high-speed, 3) low delay-sensitive and low-speed, and 4) low delay-sensitive and high-speed. However, the priority assignment of these users is challenging. Though it is obvious that the high delay-sensitive and high-speed users should be given a higher priority to use the macro BS and the MEC, where the low delay-sensitive and low-speed users should be given a lower priority, it is not clear how

priorities can be assigned to the rest two type of users. A low-speed user can be offloaded to the femtocell. However, if it has a high delay-sensitive computation task, the user may face a service failure. On the other hand, offloading a high-speed user to femtocells may result in an unnecessary HO.

Besides these issues, there is another important issue on resource unavailability during designing HO decision and offloading decision algorithms in MEC systems. Without the presence of enough available radio and computational resources, even a user with a high priority can neither perform an HO nor a radio/computation offloading. Moreover, though a BS knows its own radio and computational resource availabilities, it cannot select a proper target cell during performing an HO without the knowledge of available radio and computational resources of the target BS. Since BSs (or MECs) do not share information with each other, a proper target cell cannot be selected only based on the radio and the computational resource availabilities at the current BS.

Therefore, we propose a new way to define a user's priority to address these issues. In our definition, a user has two priorities: radio and computation priority. The radio priority is selected based on the user's speed. Assume that the radio priority of a user is $P_{radio} \in \{1, 2, \ldots, n_s\}$, where $1 > 2 > \cdots > n_s$ and n_s represents the lowest speed and the lowest priority to connect to a macro BS. Similarly, the computation priority of a user can be defined as $P_{comp} \in \{1, 2, \ldots, n_c\}$, where priority $1 > 2 > \cdots > n_c$. Each priority can be selected based on several thresholds for both speed and delay requirements, and the thresholds can vary based on the preferences of service providers. We assign radio priorities by dividing the maximum speed by n_s and computation priorities by dividing the maximum delay requirement by n_c. A weight value is assigned to each resource, which depends on the traffic congestion of the cellular network. For example, during peak traffic hours (e.g., during office hours or during special events), a large volume of communication traffic is generated.

This high volume of communication traffic keeps the radio network busy, therefore, available radio resources become low. At the same time, since most of the traffic at the macro BS is communication traffic, more computational resources can be available at the corresponding MEC. We assign weight values as w_r and w_c, where w_r represents the weight value for the radio resource and w_c represents the weight value for the computational resource. User devices can share their priorities with the BS while requesting an offloading or an HO. Then, the BS can determine the overall priority (P_u) for a user following the formula given below:

$$P_u = P_{radio}.w_r + P_{comp}.w_c. \tag{5.18}$$

In this way, the priority can fulfill all the requirements of both radio and computation offloading. For example, a user with low-speed ($P_{radio} = 3$) and a high delay-requirement ($P_{comp} = 1$) will still perform an HO to a macro BS and offload its computation tasks to the MEC even in the peak traffic hours ($w_r = 30\%$ and $w_c = 70\%$), because the $P_u = 1.6$ represents a high priority based on the priority threshold. Similarly, when the available computational resource is low at the MEC, e.g., $w_c = 30\%$ and $w_r = 70\%$, the user still performs computation offloading to the MEC because the $P_u = 2.4$ also indicates a high priority.

5.2.3 Joint Offloading Decision Algorithm

A joint offloading decision algorithm that considers both radio and computation offloading is presented in this section. The block diagram of the proposed joint offloading decision algorithm is shown in Figure 5.7. The figure presents that when a user decides to offload its computation tasks to the cloud, it sends a measurement report to the serving macro BS. The measurement report contains RSSIs from the serving macro BS, neighboring macro BSs, and femto BSs, their cell IDs, and user priority. The serving macro BS first makes a radio offloading decision and then makes

a computation offloading decision using this measurement report. A computation task is either offloaded to the MEC via the macro BS or to the remote cloud via a macro/femto BS based on the user's priority. The MEC can also be deployed in a femto BS with less computational resources. However, in this paper, we do not consider this option.

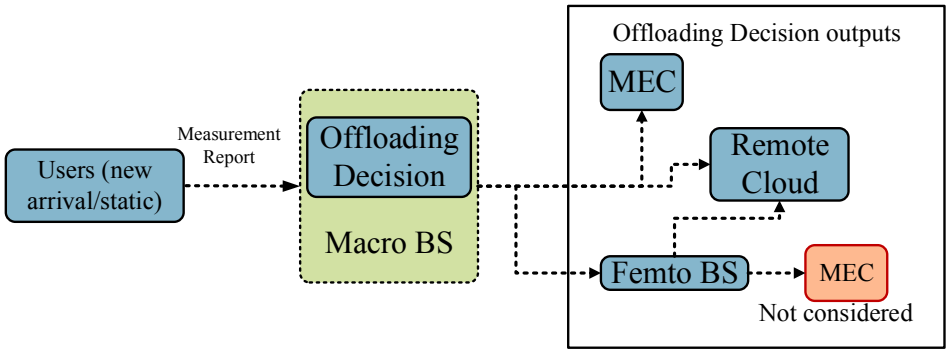

Figure 5.7: A model for joint radio and computation offloading decision.

Algorithm 18: Joint radio and computation offloading decision algorithm

if $RSSI_{serv} \geq Th_{RSSI}$ *and* $Ch_{avM} > 0$ *and* $P_u <= Th_{pr}$ **then**
  Offload to macro BS;
  if $compRes_{req} <= compRes_{avl}$ **then**
    Offload to the MEC;
  else
    Offload to the remote cloud;
  End;
else
  Select a target femtocell;
  if $RSSI_{femto} \geq Th_{femto}$ *and* $Ch_{avF} > 0$ **then**
    Offload to the femtocell;
  else
    Service fail;
  End;
End;

The joint offloading decision algorithm is presented in Algorithm 18. In our algorithm, the offloading decision is made based on RSSIs of the macro BS and the femto BS, channel availabilities of the macro BS and the femto BS, the user priority, and the computational resource availability in the MEC. If all requirements of the offloading decision are fulfilled, the user is connected to the macro BS, then computation

tasks are offloaded to the MEC or to the remote cloud based on the computational resource availability of the MEC. Otherwise, the user performs a radio offloading to a femto BS and offloads its computation tasks to the remote cloud. Before performing a radio offloading to the femto BS, the serving macro BS needs to find a proper target femtocell. To determine the target femtocell, the serving macrocell generates a target femtocell list, $list_f$, after getting the measurement report. The target femtocell list can be presented as:

$$list_f = \{(i, RSSI_{femto}(i)) : RSSI_{femto}(i) > RSSI_{femtoMin}\}, \tag{5.19}$$

where $i \in \{1, 2, \ldots, n_f\}$ represents femtocell IDs. Finally, the target femtocell (i') is selected from this list by the highest value of the RSSI as:

$$RSSI(i') = \arg\max_i (RSSI_{femto}(i)). \tag{5.20}$$

5.2.4 Handoff Decision Algorithm

In this section, the proposed HO decision algorithm is described and the joint offloading decision algorithm which is presented in the previous section is incorporated in it. The block diagram for the proposed HO decision algorithm is shown in Figure 5.8. It is observed in the figure that when a user moves out of a cellular coverage area, it sends a measurement report to the serving BS. The measurement report contains the same parameters as the joint offloading decision algorithm. The serving BS performs a target cell selection and an HO decision algorithm. The HO decision block in the figure decides whether to perform an HO to a macro BS or to perform a radio offloading to a femto BS. If the user performs an HO to a target macro BS, the target macro BS makes the decision whether to migrate the computation to the MEC or to the remote cloud based on the resource availability.

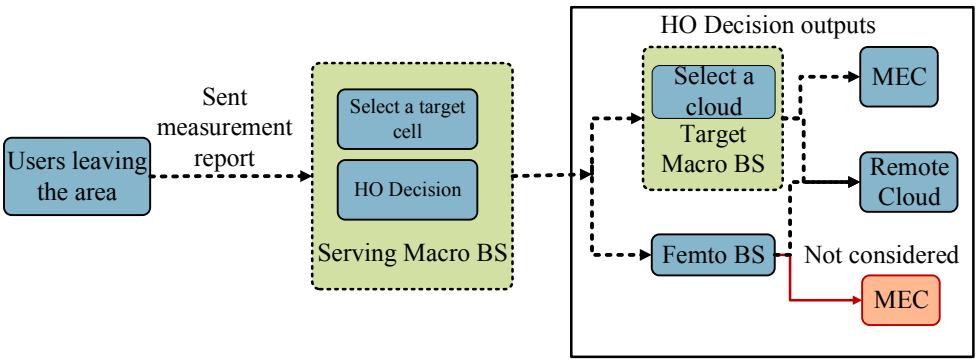

Figure 5.8: A model for HO and offloading decision.

When the RSSI of the serving BS goes below a threshold, the HO is triggered. Then, after getting the measurement report from the user, the serving BS selects a target macro or femto BS. Similar to the target femtocell selection, the maximum $RSSI$ of the target macrocell is used to select a target macro BS along with the priority of a user. The target cell list for macrocells is assumed to be $list_m$, and it can be obtained as:

$$list_m = \{(j, RSSI_{targ}(j)) : RSSI_{targ}(j) > RSSI_{min}\}, \tag{5.21}$$

where j is the cell ID for the target macro BS and $j \in \{1, 2, \ldots, n_m\}$. Then, the target macrocell (j') can be attained as:

$$RSSI(j') = \arg\max_{j}(RSSI_{targ}(j)). \tag{5.22}$$

It would be better if the target cell selection could consider the available resources (both radio and computational) from the target cells as a target cell selection parameter. However, this is not possible, since the user does not have access to this information and BSs do not share information with each other. Therefore, similar to the offloading decision, the HO decision is made based on the user's priority, available

channels, and RSSIs. The proposed HO decision algorithm is shown in Algorithm 19. In our proposed HO decision algorithm, we migrate the rest of the computation tasks to the new MEC if resources are available, otherwise, complete the computation at the old MEC and send the result via the remote cloud. Since we consider both the MEC and the remote cloud are from the same service provider, both clouds know the location of a user. The reason behind this result migration is that, in this way, the migration of the remaining computation tasks to the remote cloud may cause more migration costs and delay at the user's end than the transmission cost of the result via the remote cloud. If any of those HO decision criteria are not fulfilled, the BS requests a user to perform a radio offloading to the femtocell. The target femtocell is selected based on (5.20). If the user is not moving out of the cell coverage area, i.e., the RSSI of the serving BS is larger than the threshold, then the joint offloading decision algorithm is incorporated into the HO decision algorithm. Besides these HO and offloading decision algorithms, we need a femtocell to macrocell HO decision algorithm to ensure a seamless connection between users and the remote cloud. However, users using femtocells offload their computation tasks only to the remote cloud. Therefore, the computation offloading or the computation task migration is not an issue in this case. Only maintaining a seamless wireless connection is the main concern. As a result, we can use traditional femtocell to macrocell HO decision algorithm which depends on RSSIs of the serving femtocell and the target macrocell.

5.2.5 Determining Handoff Decision Parameters

Selecting a proper threshold when designing an appropriate HO decision is a very important issue. In our algorithms, we use multiple thresholds. How these thresholds are determined is discussed in this section.

To select the minimum RSSI for the macrocell network, we use the RSSI at the macrocell boundary. RSSIs at different distances from the macro BS is shown in Figure 5.9(a). The Okumura-Hata propagation model is used to calculate the RSSI

Algorithm 19: HO Decision algorithm

```
if RSSI_serv < Th_RSSI then
    Select a target macrocell;
    if RSSI_targ ≥ Th_RSSI + HM and Ch_avM > 0 and P_u <= Th_pr then
        HO to the target macrocell;
        if compRes_rem <= compRes_avl then
            Migrate to the MEC;
        else
            Migrate result via the remote cloud;
        End;
        RSSI_serv ← RSSI_targ
    else
        Select a the target femtocell;
        if RSSI_femto ≥ Th_femto and Ch_avF > 0 then
            HO to femtocell;
        else
            Service fail;
    End;
else
    Call Algorithm 18;
End;
```

for the macrocell network [132]. The radius of the macrocell is assumed to be 1.1km and the RSSI at 1.1km is shown -75dB, which is considered as $RSSI_{min}$. Now, if the hysteresis margin (HM) is considered as 5dB, we can obtain the Th_{RSSI} as -70dB. The optimal value of the HM is taken from [22].

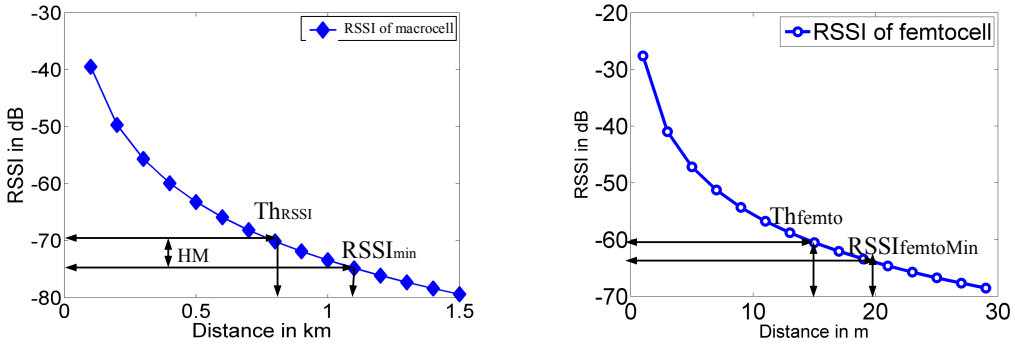

(a) $RSSI$ for a macrocell (b) $RSSI$ for a femtocell

Figure 5.9: Selection of $RSSI_{min}$, Th_{RSSI}, and HM for macrocell networks, and $RSSI_{femtoMin}$ and Th_{femto} for femtocell networks.

To determine the value of Th_{femto} the ITU-R P.1238-7 indoor path-loss model is used to calculate the RSSI at the femtocell boundary (15m) [17]. The minimum RSSI

is taken at a 20m distance from the femto BS so that the target femtocell is selected by the time the user enters the femto coverage area. RSSIs from the femto BS for different distances are shown in Figure 5.9(b).

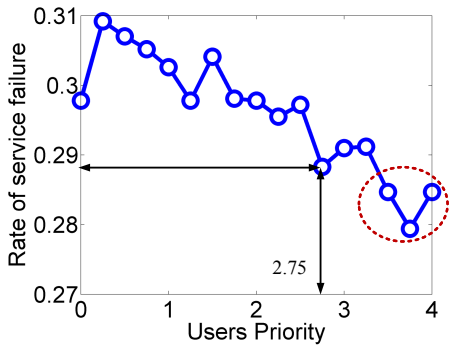

Figure 5.10: Service failure rate for different users' priority.

Optimizing the value of the priority threshold Th_{pr} is the most important and the most challenging task, because it has a high impact on both the HO and the joint offloading decisions. Whether a user should use the macrocell network or the femtocell network depends on the priority threshold. Furthermore, whether a computation task should offload to the MEC or to the remote cloud also depends on the priority threshold. If the priority threshold is not selected properly, offloading low priority users to the MEC may force the high priority users to offload to the remote cloud, which may create a high latency to end users or in the worst-case scenario, may lead to an offload failure. However, selecting a proper priority threshold is challenging because of the randomness of users' mobility, the necessity of computational resources, and resource availabilities. In this section, we choose three parameters to select a proper priority threshold: the rate of service failure, the rate of total successful offload, and the rate of successful MEC offload. These parameters are presented based on the simulation results with respect to different users' priorities (0 to 4) in Figure 5.10 and Figure 5.11. From the figures, we can observe that when the priority value is 3.75, the rate of service failure is the lowest and the rate of total successful

offloading is the highest. However, for the same priority value, the rate of successful MEC offload presents one of the lowest values. The same reason applies for the other two priority values which are 3.5 and 4. As a result, we cannot consider these values as the best value for the priority threshold. Therefore, we choose 2.75 as the priority threshold which represents the next lowest value for the rate of service failure and the next highest value for the rate of total successful offload. Moreover, the rate of successful MEC offload is also above 90%.

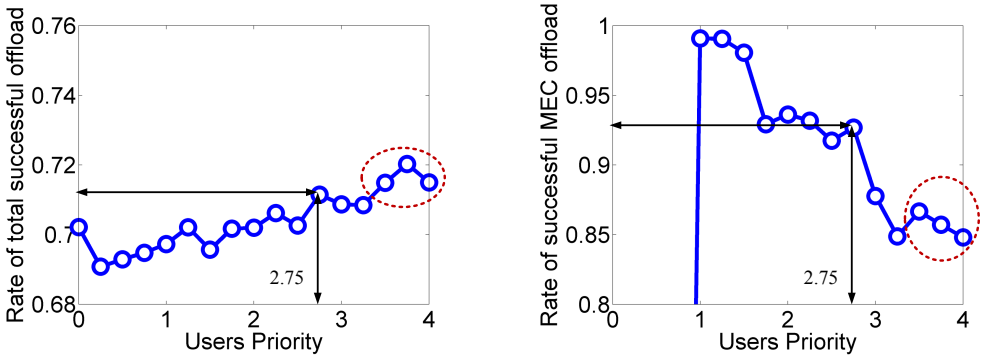

(a) Total offloading success (b) MEC offloading success

Figure 5.11: Rate of total successful offload and successful MEC offload.

5.2.6 Performance Evaluation

In this section, the performance of our proposed HO decision algorithm is presented in terms of the rate of MEC offloading success, the rate of total offloading, the rate of HO failure, and service migration cost. As the joint radio and computation offloading decision algorithm is incorporated into our proposed HO decision algorithm, the performance of the joint offloading decision is not presented separately in the paper. First, we introduce the settings of scenarios in the simulation. Then, the performance of the proposed HO decision algorithm is evaluated.

5.2.6.1 Simulation Setup

To simulate our proposed HO decision algorithm, we use our system model scenario shown in Fig. 5.6. We use three macro BSs (each with an MEC), sixteen femto BSs

placed randomly within the macrocell coverage areas and a remote cloud. The number of users varies from 0 to 30. They are placed randomly within the macro cell radius and follow a Random WayPoint mobility model. We use Net Logo 6.0.1 to simulate our proposed algorithm [121]. To reduce the randomness of the scenario, we use the average of 100 simulations for each case. The values of the parameters used in the simulation are listed in Table 5.5 [17, 22].

To evaluate the performance of our proposed HO decision algorithm, we investigate the following four performance metrics: 1) *Rate of MEC offloading success*: the probability of a computation task successfully offloaded to the MEC; 2) *Rate of total offloading success*: the probability of a computation task successfully offloaded to any cloud; 3) *Rate of HO failure*: the probability of service drop when a user fails to connect to the target cell; 4) *Service migration cost*: the cost of migrating a computation task from a serving MEC to a target MEC during an HO. In addition, we compare our proposed HO decision algorithm with three algorithms: *Femto cooperation*, *Cloud cooperation*, and *No cooperation*. The first one considers radio offloading from the macrocell to femtocell in order to reduce the radio congestion. The second one considers computation offloading with the cooperation of a remote cloud with the MEC. Finally, the third one has no cooperation of femtocells or the remote cloud. Since there is no HO decision paper available in MEC systems, we implement our proposed HO decision algorithm with these traditional radio and cloud offloading decision algorithms. Moreover, we consider two worst network conditions: low availability of radio resource and low availability of computational resource.

5.2.6.2 Rate of MEC Offloading Success

Figure 5.12 shows the results of the rate of MEC offloading success for two worst case scenarios. A low availability of radio and computational resources are represented in Figure 5.12(a) and Figure 5.12(b), respectively. In both cases, MEC offloading success rate decreases with the increment of users in the network because of the

Table 5.5: Simulation Parameters for Joint Offloading Decision Algorithm

Transmission power of macro & femto BSs	45 & 15 dBm
Available channels for macro & femto BS	100 & 10
Range of macrocell (radius)	1100 m
Range of femtocell (radius)	15 m
Minimum Macro RSSI, $RSSI_{min}$	-75 dB
RSSI threshold for macrocell, Th_{RSSI}	-70 dB
RSSI threshold for femtocell, Th_{femto}	-60 dB
Priority threshold P_u	2.75
Minimum femto RSSI $RSSI_{femtoMin}$	-68 dB
User speed	0 to 20 km/hr

limited radio and computational resources. However, we can observe from these figures that though the availability of radio resource is low, the success rate is high in case of the high computational resource availability when user number is high. This is because the MEC can allocate more computational resources to each user and finish each computation task with a low computation time, therefore, support more users. Furthermore, we compare our proposed HO decision algorithm with three algorithms, and our proposed HO decision algorithm with both femtocell and cloud cooperation shows better MEC offloading success rate than others.

5.2.6.3 Rate of Total Offloading Success

In Figure 5.13, the rate of total offloading success represents the rate of the successful offloading to the MEC and the remote cloud. The results for low radio and computational resources with respect to a different number of users are shown in Figure 5.13 (a) and Figure 5.13 (b), respectively. The figures present that our proposed HO decision algorithm with joint cooperation has almost 80% successful offloading because of the cooperation of femtocells and the remote cloud which is a bit higher than the case of remote cloud cooperation. This cooperation allows users to offload computation task to the MEC via the macrocell and to the remote cloud via the macrocell and femtocells. On the other hand, the rate of total offloading success is less than 20% for the case of femtocell cooperation and no-cooperation. Therefore, we can observe that only cooperating femtocells cannot address the issue of offloading

failure.

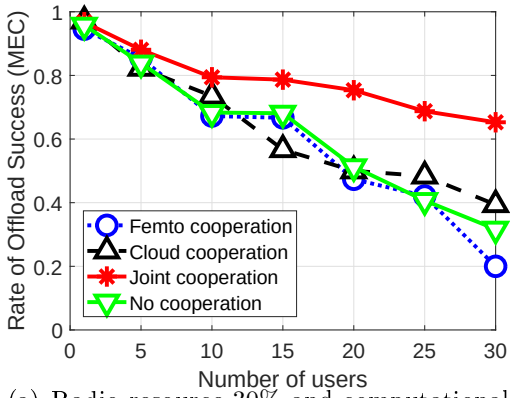

(a) Radio resource 30% and computational resource 70% available

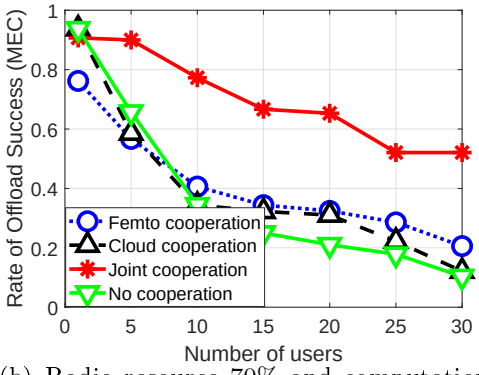

(b) Radio resource 70% and computational resource 30% available

Figure 5.12: The rate of MEC offloading success.

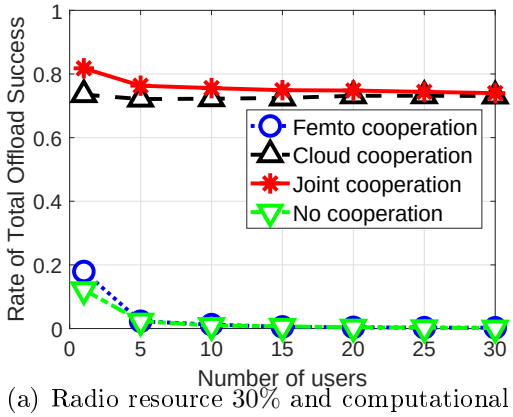

(a) Radio resource 30% and computational resource 70% available

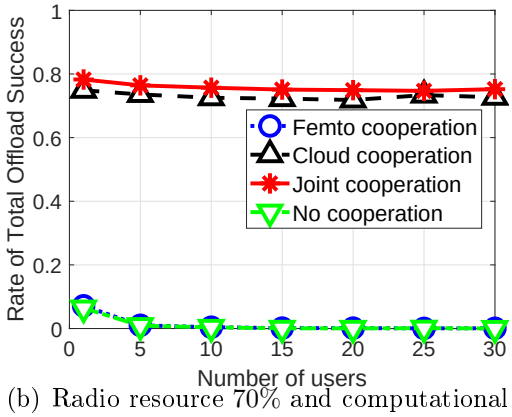

(b) Radio resource 70% and computational resource 30% available

Figure 5.13: The rate of total (MEC and remote cloud) offloading success.

5.2.6.4 Rate of HO Failure

The rate of HO failure for all four algorithms is shown in Figure 5.14. From the HO failure rate, we can observe that both our proposed algorithm and the algorithm with the femtocell cooperation have the lowest rate of HO failure as femtocells can offload radio traffic from the macrocell network. The algorithms without the cooperation of femtocells have a high HO failure rate. As a result, we can conclude that only cooperating the remote cloud cannot address the issue of HO failure in MEC deployed

macrocell networks.

5.2.6.5 Service migration Cost

As the MEC has a limited coverage area, the offloaded computation needs to be migrated when a user moves out of the coverage area. This migration has a cost and it causes extra delay to the user's end. To show how much migration cost is needed for each algorithm, we represent the cost of service migration in Figure 5.15. It is shown in the figures that our proposed HO decision algorithm with the joint cooperation has the lowest service migration cost as compared to other algorithms. The service migration cost is calculated for an exponential offloading duration (mean $1/\eta = 3$), a residence time (mean $1/\mu = 10$), and the computation task arrival rate λ (0.1 to 0.34).

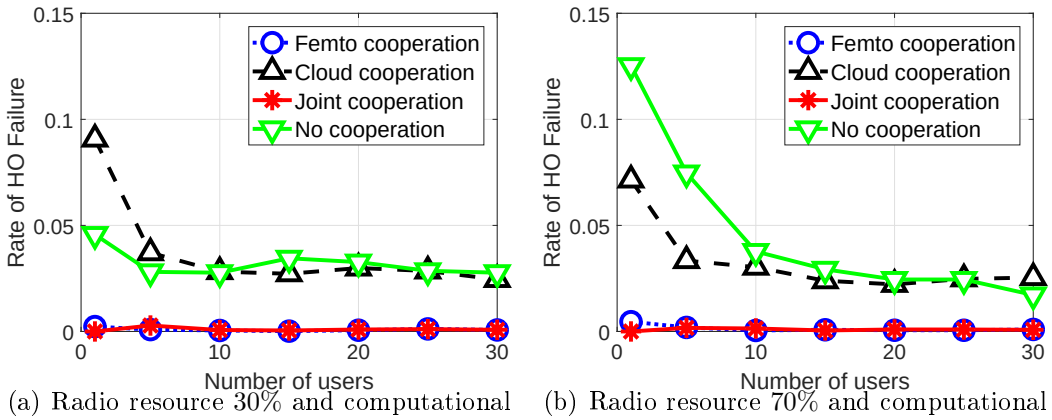

(a) Radio resource 30% and computational resource 70% available

(b) Radio resource 70% and computational resource 30% available

Figure 5.14: The rate of HO failure.

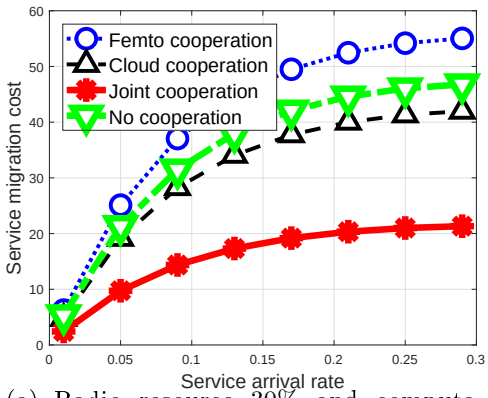

(a) Radio resource 30% and computational resource 70% available

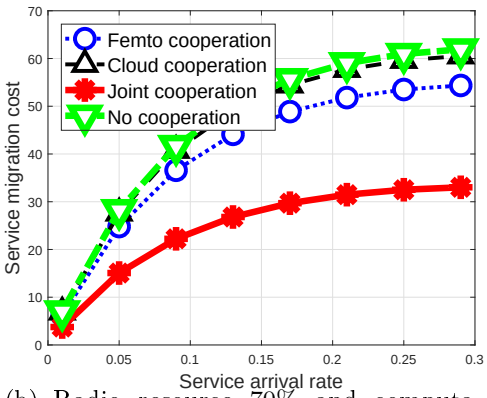

(b) Radio resource 70% and computational resource 30% available

Figure 5.15: Service migration cost.

CHAPTER 6: CONCLUSION

6.1 Conclusions

In this dissertation, six adaptive mobility management schemes are proposed to support seamless and secure mobility management in femtocell networks, CR femtocell networks, and mobile edge computing (MEC). First, two adaptive handoff (HO) decision algorithms are proposed for closed-access and open-access femtocell networks. Then, a secure target cell selection scheme is proposed for femtocell networks. An analytical model is also proposed analyze the total HO signaling cost. Later, a power control scheme along with the detection sensitivity scheme and a mobility management scheme to address the issues of heterogeneous spectrum in cognitive radio (CR) femtocells. Last, a service HO decision algorithm and a joint offloading decision are proposed to reduce the migration rate and the radio congestion.

In the adaptive HO decision algorithm, a location-fingerprint based HO decision algorithm is proposed to improve the HO performance and to offload cellular data traffic in densely deployed heterogeneous networks with femtocells. In the proposed algorithm, the hysteresis margin changes with the HO priority based on the location of users. Therefore, a fast HO can be triggered wherever necessary. The algorithm can reduce the HO failure rate and at the same time, provide better cell utilization to insure maximum data offloading. The performance of the proposed self-adaptive HO-decision algorithm is analyzed in terms of unnecessary HO rate, HO failure rate, and cell utilization by considering the challenges of indoor deployment. Simulation results show significant improvement as compared to the existing HO-decision algorithms in femtocell networks. It is observed that a proper selection of hysteresis margin and threshold can reduce unnecessary HO rate and HO failure rate without sacrificing cell

utilization.

An analytical model is designed to evaluate the HO signaling cost of macro-to-femto, femto-to-femto, and femto-to-macro HO in open-access femtocell networks. In addition, a target cell selection method and HO decision algorithms for open-access femtocell networks are proposed. The proposed algorithms are compared to five existing HO decision algorithms with respect to the total HO signaling costs and femtocell utilizations. Simulation results show that the proposed algorithms can significantly reduce the total HO signaling costs without sacrificing femtocell utilization as compared to the existing algorithms.

In the secure target cell selection scheme, the effects of two possible attacks on the HO decision process in open-access femtocell networks are discussed. Then, a target cell selection and an HO decision scheme are proposed to address these attacks by using both $RSSI$ and location database. Simulation results show that the proposed scheme can reduce the probability of a user being handed off to a malicious femtocell and can provide a better femtocell utilization. The results of total HO signaling costs show that the proposed scheme can improve the network performance without adding significant extra signaling cost.

The proposed power control scheme addresses the issue related to the transmission range changes, while the detection sensitivity selection scheme helps to reduce the effect of the sensing frequency changes. The performance of the power control scheme is analyzed in terms of femtocell utilization and probability of interference. On the other hand, the performance of the detection sensitivity selection scheme is analyzed in terms of detection error rate and false alarm rate. The proposed schemes can increase the femtocell utilization and at the same time, can reduce the interference from neighboring CR FBS and FUEs, the detection error rate, and the false alarm rate. Proposed schemes are compared with the conventional CR femtocell networks where the effect of heterogeneous frequency change is not considered. Simulation

results show significant performance improvement as compared to the conventional CR femtocell networks.

A mobility management scheme is proposed with an adaptive HO-threshold to support both inbound and outbound mobility. In addition, an HO-threshold selection scheme is proposed with the interference from PUs and neighboring femtocells taken into account and integrated with the proposed mobility management scheme. The probability of interference from both PUs and neighboring femtocells is calculated analytically. The performance of the proposed mobility management scheme is analyzed in terms of femtocell utilization, required transmission time, and throughput. The proposed scheme is compared with a traditional mobility management scheme where the channel heterogeneity is not considered. Simulation results show significant performance improvement as compared to the traditional scheme in CR femtocell networks. The proposed scheme can reduce the channel under-utilization and required transmission time. On the other hand, it can improve the throughput.

A novel architecture along with a service HO decision algorithm is presented in order to support mobile users in MEC-deployed cellular networks. The proposed scheme addressed the issue of extra signaling cost due to unnecessary HOs caused by the resource unavailability at the target MEC. In addition, an analytical model is proposed to determine the total cost of radio HO signaling, service HO signaling, and total migration. Simulation results show that the proposed system model and service HO decision algorithm can reduce the total cost due to both radio and service HOs. In addition, the joint HO and offloading decision scheme addressed the issue of mobility management along with the issue of radio and computational resource congestions. A user's priority is added to address these issues during designing the HO and the offloading decision algorithms. Simulation results show that the proposed HO decision algorithm increases the success rate of MEC, at the same time, reduces the HO failure rate and the migration cost as compared to the other proposed HO

and offloading decision algorithms.

To sum up, the proposed mobility management schemes in this dissertation are endowed with the ability to adapt to the existing practical challenges. Therefore, this research will provide important insights on next-generation femtocell networks.

6.1.1 Completed Work

In this dissertation, the following research work has been completed:

- Two HO decision algorithms for closed-access and open-accessed femtocell networks are proposed by considering the randomness of femtocell deployment.
- An analytical model to analyze the HO signaling cost in femtocell network is designed.
- A target cell selection and an HO decision scheme are developed, which help a user to select a secure target femtocell during an HO.
- A power control scheme along with an adaptive detection sensitivity scheme is designed to address the unique challenges of CR femtocell networks, such as interference, cell under-utilization, detection error, and false alarm.
- An adaptive HO-threshold selection scheme combined with the proposed mobility management scheme is developed by considering the interference from both primary users and neighboring femtocells.
- A novel service HO decision algorithm to support user mobility in MEC deployed with femto base stations is designed.
- An HO decision algorithm for MEC systems considering both radio and computation congestion issues is proposed.

6.1.2 Published and Submitted Work

The following list is a summary of my publications:

1. Wahida Nasrin and Jiang Xie, "SharedMEC: Sharing An MEC to Support Users Mobility in Mobile Edge Computing," in *Proceedings of IEEE International Conference on Communications (ICC)*, May 2018.

2. Wahida Nasrin and Jiang Xie, "An Effective Target Cell Selection Scheme in Open-Access Femtocell Networks" in *Proceedings of IEEE Global Communications Conference (GLOBECOM)*, December 2017. **(Best Paper Award)**

3. Wahida Nasrin and Jiang Xie, "Signaling Cost Analysis for Handoff Decision Algorithms in Femtocell Networks," in *Proceedings of IEEE International Conference on Communications (ICC)*, May 2017.

4. Wahida Nasrin and Jiang Xie, "Effects of Heterogeneous Frequency Changes in Cognitive Radio Femtocell Networks," in *Proceedings of IEEE Global Communications Conference (GLOBECOM)*, December 2016.

5. Wahida Nasrin and Jiang Xie, "A Mobility Management Scheme to Reduce the Impact of Channel Heterogeneity in Cognitive Radio Femtocell Networks," in *Proceedings of IEEE International Conference on Sensing, Communication and Networking (SECON)*, June 2016.

6. Wahida Nasrin and Jiang Xie, "A Self-Adaptive Handoff Decision Algorithm for Densely Deployed Closed-Group Femtocell Networks," in *Proceedings of IEEE International Conference on Sensing, Communication and Networking (SECON)*, June 2015.

7. Wahida Nasrin and Jiang Xie, "The Incorporation of Radio and Computation Offloading for Mobility Management in Mobile Edge Computing," in preparation to be submitted to *IEEE International Conference on Communications (ICC)*, October 2018.

8. Wahida Nasrin and Jiang Xie, "Adaptive Handoff Decision Algorithms for Closed-Access and Open-Access Modes in Femtocell Networks," submitted to *IEEE Transactions on Vehicular Technology*, December 2017.

9. Wahida Nasrin and Jiang Xie, "Reducing the Impact of Channel Heterogeneity on Mobile Users in Cognitive Radio Femtocell Networks," submitted to *IEEE Transaction on Cognitive Communications and Networking*, February 2018.

10. Wahida Nasrin and Jiang Xie, "A Secure Target Cell Selection Scheme for Open-Access Femtocell Networks," submitted to *IEEE Transactions on Vehicular Technology*, June 2018.

6.2 Future Work

My Ph.D. research opens up many theoretical and practical research possibilities in mobility and resource management and other related areas in wireless communications. Potential future research work includes the following research topics:

- **User association and mobility management in 5G mmWave small cells**

The mmWave small cell network is different from the traditional small cell network, and it introduces challenges of high path-loss attenuation, poor diffraction, straight constraints on hardware, vulnerable to blockage, and node mobility. One of the basic problems is the overly frequent HOs due to wrong user association between adjacent base stations, which, however, is similar to the research issues I was addressing in 5G femtocell networks. Therefore, I believe that my proposed mobility management methods can be extended to these new networks.

- **Wireless network security enhanced by adaptive mobility management**

Unlike existing mobile networks, the next-generation (5G) mobile network is introduced to support not only the increasing voice and data traffic. 5G will also serve

vertical industries, which include vehicular networks, Internet of Things (IoT), high-speed railways, etc. These new additions will bring new challenges from the security and privacy perspective. The adaptive mobility management schemes for heterogeneous networks and the secure target cell selection scheme in my previous work can be treated as powerful extensions of the traditional network security schemes to support 5G deployment.

- **Mobile Edge Computing (MEC) in the support of Internet of Things (IoT)**

One of the key technologies of 5G mobile networks is IoT. All devices in IoT need to perform computations in order to serve the required purpose, e.g., environment monitoring, building and home automation, medical and healthcare, transportation, and agriculture. However, most devices in IoT are limited in computation resources and battery life, therefore, offload their large volume of computation tasks to the cloud. MEC is a proper solution to provide computational resources to IoT devices and fulfill the offloading delay requirement. I believe each of these issues can be a potential research direction and my existing mobility management and security schemes can be extended to address these issues in IoT.

REFERENCES

[1] "Small cells, fiber and spectrum are key to 5G, AT&T exec says." https://www.rcrwireless.com/20170623/5g/201706235gsmall-cells-fiber-spectrum-5g-tag17, June 23, 2017.

[2] V. Chandrasekhar, J. G. Andrews, and A. Gatherer, "Femtocell networks: a survey," *IEEE Communications Magazine*, vol. 46, pp. 59–67, September 2008.

[3] J. G. Andrews, H. Claussen, M. Dohler, S. Rangan, and M. C. Reed, "Femtocells: past, present, and future," *IEEE Journal on Selected Areas in Communications*, vol. 30, no. 3, pp. 497–508, 2012.

[4] Cisco, "Cisco visual networking index: Global mobile data traffic forecast update, 2010-2015." Whitepaper, 2011.

[5] J. G. Andrews, H. Claussen, M. Dohler, S. Rangan, and M. C. Reed, "Femtocells: Past, present, and future," *IEEE Journal on Selected Areas in Communications*, vol. 30, pp. 497–508, April 2012.

[6] J. Mitola and G. Q. Maguire Jr, "Cognitive radio: making software radios more personal," *IEEE Personal Communications*, vol. 6, no. 4, pp. 13–18, 1999.

[7] I. F. Akyildiz, W.-Y. Lee, M. C. Vuran, and S. Mohanty, "Next generation/dynamic spectrum access/cognitive radio wireless networks: a survey," *Computer Networks*, vol. 50, no. 13, pp. 2127–2159, 2006.

[8] L. Huang, G. Zhu, and X. Du, "Cognitive femtocell networks: an opportunistic spectrum access for future indoor wireless coverage," *IEEE Wireless Communications*, vol. 20, no. 2, pp. 44–51, 2013.

[9] S.-Y. Lien, C.-C. Tseng, K.-C. Chen, and C.-W. Su, "Cognitive radio resource management for qos guarantees in autonomous femtocell networks," in *Proc. IEEE International Conference on Communications (ICC)*, pp. 1–6, 2010.

[10] H. Venkataraman and G.-M. Muntean, *Cognitive Radio and Its Application for Next Generation Cellular and Wireless Networks*. Springer, 2012.

[11] R. Xie, F. R. Yu, and H. Ji, "Energy-efficient spectrum sharing and power allocation in cognitive radio femtocell networks," in *Proc. IEEE INFOCOM*, pp. 1665–1673, 2012.

[12] E. Cuervo, A. Balasubramanian, D.-k. Cho, A. Wolman, S. Saroiu, R. Chandra, and P. Bahl, "Maui: making smartphones last longer with code offload," in *Proc. of the International Conference on Mobile Systems, Applications, and Services*, pp. 49–62, 2010.

[13] K. Kumar and Y.-H. Lu, "Cloud computing for mobile users: Can offloading computation save energy?," *IEEE Computer*, vol. 43, no. 4, pp. 51–56, 2010.

[14] Y. Mao, C. You, J. Zhang, K. Huang, and K. B. Letaief, "Mobile edge computing: Survey and research outlook," *arXiv preprint arXiv:1701.01090*, 2017.

[15] A. Ahmed and E. Ahmed, "A survey on mobile edge computing," in *Proc. of International Conference on Intelligent Systems and Control (ISCO)*, pp. 1–8, 2016.

[16] T. Zahir, K. Arshad, A. Nakata, and K. Moessner, "Interference management in femtocells," *IEEE Communication Survey and Tututorial*, vol. 15, no. 1, pp. 293–311, 2012.

[17] "Propagation data and prediction methods for the planning of indoor radio communication systems and radio local area networks in the frequency range 900 MHz to 100 GHz." Recommendation ITU-R P.1238-7, 2012.

[18] D. Xenakis, N. Passan, L. Merakos, and C. Verikoukis, "Mobility management for femtocells in LTE-Advanced: Key aspects and survey of handover decision algorithms," *IEEE Communications Surveys and Tutorials*, vol. 16, pp. 64–91, First Quarter 2014.

[19] Z. Becvar and P. Mach, "Adaptive hysteresis margin for handover in femtocell networks," in *Proc. International Conference on Wireless and Mobile Communications (ICWMC)*, pp. 256–261, 2010.

[20] W. Nasrin and J. Xie, "A mobility management scheme to reduce the impact of channel heterogeneity in cognitive radio femtocell networks," in *Proc. of IEEE International Conference on Sensing, Communication, and Networking (SECON)*, pp. 1–9, 2016.

[21] J.-M. Moon, J. Jung, S. Lee, A. Nigam, and S. Ryoo, "On the trade-off between handover failure and small cell utilization in heterogeneous networks," in *Proc. IEEE International Conference on Communication Workshop (ICCW)*, pp. 2282–2287, 2015.

[22] W. Nasrin and J. Xie, "A self-adaptive handoff decision algorithm for densely deployed closed-group femtocell networks," in *Proc. IEEE Internationa Conferance on Sensing, Communication, and Networking*, 2015.

[23] L. Wang, Y. Zhang, and Z. Wei, "Mobility management schemes at radio network layer for LTE femtocells," in *Proc. IEEE Vehicular Technology Conference*, pp. 1–5, 2009.

[24] H. Zhang, W. Ma, W. Li, W. Zheng, X. Wen, and C. Jiang, "Signalling cost evaluation of handover management schemes in LTE-advanced femtocell," in *Proc. IEEE Vehicular Technology Conference (VTC Spring)*, pp. 1–5, 2011.

[25] C.-M. Chen, Y.-H. Chen, Y.-H. Lin, and H.-M. Sun, "Eliminating rouge femtocells based on distance bounding protocol and geographic information," *Expert Systems with Applications*, vol. 41, no. 2, pp. 426–433, 2014.

[26] R. W. Lott, R. B. Gurajala, K. D. Huber, J. J. Flynn, W. G. Mansfield, J. T. Seymour, R. Neelakantan, T. J. Pitassi, J. P. Davis, and A. Downie, "Femtocell service registration, activation, and provisioning," 2013. US Patent 8,504,032.

[27] J. Xie and I. Howitt, "Multi-domain wlan load balancing in WLAN/WPAN interference environments," *IEEE Transactions on Wireless Communications*, vol. 8, no. 9, 2009.

[28] U. Narayanan and J. Xie, "Signaling cost analysis of handoffs in a mixed IPv4/IPv6 mobile environment," in *Proc. IEEE Global Telecommunications Conference (GLOBECOM)*, pp. 1792–1796, 2007.

[29] Z. Becvar, P. Mach, and M. Vondra, "Self-optimizing neighbor cell list with dynamic threshold for handover purposes in networks with small cells," *Wireless Communications and Mobile Computing*, vol. 15, no. 13, pp. 1729–1743, 2015.

[30] X. Liu and J. Xie, "Contention window-based deadlock-free MAC for blind rendezvous in cognitive radio ad hoc networks," in *Proc. of IEEE Global Communications Conference (GLOBECOM)*, pp. 1–6, 2015.

[31] Z. Feng, L. Song, Z. Han, X. Zhao, and D. Niyato, "Cell selection in two-tier femtocell networks with open/closed access using evolutionary game," in *Proc. of IEEE Wireless Communications and Networking Conference (WCNC)*, pp. 860–865, 2013.

[32] C. Dhahri and T. Ohtsuki, "Learning-based cell selection method for femtocell networks," in *Proc. of IEEE Vehicular Technology Conference (VTC)*, pp. 1–5, 2012.

[33] P. Series, "Propagation data and prediction methods for the planning of indoor radiocommunication systems and radio local area networks in the frequency range 900 MHz to 100 GHz," *ITU-R Recs*, 2012.

[34] R. Borgaonkar, K. Redon, and J.-P. Seifert, "Security analysis of a femtocell device," in *Proc. of ACM International Conference on Security of Information and Networks*, pp. 95–102, 2011.

[35] N. Golde, K. Redon, and R. Borgaonkar, "Weaponizing femtocells: The effect of rogue devices on mobile telecommunications.," in *Proc. of NDSS*, 2012.

[36] F. Van Den Broek and R. W. Schreur, "Femtocell security in theory and practice," in *Proc. of Springer Nordic Conference on Secure IT Systems*, pp. 183–198, 2013.

[37] M. Ma and D. H. Tsang, "Impact of channel heterogeneity on spectrum sharing in cognitive radio networks," in *Proc. IEEE International Conference on Communications (ICC)*, pp. 2377–2382, 2008.

[38] M. Tercero, P. G. Sánchez, Ö. Ileri, and J. Zander, "Distributed spectrum access with energy constraint for heterogeneous channels," in *Proc. International Conference onCognitive Radio Oriented Wireless Networks & Communications (CROWNCOM)*, pp. 1–5, 2010.

[39] G. Ning, J. Duan, J. Su, and D. Qiu, "Spectrum sharing based on spectrum heterogeneity and multi-hop handoff in centralized cognitive radio networks," in *Proc. Wireless and Optical Communications Conference (WOCC)*, pp. 1–6, 2011.

[40] H. Gao, H. Liu, and S. Wang, "Research of spectrum sharing method based on channel heterogeneity," in *Proc. International Conference on Computer Science and Network Technology (ICCSNT)*, pp. 1699–1705, 2012.

[41] W.-Y. Lee and I. F. Akyildiz, "Spectrum-aware mobility management in cognitive radio cellular networks," *IEEE Transactions on Mobile Computing*, vol. 11, no. 4, pp. 529–542, 2012.

[42] Y.-S. Chen, C.-H. Cho, I. You, and H.-C. Chao, "A cross-layer protocol of spectrum mobility and handover in cognitive LTE networks," *Simulation Modelling Practice and Theory*, vol. 19, no. 8, pp. 1723–1744, 2011.

[43] O. Jo and D.-H. Cho, "Seamless spectrum handover considering differential path-loss in cognitive radio systems," *IEEE Communications Letters*, vol. 13, no. 3, pp. 190–192, 2009.

[44] Z. Yang, Y. Song, and D. Wang, "An optimal operating frequency selection scheme in spectrum handoff for cognitive radio networks," in *Proc. International Conference on Computing, Networking and Communications (ICNC)*, pp. 1066–1070, 2015.

[45] D. Wang, Y. Song, and Z. Yang, "A joint power adaptation and spectrum handoff scheme in mobile cognitive radio networks," in *Proc. International Conference on Computing, Networking and Communications (ICNC)*, pp. 1061–1065, 2015.

[46] Z. Yang, Y. Song, and D. Wang, "An optimal operating frequency selection scheme in spectrum handoff for cognitive radio networks," in *Proc. International Conference on Computing, Networking and Communications (ICNC)*, 2015.

[47] F. Tariq, L. S. Dooley, and A. S. Poulton, "Analysis of coverage range expansion in closed access cognitive femtocell networks," in *Proc. International Symposium on Wireless Personal Multimedia Communications (WPMC)*, pp. 1–5, 2013.

[48] M. Patel, B. Naughton, C. Chan, N. Sprecher, S. Abeta, A. Neal, *et al.*, "Mobile-edge computing introductory technical white paper," *Mobile-edge Computing (MEC) industry initiative White Paper*, 2014.

[49] M. T. Beck, M. Werner, S. Feld, and T. Schimper, "Mobile edge computing: A taxonomy," 2014.

[50] T. Verbelen, P. Simoens, F. De Turck, and B. Dhoedt, "Cloudlets: Bringing the cloud to the mobile user," in *Proc. of the ACM Workshop on Mobile Cloud Computing and Services*, pp. 29–36, 2012.

[51] D. Calin, H. Claussen, and H. Uzunalioglu, "On femto deployment architectures and macrocell offloading benefits in joint macro-femto deployments," *IEEE Communications Magazine*, vol. 48, no. 1, 2010.

[52] J. Moon and D. Cho, "Efficient handoff algorithm for inbound mobility in hierarchical macro/femto cell networks," *IEEE Communications Letters*, vol. 13, pp. 755–757, October 2009.

[53] J. Moon and D. Cho, "Novel handoff decision algorithm in hierarchical macro/femto cell networks," in *Proc. IEEE Wireless Communications and Network Conference (WCNC)*, pp. 1–6, April 2010.

[54] P. Xu, X. Fang, R. He, and Z. Xiang, "An efficient handoff algorithm based on received signal strength and wireless transmission loss in hierarchical cell networks," *Telecommunication Systems*, vol. 52, no. 1, pp. 317–325, 2013.

[55] D. López-Pérez, A. Ladányi, A. Juttner, and J. Zhang, "OFDMA femtocells: Intracell handover for interference and handover mitigation in two-tier networks," in *Proc. IEEE Wireless Communications and Networking Conference (WCNC)*, pp. 1–6, 2010.

[56] B. Jeong, S. Shin, I. Jang, N. W. Sung, and H. Yoon, "A smart handover decision algorithm using location prediction for hierarchical macro/femto-cell networks," in *Proc. IEEE Vehicular Technology Conference (VTC Fall)*, pp. 1–5, 2011.

[57] S. Wu, "Handover strategy in HIP-based LTE femtocells networks with hybrid access model," in *Proc. IEEE International Conference in Genetic and Evolution Computing (ICGEC)*, 2012.

[58] S. Wu, X. Zhang, R. Zheng, Z. Yin, Y. Fang, and D. Yang, "Handover study concerning mobility in the two-hierarchy network," in *Proc. IEEE Vehicular Technology Conference*, pp. 1–5, 2009.

[59] P. Xu, X. Fang, J. Yang, and Y. Cui, "A user's state and SINR-based handoff algorithm in hierarchical cell networks," in *Proc. International Conference on Wireless Communications Networking and Mobile Computing (WiCOM)*, pp. 1–4, 2010.

[60] G. Yang, X. Wang, and X. Chen, "Handover control for LTE femtocell networks," in *Proc. International Conference on Electronics, Communications and Control (ICECC)*, pp. 2670–2673, 2011.

[61] M. Z. Chowdhury, W. Ryu, E. Rhee, and Y. M. Jang, "Handover between macrocell and femtocell for UMTS based networks," in *Proc. International Conference on Advanced Communication Technology (ICACT)*, vol. 1, pp. 237–241, 2009.

[62] J.-S. Kim and T.-J. Lee, "Handover in UMTS networks with hybrid access femtocells," in *Proc. International Conference on Advanced Communication Technology (ICACT)*, vol. 1, pp. 904–908, 2010.

[63] Z. Becvar and P. Mach, "Adaptive techniques for elimination of redundant handovers in femtocells," in *Proc. IEEE International Conference on Networks (ICN)*, pp. 230–234, 2011.

[64] H. Ge, X. Wen, W. Zheng, Z. Lu, and B. Wang, "A history-based handover prediction for LTE systems," in *Proc. IEEE International Symposium on Computer Network and Multimedia Technology (CNMT)*, pp. 1–4, 2009.

[65] Z. Becvar, "Efficiency of handover prediction based on handover history," *Journal of Convergence Information Technology*, vol. 4, no. 4, pp. 41–47, 2009.

[66] A. Ulvan, R. Bestak, and M. Ulvan, "Handover scenario and procedure in LTE-based femtocell networks," in *Proc. International Conference on Mobile Ubiquitous Computing, Systems, Services and Technologies*, pp. 213–218, 2010.

[67] D.-W. Lee, G.-T. Gil, and D.-H. Kim, "A cost-based adaptive handover hysteresis scheme to minimize the handover failure rate in 3GPP LTE system," *EURASIP Journal on Wireless Communications and Networking*, vol. 2010, no. 6, 2010.

[68] L.-P. David, V. Alvaro, L. Ákos, d. l. R. Guillaume, Z. Jie, *et al.*, "Intracell handover for interference and handover mitigation in OFDMA two-tier macrocell-femtocell networks," *EURASIP Journal on Wireless Communications and Networking*, vol. 2010, pp. 1–15, 2010.

[69] K. S. B. Reguiga, F. Mhiri, and R. Bouallegue, "Handoff management in green femtocell network," *Internat. J. of Comp. Apps*, vol. 27, no. 4, pp. 1–7, 2011.

[70] D. Xenakis, N. Passas, and C. Verikoukis, "A novel handover decision policy for reducing power transmissions in the two-tier LTE network," in *Proc. IEEE International Conference on Communications (ICC)*, pp. 1352–1356, 2012.

[71] L. Tang, D. Wang, and Q. Chen, "An adaptive scaling scheme for TTT in small cell," in *Proc. IET International Conference on Wireless, Mobile and Multimedia Networks (ICWMMN)*, pp. 6–11, 2013.

[72] H.-P. Lin, R.-T. Juang, and D.-B. Lin, "Validation of an improved location-based handover algorithm using GSM measurement data," *IEEE Transactions on Mobile Computing*, vol. 4, no. 5, pp. 530–536, 2005.

[73] T. Inzerilli, A. M. Vegni, A. Neri, and R. Cusani, "A location-based vertical handover algorithm for limitation of the ping-pong effect," in *Proc. IEEE International Conference on Wireless and Mobile Computing Networking and Communications (WIMOB)*, pp. 385–389, 2008.

[74] H. Zhang, X. Wen, B. Wang, W. Zheng, and Y. Sun, "A novel handover mechanism between femtocell and macrocell for LTE based networks," in *Proc. Second International Conference on Communication Software and Networks (ICCSN)*, pp. 228–231, 2010.

[75] M. Ylianttila, J. Mäkelä, and K. Pahlavan, "Analysis of handoff in a location-aware vertical multi-access network," *Computer Networks*, vol. 47, no. 2, pp. 185–201, 2005.

[76] J. Zhang, H. C. Chan, and V. C. Leung, "A location-based vertical handoff decision algorithm for heterogeneous mobile networks," in *Proc. IEEE Global Telecommunications Conference (GLOBECOM)*, pp. 1–5, 2006.

[77] T.-Y. Wu, C.-C. Lai, and H.-C. Chao, "Efficient IEEE 802.11 handoff based on a novel geographical fingerprint scheme," *Wireless Communications and Mobile Computing*, vol. 6, no. 1, pp. 127–135, 2006.

[78] T.-Y. Wu and W.-F. Weng, "Reducing handoff delay of wireless access in vehicular environments by artificial neural network-based geographical fingerprint," *IET Communications*, vol. 5, no. 4, pp. 542–553, 2011.

[79] A. Ulvan, R. Bestak, and M. Ulvan, "The study of handover procedure in LTE-based femtocell network," in *Proc. IEEE Wireless and Mobile Networking Conference (WMNC)*, pp. 1–6, 2010.

[80] D. Xenakis, N. Passas, L. Merakos, and C. Verikoukis, "Mobility management for femtocells in LTE-advanced: key aspects and survey of handover decision algorithms," *IEEE Communications Surveys & Tutorials*, vol. 16, no. 1, pp. 64–91, 2014.

[81] I. Bilogrevic, M. Jadliwala, and J.-P. Hubaux, "Security issues in next generation mobile networks: LTE and femtocells," in *Proc. of International Femtocell Workshop*, 2010.

[82] R. Rajavelsamy, J. Lee, and S. Choi, "Towards security architecture for home (evolved) NodeB: challenges, requirements and solutions," *Security and Communication Networks*, vol. 4, no. 4, pp. 471–481, 2011.

[83] J. Xiang, Y. Zhang, T. Skeie, and L. Xie, "Downlink spectrum sharing for cognitive radio femtocell networks," *IEEE Systems Journal*, vol. 4, no. 4, pp. 524–534, 2010.

[84] S.-M. Cheng, W. C. Ao, F.-M. Tseng, and K.-C. Chen, "Design and analysis of downlink spectrum sharing in two-tier cognitive femto networks," *IEEE Transactions on Vehicular Technology*, vol. 61, no. 5, pp. 2194–2207, 2012.

[85] X. Kang, R. Zhang, and M. Motani, "Price-based resource allocation for spectrum-sharing femtocell networks: A stackelberg game approach," *IEEE Journal on Selected Areas in Communications*, vol. 30, no. 3, pp. 538–549, 2012.

[86] D.-C. Oh, H.-C. Lee, and Y.-H. Lee, "Cognitive radio based femtocell resource allocation," in *Proc. International Conference on Information and Communication Technology Convergence (ICTC)*, pp. 274–279, 2010.

[87] P. Mach and Z. Becvar, "Mobile edge computing: A survey on architecture and computation offloading," *IEEE Communications Surveys & Tutorials*, 2017.

[88] P. Mach and Z. Becvar, "Cloud-aware power control for real-time application offloading in mobile edge computing," *Transactions on Emerging Telecommunications Technologies*, vol. 27, no. 5, pp. 648–661, 2016.

[89] T. Taleb and A. Ksentini, "An analytical model for follow me cloud," in *Proc. of IEEE Global Communications Conference (GLOBECOM)*, pp. 1291–1296, 2013.

[90] A. Ksentini, T. Taleb, and M. Chen, "A Markov decision process-based service migration procedure for follow me cloud," in *Proc. of IEEE International Conference on Communications (ICC)*, 2014.

[91] X. Sun and N. Ansari, "Primal: Profit maximization avatar placement for mobile edge computing," in *Proc. of IEEE International Conference on Communications (ICC)*, pp. 1–6, 2016.

[92] S. Wang, R. Urgaonkar, M. Zafer, T. He, K. Chan, and K. K. Leung, "Dynamic service migration in mobile edge-clouds," in *Proc. of IFIP Networking Conference*, pp. 1–9, 2015.

[93] A. Nadembega, A. S. Hafid, and R. Brisebois, "Mobility prediction model-based service migration procedure for follow me cloud to support QoS and QoE," in *Proc. of IEEE International Conference on Communications (ICC)*, pp. 1–6, 2016.

[94] S. Wang, R. Urgaonkar, T. He, K. Chan, M. Zafer, and K. K. Leung, "Dynamic service placement for mobile micro-clouds with predicted future costs," *IEEE Transactions on Parallel and Distributed Systems*, vol. 28, no. 4, pp. 1002–1016, 2017.

[95] R. Urgaonkar, S. Wang, T. He, M. Zafer, K. Chan, and K. K. Leung, "Dynamic service migration and workload scheduling in edge-clouds," *Performance Evaluation*, vol. 91, pp. 205–228, 2015.

[96] K. Ha, Y. Abe, Z. Chen, W. Hu, B. Amos, P. Pillai, and M. Satyanarayanan, "Adaptive VM handoff across cloudlets," *Technical report, Technical Report CMU-C S-15–113*, 2015.

[97] S. Secci, P. Raad, and P. Gallard, "Linking virtual machine mobility to user mobility," *IEEE Transactions on Network and Service Management*, vol. 13, no. 4, pp. 927–940, 2016.

[98] M. Zhang, X. Du, and K. Nygard, "Improving coverage performance in sensor networks by using mobile sensors," in *Proc. of Military Communications Conference (MILCOM)*, pp. 3335–3341, 2005.

[99] X. Du and F. Lin, "Maintaining differentiated coverage in heterogeneous sensor networks," *EURASIP Journal on Wireless Communications and Networking*, vol. 2005, no. 4, pp. 565–572, 2005.

[100] Z. Becvar, J. Plachy, and P. Mach, "Path selection using handover in mobile networks with cloud-enabled small cells," in *Proc. of IEEE International Symposium on Personal, Indoor, and Mobile Radio Communication (PIMRC)*, pp. 1480–1485, 2014.

[101] J. Plachy, Z. Becvar, and P. Mach, "Path selection enabling user mobility and efficient distribution of data for computation at the edge of mobile network," *Computer Networks*, vol. 108, pp. 357–370, 2016.

[102] X. Chen, L. Jiao, W. Li, and X. Fu, "Efficient multi-user computation offloading for mobile-edge cloud computing," *IEEE/ACM Transactions on Networking*, vol. 24, no. 5, pp. 2795–2808, 2016.

[103] L. Yang, J. Cao, H. Cheng, and Y. Ji, "Multi-user computation partitioning for latency sensitive mobile cloud applications," *IEEE Transactions on Computers*, vol. 64, no. 8, pp. 2253–2266, 2015.

[104] J. Yue, D. Zhao, and T. D. Todd, "Cloud server job selection and scheduling in mobile computation offloading," in *Proc. of IEEE Global Communications Conference (GLOBECOM)*, pp. 4990–4995, 2014.

[105] Y. Yu, J. Zhang, and K. B. Letaief, "Joint Subcarrier and CPU Time Allocation for Mobile Edge Computing.," in *Proc. of IEEE Global Communications Conference (GLOBECOM)*, pp. 1–6, 2016.

[106] S. Barbarossa, S. Sardellitti, and P. Di Lorenzo, "Joint allocation of computation and communication resources in multiuser mobile cloud computing," in *Proc. of IEEE Signal Processing Advances in Wireless Communications (SPAWC)*, pp. 26–30, 2013.

[107] S. Sardellitti, G. Scutari, and S. Barbarossa, "Joint optimization of radio and computational resources for multicell mobile-edge computing," *IEEE Transactions on Signal and Information Processing over Networks*, vol. 1, no. 2, pp. 89–103, 2015.

[108] E. Gelenbe, R. Lent, and M. Douratsos, "Choosing a local or remote cloud," in *Proc. of Network Cloud Computing and Applications (NCCA)*, pp. 25–30, 2012.

[109] T. Zhao, S. Zhou, X. Guo, Y. Zhao, and Z. Niu, "A cooperative scheduling scheme of local cloud and internet cloud for delay-aware mobile cloud computing," in *Proc. of IEEE Globecom Workshops (GC Wkshps)*, pp. 1–6, 2015.

[110] K. Mitra, C. Ahlund, *et al.*, "A mobile cloud computing system for emergency management," *IEEE Cloud Computing*, vol. 1, no. 4, pp. 30–38, 2014.

[111] C. Wang, Y. Li, and D. Jin, "Mobility-assisted opportunistic computation offloading," *IEEE Communications Letters*, vol. 18, no. 10, pp. 1779–1782, 2014.

[112] K. Lee and I. Shin, "User mobility model based computation offloading decision for mobile cloud," *Journal of Computing Science and Engineering*, vol. 9, no. 3, pp. 155–162, 2015.

[113] M. R. Rahimi, N. Venkatasubramanian, and A. V. Vasilakos, "MuSIC: Mobility-aware optimal service allocation in mobile cloud computing," in *Proc. of IEEE International Conference on Cloud Computing (CLOUD)*, pp. 75–82, 2013.

[114] S. Wang, R. Urgaonkar, T. He, M. Zafer, K. Chan, and K. K. Leung, "Mobility-induced service migration in mobile micro-clouds," in *Proc. of IEEE Military Communications Conference (MILCOM)*, pp. 835–840, 2014.

[115] 3GPP, T. 36.839, and V.11.1.0, "Radio resource control protocol specification," December 2013.

[116] Z. Yang, Z. Zhou, and Y. Liu, "From RSSI to CSI: Indoor localization via channel response," *ACM Computing Surveys*, vol. 46, pp. 1–32, November 2013.

[117] A. S. R. Zekavat and R. M. Buehrer, *RF Fingerprinting Location Techniques.* Wiley-IEEE Press, 1 ed., 2012.

[118] J. McNair, T. Tugcu, W. Wang, and J. L. Xie, "A survey of cross-layer performance enhancements for mobile IP networks," *Computer Networks*, vol. 49, no. 2, pp. 119–146, 2005.

[119] J. Xie and U. Narayanan, "Performance analysis of mobility support in ipv4/ipv6 mixed wireless networks," *IEEE Transactions on Vehicular Technology*, vol. 59, no. 2, pp. 962–973, 2010.

[120] S. Lal and D. K. Panwar, "Coverage analysis of handoff algorithm with adaptive hysteresis margin," in *Proc. 10th International Conference on Information Technology (ICIT)*, pp. 133–138, December 2007.

[121] S. Tisue and U. Wilensky, "Netlogo: A simple environment for modeling complexity," in *Proc. International Conference on Complex Systems*, pp. 16–21, 2004.

[122] W. Nasrin and J. Xie, "Effects of heterogeneous frequency changes in cognitive radio femtocell networks," in *IEEE Global Communications Conference (GLOBECOM)*, pp. 1–6, 2016.

[123] K. Lin, H. Lin, and R. Juang, "Proposed text for HO from femtocell BS to macro BS or other femtocell BS (AWD-femto)," *IEEE Standard Contribution C*, vol. 802, 2009.

[124] A. Ghasemi and E. S. Sousa, "Spectrum sensing in cognitive radio networks: requirements, challenges and design trade-offs," *IEEE Communications Magazine*, vol. 46, no. 4, pp. 32–39, 2008.

[125] J. Shim, Q. Cheng, and V. Sarangan, "Cooperative spectrum sensing with optimal sensing ranges in cognitive radio ad-hoc networks," in *Proc. International Conference on Cognitive Radio Oriented Wireless Networks (CROWNCOM)*, 2010.

[126] E. Dahlman, S. Parkvall, and J. Skold, *4G: LTE/LTE-advanced for mobile broadband*. Academic press, 2013.

[127] T. Camp, J. Boleng, and V. Davies, "A survey of mobility models for ad hoc network research," *Wireless communications and mobile computing*, vol. 2, no. 5, pp. 483–502, 2002.

[128] A. Machen, S. Wang, K. K. Leung, B. J. Ko, and T. Salonidis, "Live service migration in mobile edge clouds," *arXiv preprint arXiv:1706.04118*, 2017.

[129] W. Nasrin and J. Xie, "Signaling cost analysis for handoff decision algorithms in femtocell networks," in *Proc. of IEEE International Conference on Communications (ICC)*, pp. 1–6, 2017.

[130] J. Xie, "User independent paging scheme for mobile ip," *Wireless Networks*, vol. 12, no. 2, pp. 145–158, 2006.

[131] W. Nasrin and J. Xie, "An effective target cell selection scheme in open-access femtocell networks," in *Proc. of IEEE Global Communications Conference (GLOBECOM)*, 2017.

[132] V. Erceg, L. J. Greenstein, S. Y. Tjandra, S. R. Parkoff, A. Gupta, B. Kulic, A. A. Julius, and R. Bianchi, "An empirically based path loss model for wireless channels in suburban environments," *IEEE Journal on Selected Aeas in Communications*, vol. 17, no. 7, pp. 1205–1211, 1999.